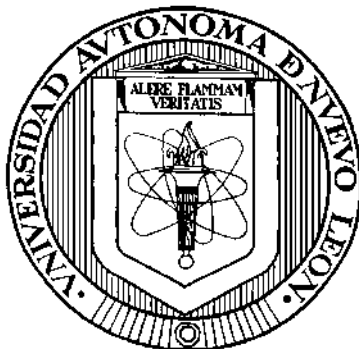


UNIVERSIDAD AUTÓNOMA DE NUEVO LEÓN

FACULTAD DE CIENCIAS QUÍMICAS



"SYNTHESIS AND CHARACTERIZATION OF NEW LUMINESCENT  
BIOSENSORS OF Al (III), DERIVATIVES FROM SCHIFF BASE WITH  
POTENTIAL USE AS PREVENTIVE DIAGNOSIS METHOD IN  
NEURODEGENERATIVE DISEASES"

BY

M.C. JESSICA CECILIA BERRONES REYES

AS PARTIAL REQUIREMENT TO OBTAIN THE DEGREE OF  
DOCTOR OF SCIENCE WITH  
ORIENTATION IN CHEMISTRY OF MATERIALS.

July 2018

SYNTHESIS AND CHARACTERIZATION OF NEW LUMINESCENT  
BIOSENSORS OF Al (III), DERIVATIVES FROM SCHIFF BASE WITH  
POTENTIAL USE AS PREVENTIVE DIAGNOSIS METHOD IN  
NEURODEGENERATIVE DISEASES

Aprobación de la Tesis:

---

Dr. Víctor Manuel Jiménez Pérez  
Presidente

---

Dr. Alberto Gómez Treviño  
Secretario

---

Dr. Boris Ildusovich Kharissov  
Vocal

---

Dr. Procoro Gamero Melo  
Vocal

---

Dr. Mario Sánchez Vásquez  
Vocal

---

Dra. Ma. Araceli Hernández Ramírez  
Sub-Directora de estudios de posgrado

SYNTHESIS AND CHARACTERIZATION OF NEW LUMINESCENT  
BIOSENSORS OF Al (III), DERIVATIVES FROM SCHIFF BASE WITH  
POTENTIAL USE AS PREVENTIVE DIAGNOSIS METHOD IN  
NEURODEGENERATIVE DISEASES

Revisión de la Tesis:

---

Dr. Víctor Manuel Jiménez Pérez  
Director de la Tesis

---

Dr. Alberto Gómez Treviño

---

Dr. Eduardo Sánchez Cervantes

---

Dr. Boris Ildusovich Kharissov

---

Dra. Ma. Araceli Hernández Ramírez  
Sub-Directora de estudios de posgrado

## RESUMEN

MC Jessica Cecilia Berrones Reyes

Julio 2018

Universidad Autónoma de Nuevo León

Facultad de Ciencias Químicas

Título del estudio: SINTESIS Y CARACTERIZACIÓN DE NUEVOS BIOSENSORES LUMINISCENTES DE Al (III), DERIVADOS DE BESES DE SCHIFF CON POTENCIAL USO COMO METODO DIAGNOSTICO PREVENTIVO EN PADECIMIENTOS NEURODEGENERATIVOS.

Número de páginas: 74

Candidato para el grado de Doctor en Ciencias con Orientación en Química de los Materiales.

Área de estudio: Química de los Materiales.

Propósito y Método de Estudio: Hoy en día, los investigadores están en búsqueda de sensores fluorescentes simples con respuesta rápida, alta sensibilidad y selectividad debido a sus múltiples aplicaciones en diagnóstico clínicos y monitoreo ambiental. Durante la última década, ha cobrado interés el desarrollar materiales que permitan no solo la detección de diferentes moléculas, sino también su obtención de imágenes dentro de las células vivas. Debido al impacto potencial de los iones de  $Al^{3+}$  en la salud humana y el medio ambiente, sensores altamente selectivos y sensibles para este metal son, por lo tanto, muy demandados.

Contribuciones y Conclusiones: En este trabajo de investigación se reportó la síntesis de cuatro nuevos compuestos derivados de bases de Schiff los cuales fueron caracterizados mediante diversas técnicas espectroscópicas y espectrométricas. Se demostró la capacidad de los cuatro compuestos de sensar iones aluminio en solución y producir una señal detectable por fluorescencia. El compuesto 2 fue capaz de sensar este metal en cultivo celular y producir imágenes celulares donde se observa aumento la intensidad de fluorescencia producida por la unión metal-ligante.

FIRMA DEL ASESOR:

---

Dr. Víctor M. Jiménez Pérez

## SUMMARY

MC Jessica Cecilia Berrones Reyes

July 2018

Universidad Autónoma de Nuevo León

Facultad de Ciencias Químicas

Study Title: SYNTHESIS AND CHARACTERIZATION OF NEW LUMINESCENT  
BIOSENSORS OF Al (III), DERIVATIVES FROM SCHIFF BASE  
WITH POTENTIAL USE AS PREVENTIVE DIAGNOSIS METHOD  
IN NEURODEGENERATIVE DISEASES

Page number: 74

Candidate for the degree of Doctor  
of Science with Orientation in in  
Chemistry of Materials.

Study area: Chemistry of Materials.

Purpose and study method: Nowadays, researchers are in enthusiastic pursuit of simple fluorescent sensors with fast response, high sensitivity and selectivity, due to their widespread applications in clinical diagnostics and environmental monitoring. Over the past decade, there has been significant interest in developing materials that allow not only the detection of different targets but also their imaging within living cells. Due to the potential impact of Al<sup>3+</sup> ions on human health and the environment, highly selective and sensitive chemosensors for this metal are hence highly demanded.

Conclusions and contribution: This research work report the synthesis of four new compounds derived from Schiff bases that were characterized by various spectroscopic and spectrometric techniques. The ability of the four compounds to sense aluminum ions in solution and produce a signal detectable by fluorescence were demonstrated. Compound 2 was able to sense this metal in cell culture and produce cellular images where the intensity of fluorescence produced by the metal-ligand bond is increased.

ASSESSOR SIGNATURE:

---

Dr. Víctor M. Jiménez Pérez

This thesis was developed at the Laboratory of materials III in the postgraduate area of Facultad de Ciencias Químicas from Universidad Autónoma de Nuevo León under the management of Ph.D. Victor Manuel Jiménez Pérez.

This project was carried out with the financial support from CONACYT (558050), and complemented by two short stays under the collaboration and counseling of Ph.D. Steven Magennis and Ph.D. Alberto Gómez.

## DIVULGATION PROJECT AND STAYS PERFORMED

The study realized in this thesis generated a publication:

- Jessica C. Berrones-Reyes, C.C. Vidyasagar, Blanca M. Muñoz Flores, Víctor M. Jiménez-Pérez. Luminescent molecules of main group elements: Recent advances on synthesis, properties and their application on fluorescent bioimaging (FBI). *J Lumin.*, **2018**, 195, 290-313.

One short stay was performed:

- January 8<sup>th</sup> to Jun 30<sup>th</sup> 2017. Stay in the department of Chemistry of the University of Glasgow, under the management of Ph.D. Steve Magennis.

## **ACKNOWLEDGEMENTS**

I want to thank CONACYT and the Faculty of Chemical Sciences of the UANL for the support and the facilities in the development of this research work.

Thanks to Ph.D. Victor Jiménez Pérez, director of my thesis, for their support, time, knowledge taught, and for be my guide in the development of this work. I am also grateful to Ph.Ds Alberto Gómez, Steven Magennis and Blanca Muñoz for their support and generous collaboration in this project.

Thanks to my thesis committee, Ph.Ds Alberto Gómez, Eduardo Sánchez and Boris Kharissov, for their corrections, suggestions and interest, in the review of this research work.

I greatly appreciate the support of my classmates, for their unconditional presence, their helpful contributions, for their comments and suggestions made during the course of this investigation.

But most of all I thank my family, who throughout my life have ensured my welfare and education being my support at all times so that I could achieve my dreams, for motivating me and shake my hand when I felt that the road was finished.



I dedicate this thesis

TO MY PARENTS. They put their complete trust in me in every challenge that I face, without hesitation or a moment in my intelligence and ability. It is for them that I am what I am now, with you forever, my heart and my thanks.

MY SIBLINGS. Thanks to those important people in my life who were always ready to give me all your help.

MY GRANDPARENTS. For his infinite love, affection, understanding and support, for your prayers and wise counsel

TO GOD. Because he has been with me every step I take, giving me strength to continue.

With all my love for all people who believed in me

## CONTENTS

Chapter	Page
1. INTRODUCTION . . . . .	1
2. BACKGROUND . . . . .	6
2.1 Luminiscent probes . . . . .	6
2.2 Luminiscent probes for metal cations. . . . .	8
2.3 Aluminum sensors . . . . .	9
2.4 Schiff bases and naphthalene derivatives . . . . .	11
3. HYPOTHESIS. . . . .	12
4. GENERAL OBJECTIVE. . . . .	12
4.1 Specific Objectives . . . . .	12
5. MATERIALS AND METHODS . . . . .	13
5.1 Materials . . . . .	13
5.1.1 Synthesis and characterization . . . . .	13
5.1.2 Bioassays . . . . .	14
5.2 Methods . . . . .	14
5.2.1 Synthesis procedure of compounds 1-4 . . . . .	14
5.2.1.1 ( <i>S,E</i> )-11-amino-8-((2,4-di- <i>tert</i> -butyl-1-hydroxybenzylidene) amino)-11-oxopentanoic acid. <b>(1)</b> . . . . .	16
5.2.1.2 ( <i>S,E</i> )-11-amino-8-(((1-hydroxynaphthalen-10-yl)methylene)amino)-11-oxopentanoic acid. <b>(2)</b> . . . . .	17
5.2.1.3 (16 <i>S</i> ,12 <i>S</i> ,13 <i>S</i> ,14 <i>R</i> ,15 <i>S</i> )-15-(hydroxymethyl)-12-((( <i>E</i> )-(1-hydroxynaphthalen-10yl)methylene)amino) tetrahydro-2 <i>H</i> -pyran-16,13,14-triol. <b>(3)</b> . . . . .	18

4.2.1.4	( <i>E</i> )-17-hydroxy-12-(((1-hydroxynaphthalen-10-yl)methylene)amino)benzoic acid. <b>(4)</b> . . . . .	20
5.2.2	Fluorescence Measuremen . . . . .	21
5.2.3	Fluorescence Imaging of Al <sup>3+</sup> in living cells . . . . .	21
5.3	Waste disposal . . . . .	22
6.	RESULTS AND DISCUSSION . . . . .	23
6.1	Synthesis . . . . .	23
6.2	Chemical structure elucidation . . . . .	24
6.2.1	Absorption and emission analysis . . . . .	25
6.2.2	Analysis of NMR data . . . . .	27
6.2.3	Analysis of IR data. . . . .	28
6.2.4	High resolution mass spectrometry analysis . . . . .	29
6.3	Fluorescence Measurement . . . . .	31
6.3.1	Aluminum sensing. . . . .	31
6.3.2	Quantum yield determination . . . . .	32
6.3.3	Selectivity studies . . . . .	33
6.3.4	Fluorescent competitive experiments . . . . .	35
6.3.5	Sensitive quantitation of Al <sup>3+</sup> . . . . .	37
6.3.6	Detection limit . . . . .	40
6.3.7	Binding stoichiometry . . . . .	42
6.4	Fluorescence Imaging of Al <sup>3+</sup> in Living Cells . . . . .	43
7.	CONCLUSION . . . . .	47
7.1	Perspectives. . . . .	48
8.	REFERENCES . . . . .	49
9.	APPENDIX . . . . .	55
10.	AUTOBIOGRAPHIC SUMMARY. . . . .	74

## LIST OF TABLES

Table		Page
1.	Absorption and emission data of compounds <b>1-4</b> . . . . .	25
2.	Selected $^1\text{H}$ and $^{13}\text{C}$ signals. . . . .	28
3.	IR data of compounds <b>1-4</b> . . . . .	29
4.	Quantum yield values . . . . .	33
5.	LOD data of compounds <b>1-4</b> . . . . .	41

## LIST OF FIGURES

Figure	Page
1. New compounds derived from Schiff base proposed . . . . .	5
2. Structure for some fluorescent chemosensors for metal ions .	9
3. Schiff bases 1-4 . . . . .	24
4. UV spectra of compounds <b>1-4</b> in acetonitrile/water (1:1). . . .	26
5. Emission spectra of compounds <b>1-4</b> in acetonitrile/water (1:1).	26
6. Numbering of a) compound <b>1</b> ; b) compound <b>2, 3</b> and <b>4</b> . . . .	27
7. Graphic of the increment in the fluorescence intensity of a) Compound <b>1</b> , b) Compound <b>2</b> , c) Compound <b>3</b> and d) Compound <b>4</b> , in absence and presence of Al <sup>3+</sup> ions . . . . .	31
8. Photographs of a) Compounds <b>1 - 4</b> and b) compounds <b>1 - 4</b> in presence of Al <sup>3+</sup> ions (acetonitrile/H <sub>2</sub> O = 1:1) under UV lamp (365 nm). . . . .	32
9. Fluorescence spectra of a) Compound <b>1</b> , b) Compound <b>2</b> , c) Compound <b>3</b> and d) Compound <b>4</b> , in presence of different metal ions (50 μM), (acetonitrile/H <sub>2</sub> O = 1:1) . . . . .	34
10. Graphic of the fluorescence intensity of compounds <b>1-4</b> (10 μM) upon addition of Al <sup>3+</sup> (50 μM), in presence of various metal ions (50 μM). Compound <b>1</b> excited at 330 nm (blue bars), compound <b>2</b> excited at 390 nm (red bars), compound <b>3</b> excited at 390 nm (green bars) and compound <b>4</b> excited at 440 nm (purple bars) .	36

11.	a) UV–Vis and b) fluorescence spectra (excited at 330 nm) of Compound <b>1</b> (10µM) in presence of different concentrations of Al <sup>3+</sup> (0-40 µM). . . . .	38
12.	a) UV–Vis and b) fluorescence spectra (excited at 390 nm) of Compound <b>2</b> (10µM) in presence of different concentrations of Al <sup>3+</sup> (0-40 µM). . . . .	38
13.	a) UV–Vis and b) fluorescence spectra (excited at 390 nm) of Compound <b>3</b> (10µM) in presence of different concentrations of Al <sup>3+</sup> (0-40 µM). . . . .	39
14.	a) UV–Vis and b) fluorescence spectra (excited at 440 nm) of Compound <b>4</b> (10µM) in presence of different concentrations of Al <sup>3+</sup> (0-40 µM). . . . .	39
15.	Changes of emission intensity of compounds <b>1-4</b> at a) 465 nm (Compound <b>1</b> ); b) 433 nm (Compound <b>2</b> ); c) 433 nm (Compound <b>3</b> ) and c) 505 nm (Compound <b>4</b> ). . . . .	40
16.	Comparison of the limits of detection between compounds <b>1-4</b> and molecules previously reported (5 <sup>xliii</sup> , 6 <sup>ix</sup> and 7 <sup>xliiv</sup> ). . . . .	46
17.	Job’s plot for the complexation of a) compound <b>1</b> ; b) compound <b>2</b> ; c) compound <b>3</b> ; d) compound <b>4</b> , with Al <sup>3+</sup> in a mixture acetonitrile : water (1:1) . . . . .	43
18.	Confocal microscopic images of human epithelial cells Hs27 treated with (1) compound <b>1</b> , (2) compound <b>2</b> , (3) compound <b>3</b> and (4) compound <b>4</b> (20 µM); images in the absence (a) and presence (b) of Al <sup>3+</sup> (100 µM). Incubation temperature is 37 °C. . . . .	44
19.	Confocal microscopic images of human epithelial cells Hs27 treated with compound <b>2</b> (20 µM) in the absence (a) and presence (b) of Al <sup>3+</sup> (100 µM); bright-field (1), fluorescent (2) and the overlay image (3). Incubation temperature is 37 °C. . . . .	46

## LIST OF SCHEMES

Scheme	Page
1. Principal sources of Al <sup>3+</sup> contamination. . . . .	1
2. Advantages of fluorometric methods. . . . .	4
3. Components of a chemosensor . . . . .	7
4. Synthesis of the four new compounds derived from Schiff base.	15
5. Proposed fragmentation of compounds <b>1</b> and <b>2</b> . . . . .	30
6. Proposed fragmentation of compound <b>3</b> . . . . .	30
7. Proposed fragmentation of compound <b>4</b> . . . . .	30

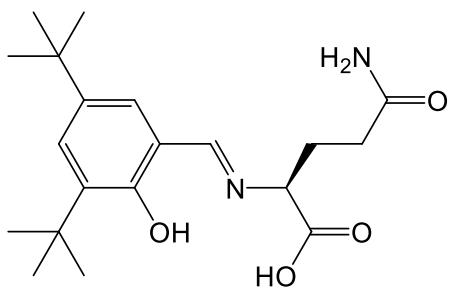
## LIST OF ABBREVIATIONS

<b>ATR</b>	attenuated total reflection	<b>μM</b>	micromolar
<b>CO<sub>2</sub></b>	carbon dioxide	<b>MP</b>	melting point
<b><sup>13</sup>C</b>	carbon NMR	<b>ml</b>	milliliter
<b>°C</b>	Celsius degrees	<b>mmol</b>	milimol
<b>δ</b>	chemical shift	<b>mM</b>	milimolar
<b>COSY</b>	correlation spectroscopy	<b>nm</b>	nanometer
<b>J</b>	coupling constant	<b>NMR</b>	Nuclear magnetic resonance
<b>CD<sub>3</sub>OD</b>	deuterated methanol	<b>ppm</b>	parts per million
<b>DMSO</b>	dimethyl sulfoxide	<b>PBS</b>	phosphate-buffered saline
<b>DMEM</b>	Dulbecco's Modified Eagle's medium	<b>KOH</b>	potassium hydroxide
<b>HETCOR</b>	2-D heterocorrelation	<b>pH</b>	potential of Hydrogen

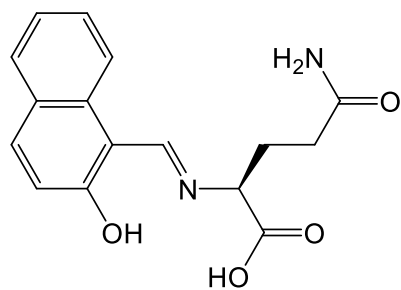


<b>FBS</b>	fetal bovine serum	$^1\text{H}$	proton NMR
<b>g</b>	grams	$\phi$	quantum yield
<b>HOMO</b>	Highest occupied molecular orbital	$\sigma$	standard deviation
<b>Hrs</b>	Hours	$(\text{CH}_3)_4\text{Si}$	tetramethylsilane
<b>Hs27</b>	human epithelial cells	<b>TOF</b>	time of flight
<b>IR</b>	infrared spectroscopy	<b>UV</b>	ultraviolet
<b>K</b>	Kelvin degrees	<b>Vis</b>	Visible region
<b>Kg</b>	kilograms	$\lambda$	wavelength
<b>LOD</b>	limit of detection	<b>H<sub>2</sub>O</b>	water
<b>L</b>	litre	<b>WHO</b>	World Health Organization
<b>LUMO</b>	Lowest unoccupied molecular orbital	<b>ZnSe</b>	Zinc selenide
<b>MHz</b>	Megahertz		

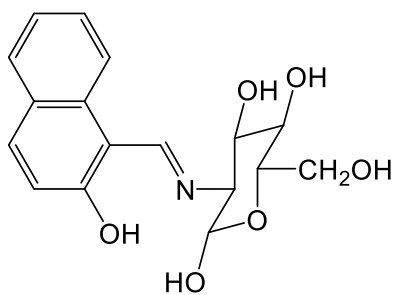
## LIST OF ORGANIC COMPOUNDS



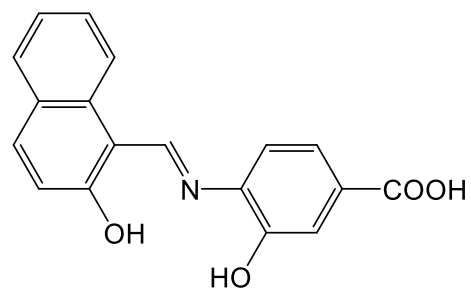
1



2



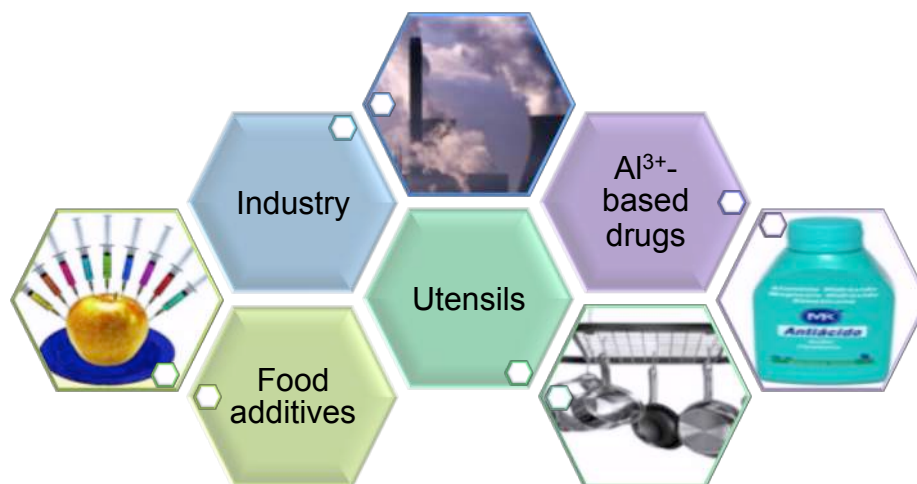
3



4

## 1.INTRODUCTION

Aluminum is a silvery-white metal, is considered the most plentiful metallic element in the earth's crust.<sup>i</sup> Due to high reactivity, aluminum does not exist as the metal in the environment; it exists in a combined state with other elements. In nature it is found in soil, rocks (particularly igneous rocks), and clays as aluminosilicate minerals. It is deadly to growing plants and kills fish in acidified water. Principal sources of  $Al^{3+}$  contamination in human beings are food additives, aluminum-based pharmaceuticals, occupational dusts, aluminum containers, cooking utensils, paper industry, dye production and the textile industry (**Scheme 1**).<sup>ii</sup>



**Scheme 1.** Principal sources of  $Al^{3+}$  contamination.

Aluminum intake from foods, particularly those containing aluminum compounds used as food additives, represents the major route of aluminum exposure for the general public, excluding persons who regularly ingest aluminum-containing antacids and buffered analgesics, for whom intakes may be as high as 5 g/day (WHO, 1997). At an average adult intake of aluminum from food of 5 mg/day and a drinking-water aluminum concentration of 0.1 mg/L, the contribution of drinking-water to the total oral exposure to aluminum will be about 4%. The contribution of air to the total exposure is generally negligible.<sup>ii</sup>

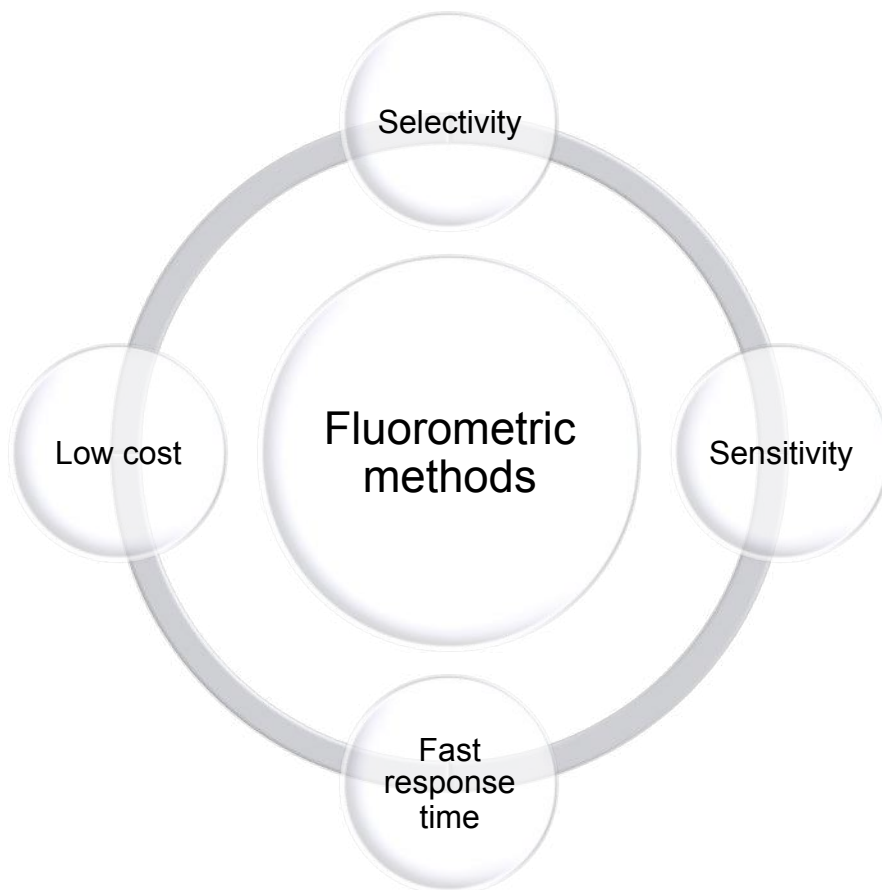
In 1989, World Health Organization (WHO) listed  $\text{Al}^{3+}$  to be one of the food pollution sources and limited  $\text{Al}^{3+}$  concentration to 200 mg/L (7.41  $\mu\text{M}$ ) in drinking water. Tolerable weekly aluminum dietary intake in the human body is estimated to be 7 mg/kg of the body weight.<sup>iii</sup>

Many studies show that aluminum is a neurotoxin. It is widely bioavailable to humans and has a direct and active access to the brain where it accumulates in a region-specific manner that highly implicates its involvement in the damage of the human nervous system and induce several health hazards<sup>iv</sup> such Alzheimer's disease,<sup>v</sup> Parkinson's disease, amyotrophic lateral sclerosis,<sup>vi</sup> etc.

As a result of the close relationship between  $\text{Al}^{3+}$  and human health, the investigation of reliable detection methods for  $\text{Al}^{3+}$  becomes more and more important. To date, some conventional methods with high sensitivity for

Al<sup>3+</sup> detection based on atomic absorption or emission spectroscopy have been developed. However, these methods require expensive instruments and intricate sample preparation processes. It is necessary to find other ways to design new chemosensors for Al<sup>3+</sup>, and fluorometric and colorimetric methods appear to be a favorable alternative for their simplicity and selectivity.<sup>vii</sup>

Fluorescent techniques are attractive and versatile tools for both analytical sensing and optical imaging because of their nondestructive methodology, high sensitivity, fast response time, technical simplicity and wide range of available indicator dyes (**Scheme 2**).<sup>viii,ix</sup> Recently, fluorescent probes have had significant interest because of their potential applications in medicinal and environmental research. Thus, many fluorescent chemosensors specific for Hg<sup>2+</sup>, Cu<sup>2+</sup>, Zn<sup>2+</sup> or other transition metals have been developed.<sup>x</sup> Compared to these transition metal ions, only a few fluorescent chemosensors have been reported for detection of Al<sup>3+</sup>.<sup>xi</sup> Jang *et al.* synthesized a colorimetric fluorescent chemosensor based on Schiff bases, useful in the detection of Al<sup>3+</sup> and Cu<sup>2+</sup>.<sup>xii</sup>



**Scheme 2.** Advantages of fluorometric methods.

Metal complexes of Schiff base ligands have showed several properties like selective extraction,<sup>xiii</sup> antitumor activity,<sup>xiv</sup> antioxidative activity,<sup>xv</sup> and attractive electronic and photo physical properties.<sup>xvi</sup> In addition, Schiff base derivatives having a fluorescent moiety are appealing tools for designing optical probes for metal ions.<sup>xvii</sup> The poor coordination ability of  $\text{Al}^{3+}$  compared to the transition metal ions<sup>xviii</sup> makes the development of an  $\text{Al}^{3+}$  fluorosensor difficult. Most of the reported  $\text{Al}^{3+}$  sensors suffer from interference caused by  $\text{Fe}^{3+}$  and  $\text{Cu}^{2+}$ ,<sup>xix</sup> poor water solubility and tedious synthetic methods of preparation.<sup>xx</sup> So

far, it has not been considered the biocompatible molecular design using biological fragments.

Recently, we have reported a series of eight new luminescent organotin compounds derived from Schiff bases and their application on fluorescent bioimaging where at least three complexes showed stain cell.<sup>xxi</sup> Based on the above, we propose in this project the synthesis, chemical and optical characterization, and determination of biological activity for sensing  $Al^{3+}$  of four new compounds derived from Schiff base (**Figure 1**), using a naphthalene moiety as fluorophore and an organic molecule or biological fragment to improve the solubility and increase biocompatibility.

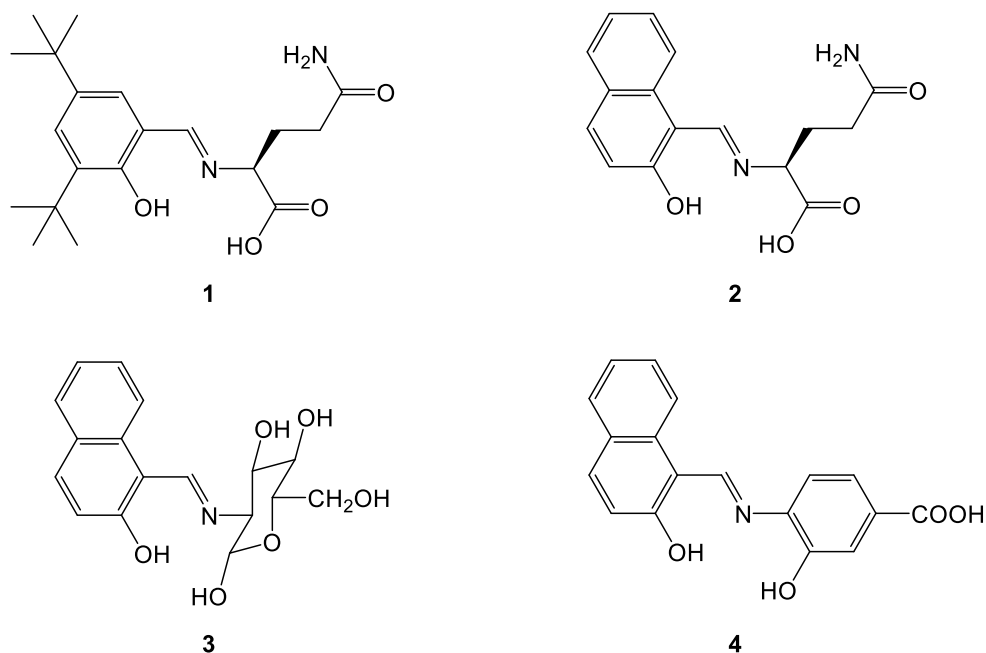


**Figure 1.** New compounds derived from Schiff base proposed.

## **2.BACKGROUND**

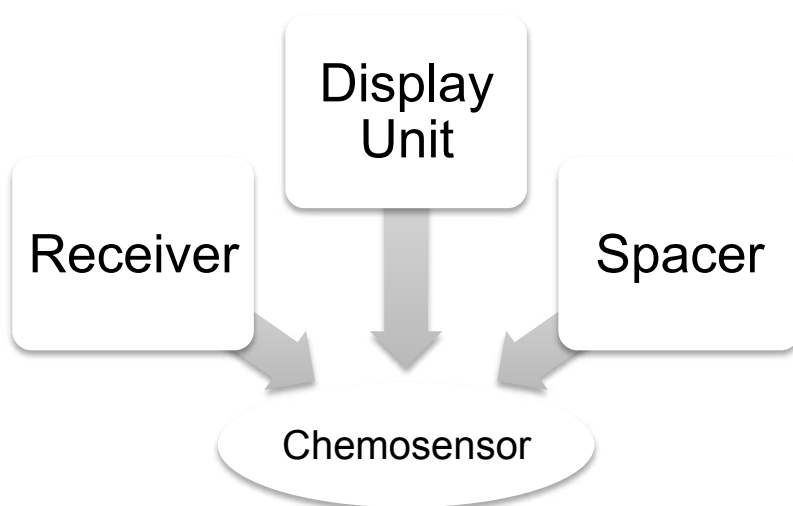
### **2.1 Luminescent Probes**

One of the main challenges currently facing in the area of supramolecular chemistry is the development of molecular systems capable of binding to specific substrates with high selectivity and specificity. This selective bonding process selective between a receiver and a substrate it is called molecular recognition and is the foundation of functioning of most biologic processes.<sup>xxii</sup>

There are numerous experimental methods for the detection of analytes, such as atomic absorption spectrometry, chromatography, etc. These techniques are expensive and generally difficult to continuous monitoring. In contrast, fluorescence-based methods offer distinct advantages in selectivity, sensitivity, real-time response and low cost.<sup>xxiii</sup> On the other hand, one of the research lines in supramolecular chemistry focuses on the design and synthesis of molecular receptors capable of selectively binding to an analyte of interest (molecule, cation or anion), based on suitable chemical and structural characteristics. The selection of receptor molecules with the capability of indicating its link with the substrate by transmitting a signal type has led to the obtaining of so-called molecular optical sensors or chemosensors.



There are two basic processes in analyte detection: molecular recognition and signal transduction. To efficiently carry out these two processes, chemosensory usually consist of three components: a receiver (to bind to a specific analyte), a display unit (charged with giving the answer) and a spacer (which changes the geometry electronic system modulates the interaction between the two units (**Scheme 3**).<sup>xxiv</sup> Due to its properties, chemosensory offer interesting and attractive potential applications in the field of analytical; in fact, they allow us to carry out measurements in real time and space when used immobilized on surfaces or even free in solution.<sup>xxv</sup>



**Scheme 3.** Components of a chemosensor.

Nowadays, researchers are in enthusiastic pursuit of fluorescent sensors due to their widespread applications in clinical diagnostics, environmental

monitoring, etc. Driven by the increasing demand for simple fluorescent sensors with fast response, and high sensitivity and selectivity, over the past decade, there has been significant interest in developing materials that allow not only the detection of different targets but also their imaging within living cells.

## 2.2 Luminescent probes for metal cations

The detection of metal cations is of great importance in different areas such as chemistry, biology, clinical biochemistry and environmental. Sodium, potassium, magnesium and calcium ions are involved in important biological processes as are the transmission of nerve impulses, muscle contraction, regulation of cell activity, etc. Zinc, on the other hand, is an essential component of many enzymes (e.g., carbonic anhydrase) and plays an important role in enzyme regulation, gene expression, neurotransmission, etc.<sup>xxvi</sup>

With respect to the toxicity of many metal ions it is well known that mercury, lead and cadmium are toxic for the organism and its early detection in the environment is of great importance.<sup>xxvii</sup> Likewise, it has been reported that aluminum accumulation in the organism may contribute to the appearance of certain neurodegenerative diseases. Because of the above, it is important to have efficient and practical detection methods for some metal cations.

It has been reported some useful molecules capable to sensing important metal cations, Fabbrizzi *et al.*<sup>xxviii</sup> showed that dioxotetramine **A (Figure 2)**, which contains an anthracene unit, is a good sensor for Ni<sup>2+</sup> and Cu<sup>2+</sup> ions.

Compound **B** reported by Ma *et al.*<sup>xxx</sup> showed high sensitivity and a dual response towards  $\text{Pb}^{2+}$  ions in a solvent mixture of water/DMSO. Dong *et al.*<sup>xxx</sup> reported the fluorescent probe **C** based on a naphthalimide and alkyne acting with radiometric response to  $\text{Hg}^{2+}$  and  $\text{Au}^{3+}$  ions in aqueous solution.

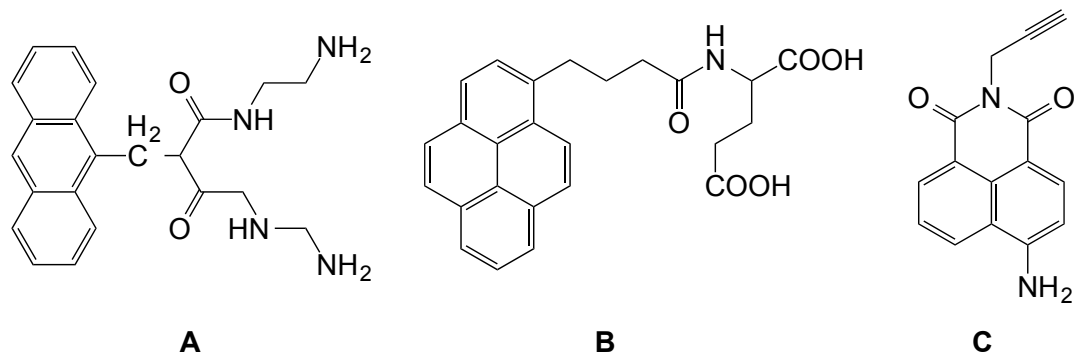


**Figure 2.** Structure for some fluorescent chemosensors for metal ions.

### 2.3 Aluminum sensors

Aluminum is the third most prevalent element and the most abundant metal in the earth's crust. But evidences suggest that aluminum has severe toxicity in the central nervous system, which can cause idiopathic Parkinson's disease, impairment of memory and Alzheimer's disease.<sup>xxxi</sup> Aluminum is found in its ionic form in most animal and plant tissues as well as in natural waters. Main sources of  $\text{Al}^{3+}$  to accumulate on human beings are food additives, aluminum-based pharmaceuticals, cosmetics, occupational dusts, aluminum containers and cooking utensils.<sup>xxxii</sup>

Due to the potential impact of  $\text{Al}^{3+}$  ions on human health and the environment, highly selective and sensitive chemosensors for  $\text{Al}^{3+}$  are hence highly demanded. Consequently, it is a challenging work to design and synthesize a highly selective and sensitive chemosensor for  $\text{Al}^{3+}$  in acid aqueous medium. Known methods for aluminum detection, such as graphite furnace atomic absorption spectrometry and inductively coupled plasma atomic emission spectrometry, are generally expensive and time-consuming in practice. Comparatively, optical detection, particularly fluorescence methods, shows unique potential for high sensitivity. Compared to transition metals, the detection of  $\text{Al}^{3+}$  has always been problematic due to the lack of spectroscopic characteristics and poor coordination ability. To the best of our knowledge, only a few fluorescent chemosensors have been reported for detection of  $\text{Al}^{3+}$  with moderate success to date. Thus, it is still highly desirable to develop new or improved methods for the selective evaluation of  $\text{Al}^{3+}$  ions in aqueous environments.<sup>xxxiii</sup>

Have been reported aluminum sensors based on polymer derivatives,<sup>xxxiv</sup> pyrimidine,<sup>xxxv</sup> coumarin derivatives<sup>xxxvi</sup> and Schiff bases,<sup>xxxvii</sup> these molecules demonstrate a new cost-effective, rapid, and simple key to the inspection of  $\text{Al}^{3+}$  ions in water samples in the presence of a complex matrix.

## **2.4 Schiff bases and naphthalene derivatives**

Lately new compounds with biological activity have been developed from Schiff bases. These molecules possess the azomethine fragment (-N = CH), which is the key to the design of new compounds with anticonvulsant, antidepressant, analgesic, anti-inflammatory and anti-malarial activity.<sup>xxxviii</sup> Their analysis has been a pattern to develop new Schiff bases compounds with diverse biological activity. It has been described the synthesis of complexes derivatives of Schiff bases that have high thermal stability to air and moisture. The investigations of Schiff bases compounds with other application like chemosensors are currently ongoing.

In addition, naphthalene moiety has been proved as an ideal fluorophore, and its correlative derivatives have been synthesized as effective fluorescent probe in determination of some metal ions.<sup>xxxix</sup> Recently, highly selective fluorescent probe for Al<sup>3+</sup> using naphthalene derivate has been reported;<sup>xl</sup> they exhibited high signal response toward and showed good application prospect, but all the fluorescent sensors need organics solvent to enhance the dissolving property of the sensors during the process of measuring.

### 3. HYPOTHESIS

Schiff bases compounds have a good aluminum sensing capability in cell culture.

#### **4. GENERAL OBJECTIVE**

Synthesize and characterize four new Schiff bases compounds and test its aluminum sensing capability in cell culture.

##### **4.1 Specific Objectives**

- Synthesize four new Schiff bases compounds by a conventional method.
- Spectroscopic ( $^1\text{H}$  and  $^{13}\text{C}$  NMR; IR) and optical (UV-vis, fluorescence) characterization of synthesized compounds.
- Measure the fluorescence spectra of the four new compounds with aluminum and other metals.
- Perform imaging detection assays of aluminum in cell culture.

#### **5. MATERIALS AND METHODS**

## **5.1 Materials**

### **5.1.1 Synthesis and characterization**

All starting materials were purchased from Sigma-Aldrich Chemical Company. Solvents were used without further purification. Melting points were determined on an Electrothermal Mel-Temp apparatus, and are not corrected. Infrared spectra were recorded using a Burker Tensor 27-FT-IR spectrophotometer equipped with a Pike Miracle™ ATR accessory with a single reflection ZnSe ATR crystal. Multinuclear magnetic resonance experiments as <sup>1</sup>H, and <sup>13</sup>C NMR spectra were recorded on a Bruker advance DPX 400. Chemical shifts (ppm) are relative to (CH<sub>3</sub>)<sub>4</sub>Si for <sup>1</sup>H and <sup>13</sup>C. Mass spectra were recorded on an AB Sciex API 2000™ LC/MS/MS System. UV-Vis absorption spectra were measured on a Shimadzu 2401 PC spectrophotometer. The emission spectra have been recorded with a Fluorolog 3 spectrofluorometer, by exciting 10 nm below the longer wavelength absorption band.

### **5.1.2 Bioassays**

Human epithelial cells Hs27 (ATCC-CRL-1634) were employed to obtain the cell images and to test the cytotoxic effects of compounds **1** to **4**. Hs27 cells were maintained in Dulbecco's Modified Eagle Media (DMEM, Invitrogen Life

Technologies) with 4 mM L-glutamine and supplemented with 10% fetal bovine serum (Gibco Life Technologies), 100 IU/mL of penicillin, and 100 g/mL of streptomycin. Culture of cell line was carried out at 37 °C in an incubator with 95% air and 5% CO<sub>2</sub> atmosphere.

Equipment:

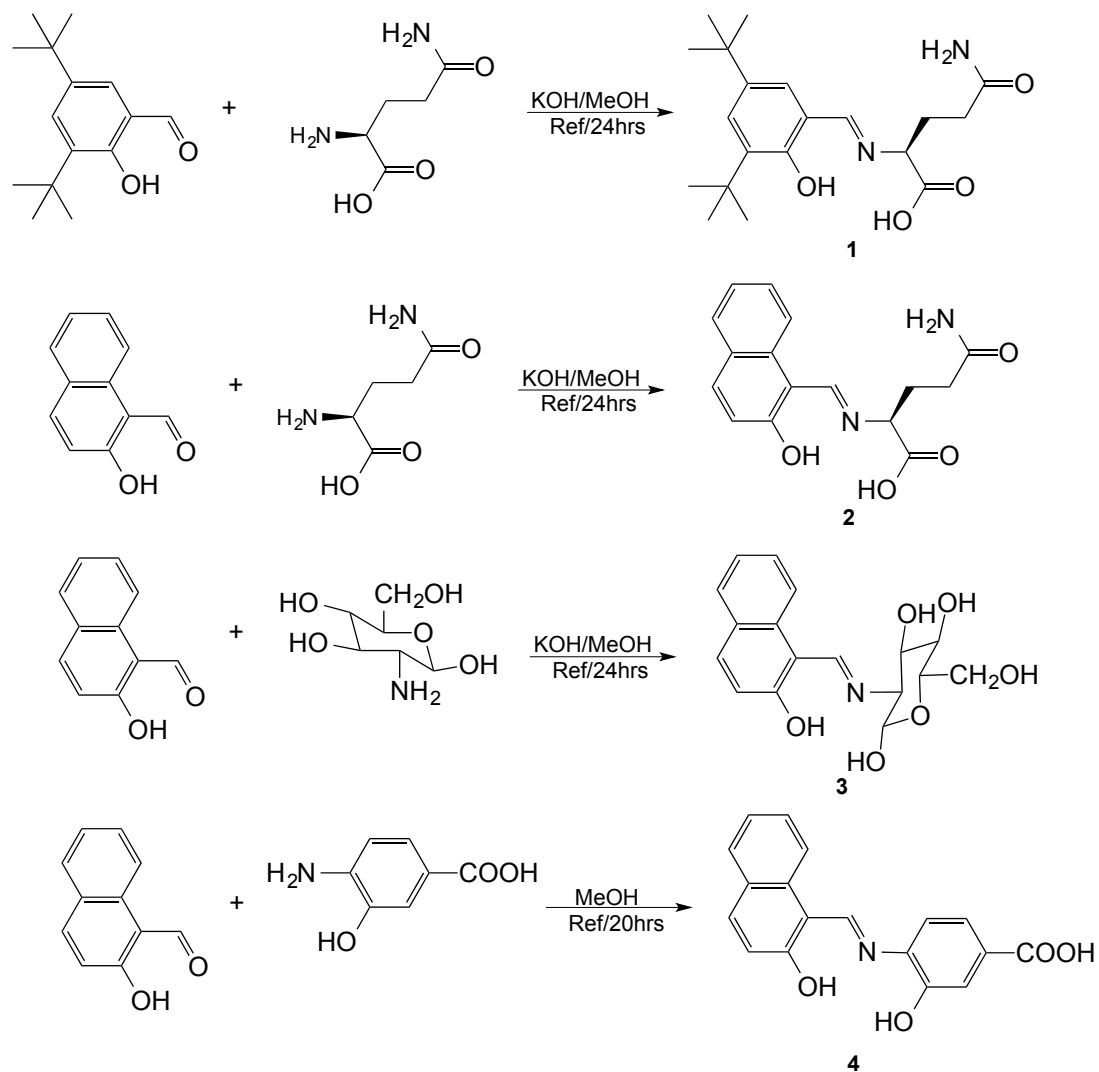
- Incubator for cell culture.
- Bell laminar flow biosafety Nuair A-425-400 model.
- Confocal laser microscopy (Olympus BX61WI).

## 5.2 Methods

### 5.2.1 Synthesis procedure of compounds 1-4.

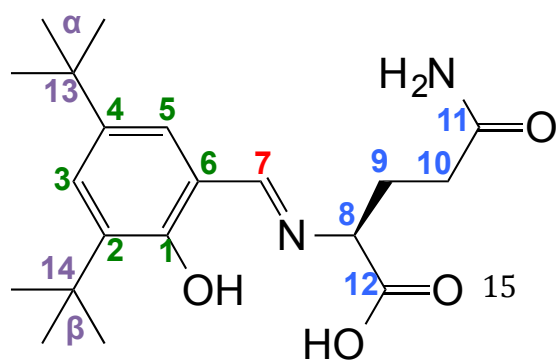
Compounds **1-4 (Scheme 4)** were synthesized by adding a methanolic solution of 3,5-di-*tert*-butyl-2-hydroxybenzaldehyde to the equimolar methanolic solution of L-glutamine in presence of KOH for compound **1**, and by adding a methanolic solution of 2-hydroxynaphthaldehyde to the equimolar methanolic solution of L-glutamine for compound **2**, L-glucosamine for compound **3**, and 4-amino-3-hydroxybenzoic acid for compound **4**, in presence of KOH, following by boiling under reflux for 24 hours and using a Dean-Stark trap to promote dehydration.





**Scheme 4.** Synthesis of the four new compounds derived from Schiff base.

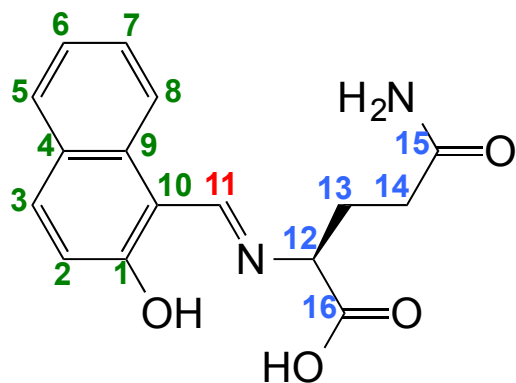
**5.2.1.1** (*S,E*)-11-amino-8-((2,4-di-*tert*-butyl-1-hydroxybenzylidene) amino)-11-oxopentanoic acid. (**1**)



A solution of 3,5-di-*tert*-butyl-2-hydroxybenzaldehyde

(0.23 g, 1 mmol) and L-glutamine (0.14 g, 1 mmol) in methanol was heated to reflux for 24 hrs in a Dean-Stark trap for the azeotropic removal of water, and allowed to cool to room temperature. All volatiles were removed under vacuum. Yield: 56%. Yellow solid. MP: 176 °C <sup>1</sup>H-NMR (400.13 MHz, CD<sub>3</sub>OD, 298 K) δ: 1.28 (s, 9H, CH<sub>3</sub>-α), 1.38 (s, 9H, CH<sub>3</sub>-β), 2.23 (m, 2H, <sup>3</sup>J=4.48 Hz, H-9), 2.25(m, 2H, <sup>3</sup>J=3.6, H-10), 3.38 (m, 1H, <sup>3</sup>J=4.96, H-8), 7.15 (d, 1H, <sup>3</sup>J=2.44, H-5), 7.33 (d, 1H, <sup>3</sup>J=2.44, H-3), 8.3 (s, 1H, H-7). <sup>13</sup>C-NMR (100.61 MHz, CD<sub>3</sub>OD, 298 K) δ: 29.94 (C-β), 31.63 (C-9), 31.92 (C-α), 33.46 (C-10), 34.98 (C-13), 35.89 (C-14), 75.69 (C-8), 119.70 (C-6), 127.54 (C-5), 127.67 (C-3), 137.42 (C-2), 140.97 (C-4), 159.49 (C-1), 167.75 (C-7), 178.61 (C-11), 178.82 (C-12). COSY correlation [δ<sub>H</sub>/ δ<sub>H</sub>]: 7.15/7.33 (H-3/H-5), 2.23/2.25 (H-9/H-10), 2.23/3.38 (H-9/H-8). HETCOR correlation [δ<sub>H</sub>/ δ<sub>C</sub>]: 1.28/31.92 (H-α/C-α), 1.38/29.94 (H-β /C-β), 2.23/31.63 (H-9 /C-9), 2.25/33.46 (H-10 /C-10), 3.38/75.69 (H-8 /C-8), 7.15/127.54 (H-5 /C-5), 7.33/127.67 (H-3 /C-3), 8.3/167.75 (H-7 /C-7). IR-ATR ν<sub>max</sub> cm<sup>-1</sup>: 3180, 2950, 1680, 1600 (C=N), 1590, 1360, 780. UV/Vis: λ<sub>max</sub> (nm) = 423 (Acetonitrile/Water 1:1). TOF calc. for [(C<sub>20</sub>H<sub>31</sub>N<sub>2</sub>O<sub>4</sub>+H)<sup>+</sup>]: 363.227834; Found: 363.228060 (error = 0.225763 ppm).

**5.3.1.2** (*S,E*)-11-amino-8-(((1-hydroxynaphthalen-10-yl)methylene)amino)-11-oxopentanoic acid. (**2**)

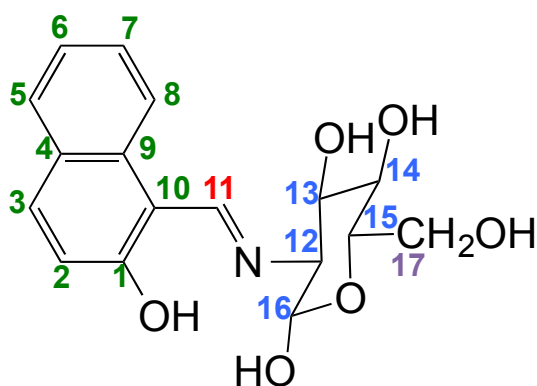


A solution of 2-hydroxynaphthaldehyde (0.17 g, 1 mmol) and L-glutamine (0.14 g, 1 mmol) in methanol was heated to reflux for 24 hrs in a Dean-Stark trap for the azeotropic removal of

water, and allowed to cool to room temperature. All volatiles were removed under vacuum. Yield: 86%. Yellow solid. MP: 180 °C.  $^1\text{H-NMR}$  (400.13 MHz,  $\text{CD}_3\text{OD}$ , 298 K)  $\delta$ : 2.29 (m, 2H,  $^3\text{J}=3.28$  Hz, H-13), 2.32 (m, 2H,  $^3\text{J}=5.04$  Hz, H-14), 4.25 (m, 1H,  $^3\text{J}=4.88$  Hz, H-12), 6.71 (d, 1H,  $^3\text{J}=9.36$  Hz, H-2), 7.15 (t, 1H,  $^3\text{J}=7.88$  Hz, H-6), 7.38 (t, 1H,  $^3\text{J}=7.04$  Hz, H-7), 7.53 (d, 1H,  $^3\text{J}=7.84$  Hz, H-5), 7.66 (d, 1H,  $^3\text{J}=9.36$  Hz, H-3), 7.96 (d, 1H,  $^3\text{J}=8.36$  Hz, H-8), 8.94 (s, 1H, H-11).  $^{13}\text{C-NMR}$  (100.61 MHz,  $\text{CD}_3\text{OD}$ , 298 K)  $\delta$ : 31.58 (C-13), 32.36 (C-14), 65.95 (C-12), 107.58 (C-10), 119.39 (C-8), 123.65 (C-6), 126.55 (C-2), 127.19 (C-4), 129.39 (C-7), 130.07 (C-5), 136.07 (C-9), 139.81 (C-3), 158.79 (C-11), 175.94 (C-16), 177.71 (C-15). COSY correlation [ $\delta_{\text{H}}/\delta_{\text{H}}$ ]: 2.29/2.32 (H-13/H-14), 2.29/4.25 (H-13/H-12), 6.71/7.66 (H-2/H-3), 7.15/7.53 (H-6/H-5), 7.15/7.38 (H-6/H-7), 7.38/7.96 (H-7/H-8). HETCOR correlation [ $\delta_{\text{H}}/\delta_{\text{C}}$ ]: 2.29/31.58 (H-13/C-13), 2.32/32.36 (H-14/C-14), 4.25/65.95 (H-12/C-12), 6.71/126.55 (H-2/C-2), 7.15/123.65 (H-6/C-6), 7.38/129.39 (H-7/C-7), 7.53/130.07 (H-5/C-5), 7.66/139.81 (H-3/C-3), 7.96/119.39 (H-8/C-8), 8.94/158.79 (H-11/C-11). IR-ATR  $\nu_{\text{max}}$   $\text{cm}^{-1}$ : 3375, 3010, 1670, 1630 (C=N), 1605, 1310, 740. UV/Vis:  $\lambda_{\text{max}}$  (nm)

= (400) 417 (Acetonitrile/Water 1:1). TOF calc. for  $[(C_{16}H_{17}N_2O_4+H)^+]$ : 301.118283; Found: 301.118528 (error = 0.244323 ppm).

**5.3.1.3** (16*S*,12*S*,13*S*,14*R*,15*S*)-15-(hydroxymethyl)-12-(((*E*)-(1-hydroxynaphthalen-10yl)methylene)amino)tetrahydro-2*H*-pyran-16,13,14-triol.**(3)**



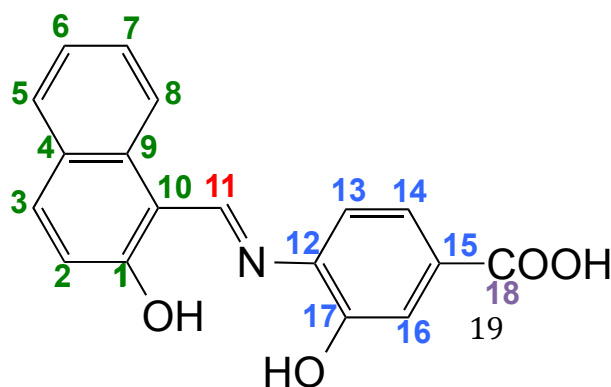
A solution of 2-hydroxynaphthaldehyde (0.17 g, 1 mmol) and D-glucosamine (0.18 g, 1 mmol) in methanol was heated to reflux for 24 hrs in a Dean-Stark trap for the azeotropic removal of water, and allowed to cool to room temperature. All volatiles were removed under vacuum. Yield: 96%. Yellow solid. MP: 202 °C.  $^1\text{H-NMR}$  (400.13 MHz,  $\text{CD}_3\text{OD}$ , 298 K)  $\delta$ : 3.41 (t, 1H,  $^3J=9.56$  Hz, H-14), 3.57 (dd, 1H,  $^3J=3.56, 10.08$  Hz, H-12), 3.78 (dd, 2H,  $^3J=4.96, 12.56$  Hz, H-17), 3.80 (t, 1H,  $^3J=10.76$  Hz, H-13), 3.88 (m, 1H, H-15), 5.32 (d, 1H,  $^3J=3.52$  Hz, H-16), 6.70 (d, 1H,  $^3J=9.40$  Hz, H-2), 7.17 (t, 1H,  $^3J=7.12$  Hz, H-6), 7.40 (t, 1H,  $^3J=7.12$  Hz, H-7), 7.55 (d, 1H,  $^3J=7.16$  Hz, H-5), 7.69 (d, 1H,  $^3J=9.40$  Hz, H-3), 7.95 (d, 1H,  $^3J=8.36$  Hz, H-8), 8.92 (s, 1H, H-11).  $^{13}\text{C-NMR}$  (100.61 MHz,  $\text{CD}_3\text{OD}$ , 298 K)  $\delta$ : 62.70 (C-17), 66.93 (C-12), 71.83 (C-14), 73.35 (C-13), 73.41 (C-15), 92.75 (C-16), 107.34 (C-10), 119.27 (C-8), 123.79 (C-6), 126.65 (C-2), 127.13 (C-4), 129.54 (C-7),

130.10 (C-5), 136.08 (C-9), 140.26 (C-3), 160.11 (C-11), 182.07 (C-1). COSY correlation [ $\delta_{\text{H}}/\delta_{\text{H}}$ ]: 3.41/3.80 (H-14/H-13), 3.41/3.88 (H-14/H-15), 3.57/3.80 (H-12/H-13), 3.57/5.32 (H-12/H-16), 3.78/3.88 (H-17/H-15), 6.70/7.69 (H-2/H-3), 7.17/7.40 (H-6/H-7), 7.17/7.55 (H-6/H-5), 7.40/7.95 (H-7/H-8). HETCOR correlation [ $\delta_{\text{H}}/\delta_{\text{C}}$ ]: 3.41/71.83 (H-14/C-14), 3.57/66.92 (H-12/C-12), 3.78/62.70 (H-17/C-17), 3.80/73.35 (H-13/C-13), 3.88/73.41 (H-15/C-15), 5.32/92.75 (H-16/C-16), 6.70/126.65 (H-2/C-2), 7.17/123.79 (H-6/C-6), 7.40/129.52 (H-7/C-7), 7.55/130.10 (H-5/C-5), 7.69/140.26 (H-3/C-3), 7.95/119.27 (H-8/C-8), 8.92/160.11 (H-11/C-11). IR-ATR  $\nu_{\text{max}}$   $\text{cm}^{-1}$ : 3265, 2920, 1605 (C=N), 1600, 1360, 1030, 780. UV/Vis:  $\lambda_{\text{max}}$  (nm) = (400) 417 (Acetonitrile/Water 1:1). TOF calc. for  $[(\text{C}_{17}\text{H}_{20}\text{NO}_6+\text{H})^+]$ : 334.128514; Found: 334.128649 (error = 0.134931 ppm).

### 5.3.1.4

(*E*)-17-hydroxy-12-(((1-hydroxynaphthalen-10-yl)methylene)amino)benzoic acid. (**4**)

(*E*)-17-hydroxy-12-(((1-hydroxynaphthalen-10-yl)methylene)amino)benzoic acid. (**4**)



A solution of 2-hydroxynaphthaldehyde (0.17 g, 1 mmol) and 4-

amino-3-hydroxybenzoic acid (0.15 g, 1 mmol) in methanol was heated to reflux for 20 hrs in a Dean-Stark trap for the azeotropic removal of water, and allowed to cool to room temperature. All volatiles were removed under vacuum. Yield: 92%. Yellow solid. MP: 312 °C. <sup>1</sup>H-NMR (400.13 MHz, (CD<sub>3</sub>)<sub>2</sub>SO, 298 K) δ: 6.74 (d, 1H, <sup>3</sup>J=9.4 Hz, H-2), 7.28 (t, 1H, <sup>3</sup>J=7.56 Hz, H-6), 7.49 (t, 1H, <sup>3</sup>J=7.04 Hz, H-7), 7.51 (dd, 1H, <sup>3</sup>J=8.44/1.76 Hz, H-14), 7.56 (d, 1H, <sup>3</sup>J=2.12 Hz, H-16), 7.66 (d, 1H, <sup>3</sup>J=8.56 Hz, H-5), 7.80 (d, 1H, <sup>3</sup>J=9.44 Hz, H-3), 8.04 (d, 1H, <sup>3</sup>J=8.52 Hz, H-13), 8.38 (d, 1H, <sup>3</sup>J=8.4 Hz, H-8), 9.49 (s, 1H, H-11), 10.80 (s, 1H, H-18). <sup>13</sup>C-NMR (100.61 MHz, (CD<sub>3</sub>)<sub>2</sub>SO, 298 K) δ: 108.25 (C-10), 116.42 (C-16), 116.96 (C-8), 120.02 (C-13), 121.25 (C-14), 123.54 (C-6), 125.31 (C-2), 126.06 (C-4), 128.17 (C-15), 128.36 (C-7), 129.13 (C-5), 132.45 (C-12), 133.87 (C-9), 138.55 (C-3), 147.85 (C-17), 149.11 (C-11), 166.92 (C-18), 179.02 (C-1). COSY correlation [δ<sub>H</sub>/ δ<sub>H</sub>]: 6.74/7.80 (H-2/H-3), 7.28/7.49 (H-6/H-7), 7.28/7.66 (H-6/H-5), 7.49/8.38 (H-7/H-8), 7.51/8.04 (H-14/H-13). HETCOR correlation [δ<sub>H</sub>/ δ<sub>C</sub>]: 6.74/125.31 (H-2/C-2), 7.28/123.54 (H-6/C-6), 7.49/128.36 (H-7/C-7), 7.51/121.25 (H-14/C-14), 7.56/116.42 (H-16/C-16), 7.66/129.13 (H-5/C-5), 7.80/138.55 (H-3/C-3), 8.04/120.02 (H-13/C-13), 8.38/116.96 (H-8/C-8), 9.49/149.11 (H-11/C-11). IR-ATR ν<sub>max</sub> cm<sup>-1</sup>: 3000, 1685, 1620 (C=N), 1600, 1300, 1200, 740. UV/Vis: λ<sub>max</sub> (nm) = (451) 474 (Acetonitrile/Water 1:1). TOF calc. for [(C<sub>18</sub>H<sub>14</sub>NO<sub>4</sub>+H)<sup>+</sup>]: 308.091734; Found: 308.091166 (error = -0.568548 ppm).

## 5.2.2 Fluorescence Measurement

Stock solutions of various metal ions (50  $\mu\text{M}$ ) were prepared with ultrapure water, respectively. A stock solution of each compound (10  $\mu\text{M}$ ) was prepared with a mixture acetonitrile/DMSO (95:5). For a typical detection, each compound solution was mixed with the stock aqueous solution of one metal ion. After the incubation at room temperature for 30 min, the corresponding fluorescence spectrum was recorded.

### **5.2.3 Fluorescence Imaging of $\text{Al}^{3+}$ in Living Cells**

Human epithelial cells Hs27 (ATCC-CRL-1634) were seeded in 6-well plates at a density of  $1 \times 10^5$  cells per well in 2 mL of Dulbecco's Modified Eagle Media (DMEM, Invitrogen Life Technologies) supplemented with 10% fetal bovine serum (Gibco Life Technologies) 100 IU/mL of penicillin, and 100 g/mL of streptomycin. Cells were maintained at 37 °C in a controlled humid atmosphere of 5%  $\text{CO}_2$  and 95% air. Twenty-four hours later the medium was renewed and cells were loaded with  $\text{Al}^{3+}$  at concentrations of 100 and 50  $\mu\text{M}$  (37 °C for 60 min). After removal of free  $\text{Al}^{3+}$  by washing with media, cells were exposed to the compounds (20  $\mu\text{M}$ ) and incubated for 30 minutes, and finally washed with PBS. Untreated cells were used as controls. Fluorescence images were collected using a confocal laser microscopy (Olympus BX61WI).

### **5.3 Waste disposal**

The laboratory safety and disposal of the waste generated in this research project were done according to the Internal Rules and Safety of the Faculty of Chemical Sciences, UANL.

Both, chemical and biological waste that were used shall be placed in various containers; the remaining biological and physical reusable material were sterilized by moist heat.

## **6. RESULTS AND DISCUSSION**

### **6.1 Synthesis**

We carried out the synthesis of Schiff bases **1-4** (**Figure 3**) by condensation reaction of the appropriate benzaldehyde or naphthaldehyde with the corresponding amine (e. g. L-glutamine, L-glucosamine, or 4-amino-3-hydroxybenzoic acid) for 24 hours. The products were obtained after filtration of



the crude reaction and precipitation using hexane as yellow powders, and were isolated with yields from 56 to 97%. The low yields of L-glutamine compounds (56-86%) could be attributed to the partial solubility of the amino acid in methanol, only the fraction that solubilizes in methanol is the one that reacts, this values are consistent with previous reports of L-glutamine Schiff base complexes.<sup>xli</sup>

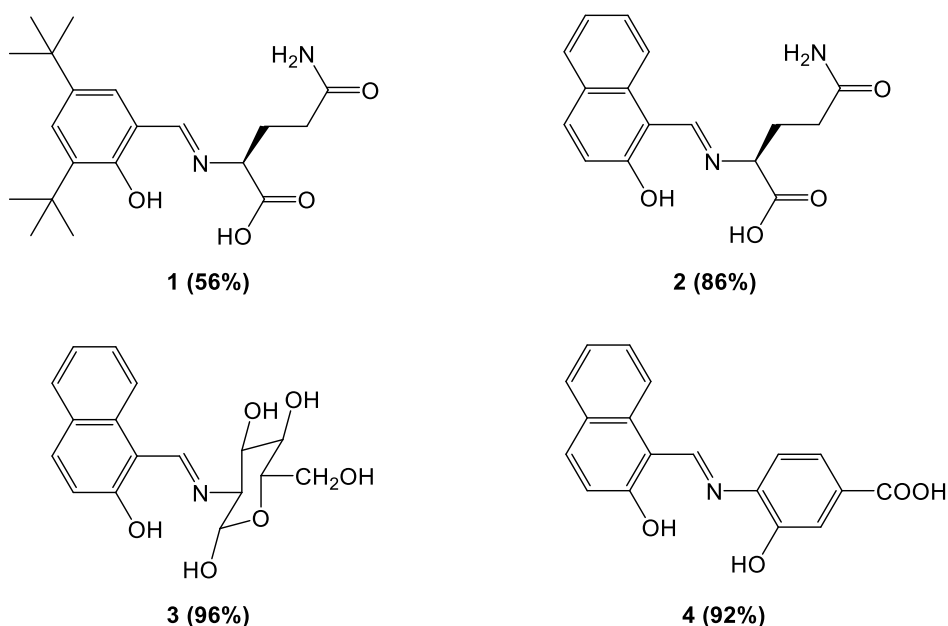


**Figure 3.** Schiff bases 1-4.

All compounds were completely soluble in DMSO, and partially soluble in organic solvents such as methanol and ethanol. The high solubility of the molecules in polar solvents, is due to the presence of functional groups like hydroxyl (-OH), carboxyl (-COOH) and amino (-NH<sub>2</sub>), that makes the molecules

more polar and presents more affinity for polar solvents like DMSO and water. This property is favorable to perform the biological assays.

## 6.2 Chemical structure elucidation

Schiff bases were characterized by UV-Vis, spectroscopic methods (IR, 1 and 2D-NMR) and mass spectrometry.

### 6.2.1 Absorption and emission analysis

The UV-Vis spectra of the compounds were obtained in mixture acetonitrile/ water (1:1). The structures of the four molecules presents  $n-\pi^*$  and  $\pi-\pi^*$  electronic transitions (**Figure 4**). In general all of the compounds exhibit a main peak in the visible, with maximum wavelength ranging between 342 and 474 nm, which can be attributed to the HOMO–LUMO electronic transitions.

The emission spectrum, showed wavelengths for compounds **1-4** between 433 to 505 nm (**Figure 5**), being the compound **4** the most red-shifted, attributed to the presence of the carboxylic acid substituent that produce an electro subtractor effect that causes the displacement a low frequency. The data are represented in **Table 1**.

**TABLE 1**  
Absorption and emission data of compounds **1-4**

Compound	Max. Absorption (nm)	Emission (nm)
1	342	465
2	(400) 417	433
3	(400) 417	433
4	(450) 474	505

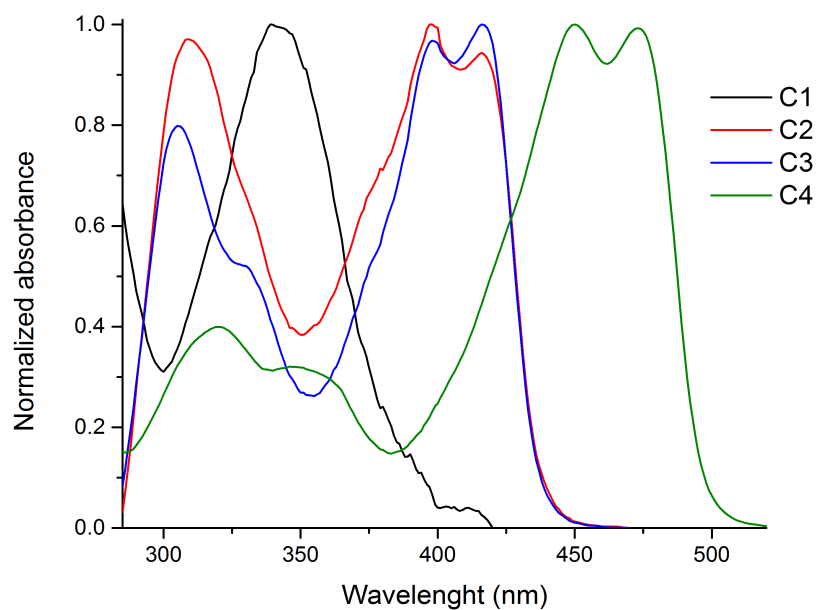


**Figure 4.** UV spectra of compounds **1-4** in acetonitrile/water (1:1).

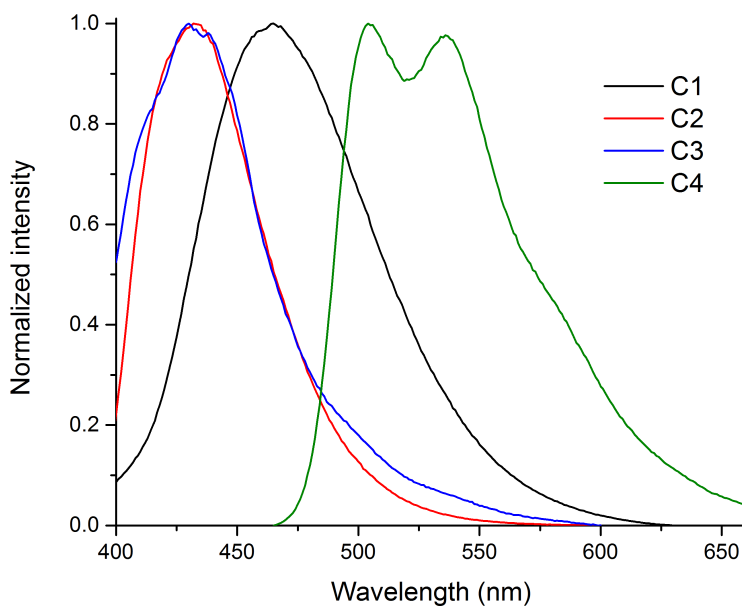


**Figure 5.** Emission spectra of compounds **1-4** in acetonitrile/water (1:1).

### 6.2.2 Analysis of NMR data

NMR spectroscopy is a reliable and powerful tool to obtain information about the structure,  $^1\text{H}$  and  $^{13}\text{C}$  analyses, collectively provide highly valuable information and hence are used for the characterization of compounds.

$^1\text{H}$ -NMR spectra confirmed the formation of Schiff bases **1-4** (see appendix), with signals for H-7 (compounds **1**) and H-11 (compounds **2, 3** and **4**) in the range of 8.30 to 9.49 ppm, (**Table 2**) typical from an imine proton according to the reports from Santillan et al.<sup>xlii</sup> In the  $^{13}\text{C}$  NMR spectra, the principal signals correspond to C-11/C-7 (C=N) between 149.11 to 167.75 ppm, C-1 (C-O) with shifts between 159.49 to 182.07 ppm, for compounds **1** to **3** C-8

(N-C) that appear between 65.95 to 75.69 ppm and for compound **4** C-12 that belongs to an aromatic system (N-C) in 132.45 ppm.

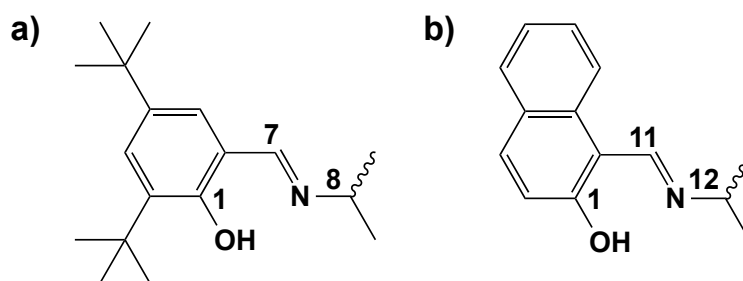


**Figure 6.** Numbering of a) compound **1**; b) compound **2**, **3** and **4**.

**TABLE 2**  
Selected  $^1\text{H}$  and  $^{13}\text{C}$  signals

	$^1\text{H}$		$^{13}\text{C}$	
	H11/H7	C11/C7	C1	C12/C8
<b>1</b>	8.30	167.75	159.49	75.69
<b>2</b>	8.94	158.79	181.07	65.95
<b>3</b>	8.92	160.11	182.07	66.93
<b>4</b>	9.49	149.11	179.02	132.45

### 6.2.3 Analysis of IR data

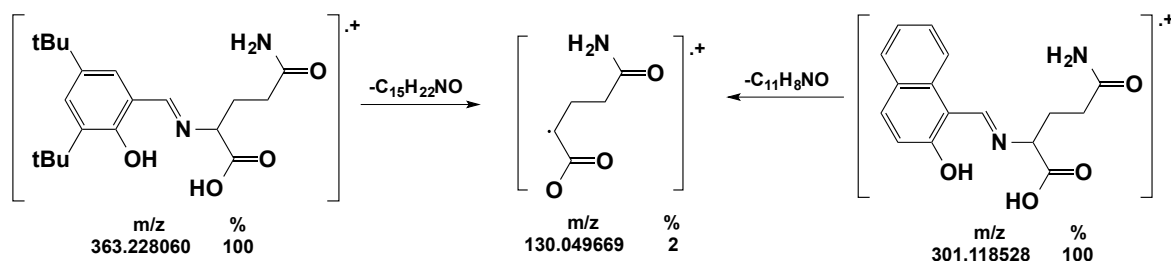
The IR spectral analysis showed the imine (C=N) stretching vibration bands for compounds **1-4** in 1600-1630  $\text{cm}^{-1}$ , previous reports showed a ligand derived from Schiff base with C=N band in 1618  $\text{cm}^{-1}$ .<sup>vii</sup> Spectra of compounds **1** and **2** displayed the characteristic signal of the aromatic groups, while compounds **3** and **4** presented the typical band of the O-H group. Principal values are listed in **Table 3**.

**TABLE 3**  
IR data of compounds **1-4**

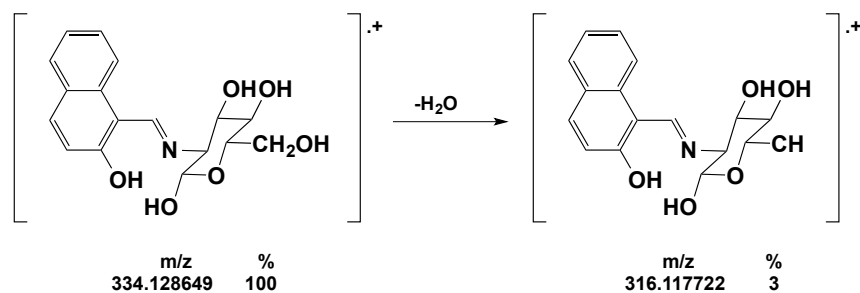
	<b>1</b>	<b>2</b>	<b>3</b>	<b>4</b>
<b>C-H arom.</b>	3180 $\text{cm}^{-1}$	3010 $\text{cm}^{-1}$	-	-
<b>C=N</b>	1600 $\text{cm}^{-1}$	1630 $\text{cm}^{-1}$	1600 $\text{cm}^{-1}$	1620 $\text{cm}^{-1}$
<b>C=O stre.</b>	1680 $\text{cm}^{-1}$	1670 $\text{cm}^{-1}$	-	1685 $\text{cm}^{-1}$
<b>O-H stre.</b>	-	-	3265 $\text{cm}^{-1}$	3000 $\text{cm}^{-1}$
<b>C-H arom. IP</b>	1360 $\text{cm}^{-1}$	1310 $\text{cm}^{-1}$	1200 $\text{cm}^{-1}$	1300 $\text{cm}^{-1}$
<b>C-H arom. OP</b>	780 $\text{cm}^{-1}$	740 $\text{cm}^{-1}$	760 $\text{cm}^{-1}$	740 $\text{cm}^{-1}$

#### 6.2.4 High resolution mass spectrometry analysis.

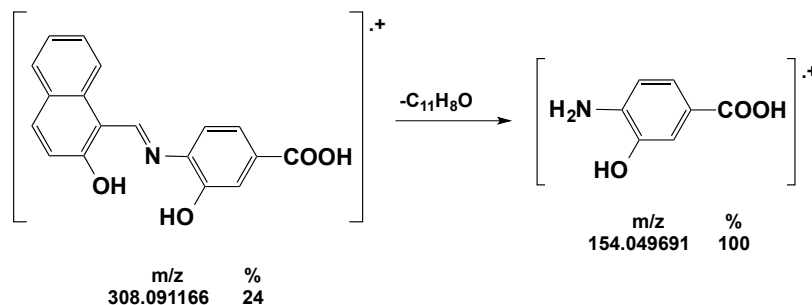
The mass spectra of the four molecules were obtained by the TOF method. The spectra of compounds **1**, **2** and **3** showed the peak base corresponds to the molecular ion peak and it is consistent with the theoretical molecular mass (errors: 0.621547 for compound **1**, 0.811386 for compound **2** and 0.403831 for compound **3**). (**Scheme 5** and **6**) while compound **4**, presents a base peak after loss of the naphthaldehyde fragment and the peak of the molecular ion represent the 24% compared to the peak base (error: -1.845385) (**Scheme 7**).



**Scheme 5.** Proposed fragmentation of compounds **1** and **2**.



**Scheme 6.** Proposed fragmentation of compound **3**.



**Scheme 7.** Proposed fragmentation of compound **4**.

### 6.3 Fluorescence Measurement.

#### 6.3.1 Aluminum sensing

The aluminum sensing behavior of the molecules was first measured. The emission spectrum of each compound was obtained as well as each compound in presence of  $\text{Al}^{3+}$  ions in a mixture acetonitrile/ $\text{H}_2\text{O}$  = 1:1 (see appendix). Both signals were compared as we can see in **figure 7** and we noticed that the emission signal is ten times higher when the metal is added for compounds **1-4**, evidencing the capacity of the four compounds to generate a signal in presence of this metal.



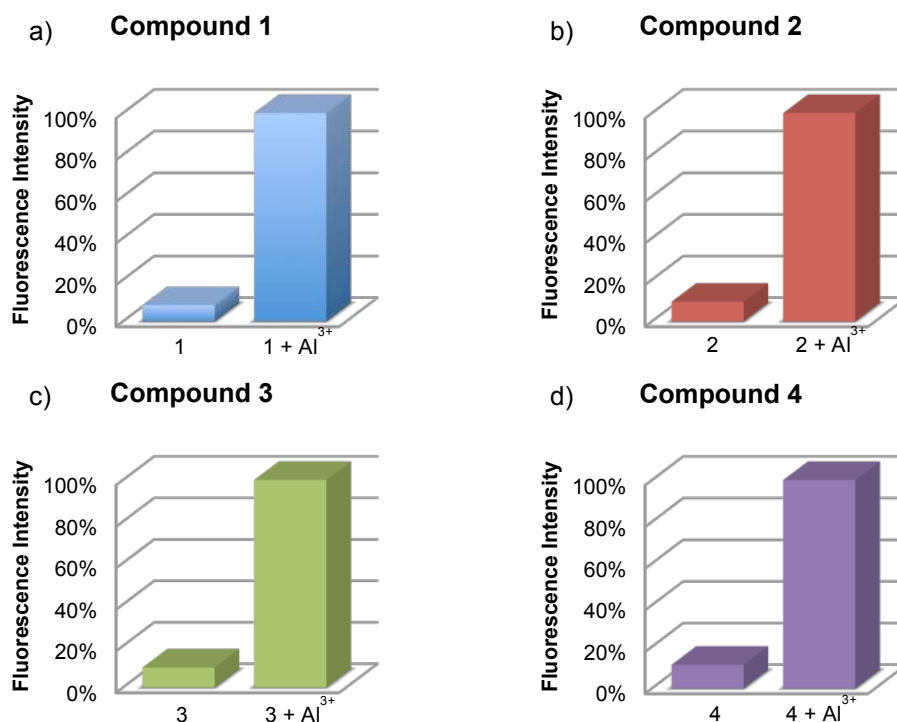


**Figure 7.** Graphic of the increment in the fluorescence intensity of a) Compound **1**, b) Compound **2**, c) Compound **3** and d) Compound **4**, in absence and presence of  $\text{Al}^{3+}$  ions.

### 6.3.2 Quantum yield determination

Quantum yield measurements were performed to the four compounds after and before the exposure of  $\text{Al}^{3+}$  in order to compare the fluorescence emission (**Figure 8**). Compounds **1** to **4** exhibited low fluorescence emission at 465, 433, 433 and 505 nm respectively with a small fluorescence quantum yield ( $\phi = 1.33 - 2.02\%$ ) upon excitation at 330 nm (compound **1**), 390 nm (compounds **2** and **3**) and 440nm (compound **4**). After the addition of  $\text{Al}^{3+}$  the fluorescence enhancement was evident ( $\phi = 2.24 - 64.91\%$ ). Compound **2** and **4** in presence of  $\text{Al}^{3+}$  were the molecules that showed better quantum yield, increasing from

2.02 to 34.02 (compound **2**) and 1.64 to 63.91 (compound **4**), an increment of 17 and 40 times respectively, as we can see in **table 4**.

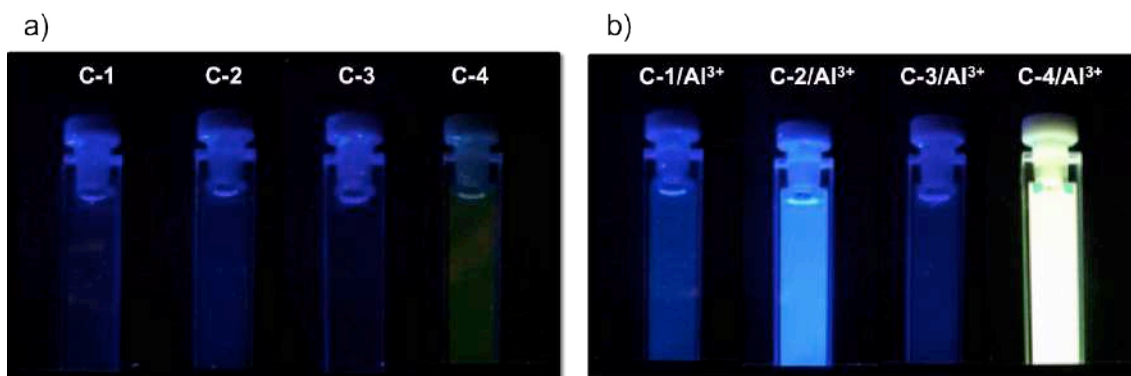


**Figure 8.** Photographs of a) Compounds **1 - 4** and b) compounds **1 - 4** in presence of Al<sup>3+</sup> ions (acetonitrile/H<sub>2</sub>O = 1:1) under UV lamp (365 nm).

**TABLE 4**  
Quantum yield values

	$\phi$ [%]		$\phi$ [%]
<b>C-1</b>	1.33	<b>C-1 / Al<sup>3+</sup></b>	14.04
<b>C-2</b>	2.02	<b>C-2 / Al<sup>3+</sup></b>	34.02
<b>C-3</b>	0.38	<b>C-3 / Al<sup>3+</sup></b>	2.24
<b>C-4</b>	1.64	<b>C-4 / Al<sup>3+</sup></b>	63.91

### 6.3.3 Selectivity studies

To determinate the selectivity of the compounds, 9 metal ions with different valences ( $\text{Fe}^{3+}$ ,  $\text{Zn}^{2+}$ ,  $\text{Cu}^{2+}$ ,  $\text{Cd}^{2+}$ ,  $\text{Pb}^{2+}$ ,  $\text{Ni}^{2+}$ ,  $\text{Co}^{2+}$ ,  $\text{Ag}^+$ ,  $\text{Hg}^{2+}$ ) was examined as the alternative of  $\text{Al}^{3+}$  for the incubation with the four complexes. The criterion used to select these metals was that we want to use these complexes for sensing in biological media, and we have to be sure that other common metals in this media will not interfere. The emission spectrum was obtained by exciting each compound 10 nm under the absorbance wavelength (**figure 9**). Photographs of the solutions of the experiment under UV lamp (365 nm) were taken (see appendix).

Compound **1** presented weak fluorescence emission by itself, and in presence of  $\text{Zn}^{2+}$  ions, the signal increased significantly, making evident its high affinity for this metal, followed by  $\text{Al}^{3+}$  ions with also considerable fluorescence emission (**figure 9a**). None of the other ions could turn on the fluorescence of this compound under the same conditions.

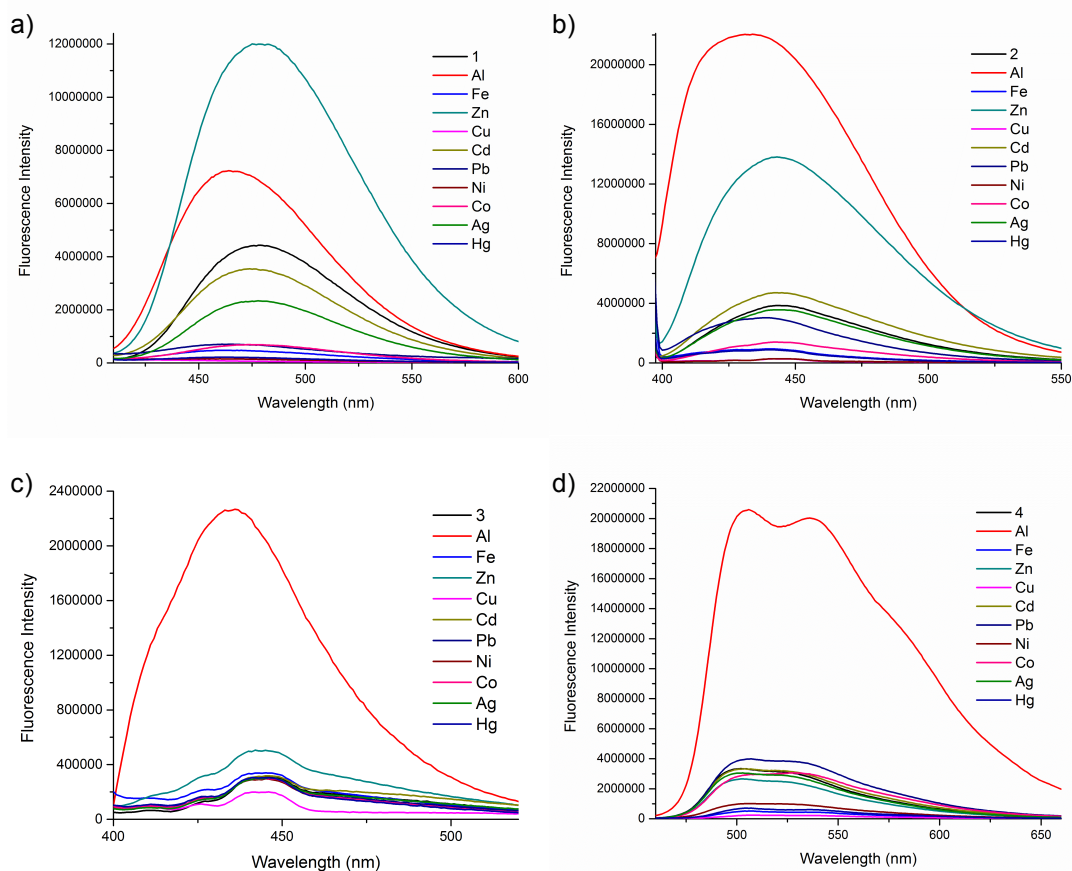


**Figure 9.** Fluorescence spectra of a) Compound **1**, b) Compound **2**, c) Compound **3** and d) Compound **4**, in presence of different metal ions (50  $\mu$ M), (acetonitrile/H<sub>2</sub>O = 1:1).

Compound **2** displayed a high emission peak when Al<sup>3+</sup> ions were present, (**figure 9b**) also, a lower signal is observed when this complex was in existence with Zn<sup>2+</sup> ions. If we compare the structure of compound **1** and **2**, we can observe that the difference is in the fluorophore moiety, so it seems like the naphthaldehyde fraction favors the aluminum sensing, as we will observe with the other molecules with this fraction as well.

Compound **3** and **4** exhibited a remarkable affinity by  $\text{Al}^{3+}$  ions, no other metal can show significant fluorescent emission, being this two complexes the most selective for sensing  $\text{Al}^{3+}$  ions (**figures 9c and d**).

#### 6.3.4 Fluorescent competitive experiments

In order to show the high selectivity of the compounds toward  $\text{Al}^{3+}$ , the fluorescent competitive studies of other metal ions were also investigated. We prepared solutions of each metal with  $\text{Al}^{3+}$ , in equivalent amounts, and then this solution was added to the solution of each complex.

The fluorescence intensities were recorded, respectively. As shown in **figure 10**, the fluorescence emission intensity of compounds **1**, **2**, **3** and **4** in presences of  $\text{Zn}^{2+}$ ,  $\text{Cd}^{2+}$ ,  $\text{Pb}^{2+}$ ,  $\text{Ni}^{2+}$ ,  $\text{Co}^{2+}$  and  $\text{Ag}^+$ , did not show significant variation by comparison with the fluorescence intensity of each compound with aluminum. By the other hand, when metals such  $\text{Fe}^{3+}$ ,  $\text{Cu}^{2+}$  and  $\text{Hg}^{2+}$  are present, the fluorescence is quenched about 45 to 90% compared with the fluorescence obtained only with  $\text{Al}^{3+}$ ; in spite of the low response, the signal can be detectable. This fluorescence quenching mechanism of the compounds may be attributed to the charge transfer effect. This effect may occur when the excited compound encounters metal ions that act as electron-accepting groups, the partial electrons will transfer to the metal cations. Therefore, the number of emitted electrons will decrease. As a result, the fluorescence is quenched.

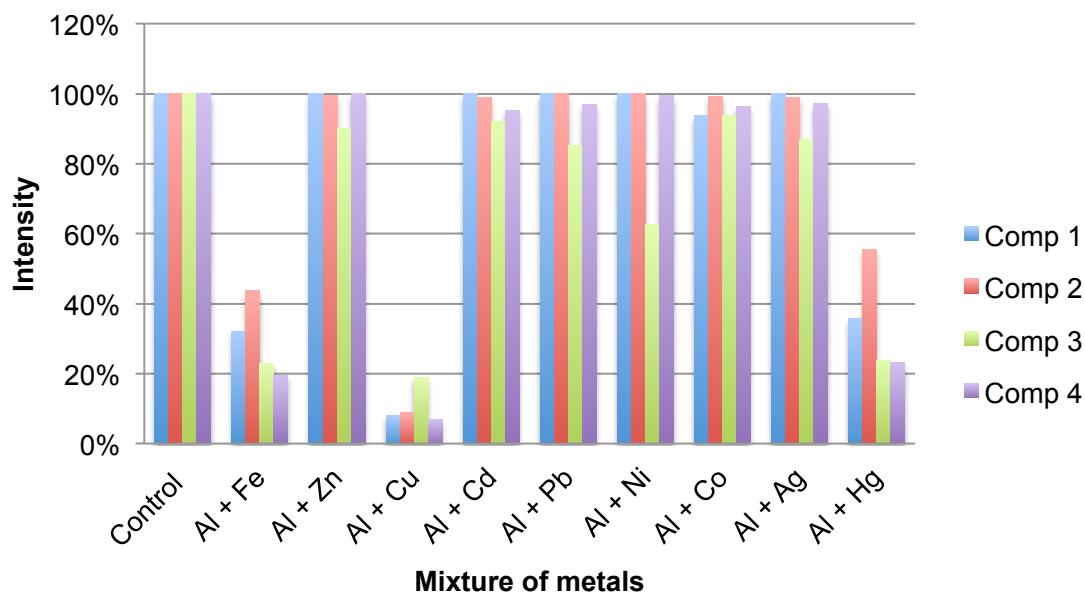


**Figure 10.** Graphic of the fluorescence intensity of compounds **1-4** (10  $\mu\text{M}$ ) upon addition of  $\text{Al}^{3+}$  (50  $\mu\text{M}$ ), in presence of various metal ions (50  $\mu\text{M}$ ). Compound **1** excited at 330 nm (blue bars), compound **2** excited at 390 nm (red bars), compound **3** excited at 390 nm (green bars) and compound **4** excited at 440 nm (purple bars).

### 6.3.5 Sensitive quantitation of $\text{Al}^{3+}$

The absorption titrations and fluorescence emission of compounds **1-4** towards  $\text{Al}^{3+}$  (concentration from 1.25 to 40  $\mu\text{M}$ ) were carried out in a mixture acetonitrile/water (1:1).

The fluorescence intensity of compounds **1-4** gradually increased with the progressive addition of  $\text{Al}^{3+}$  as we can see in **figures 11, 12, 13** and **14**. Upon

gradual addition of  $\text{Al}^{3+}$  to a solution of each compound, the absorption spectra showed changes in the intensity of the bands. **Figure 11** corresponds to the absorption graph for compound **1**, where we can appreciate an increasing in the absorption bands at 265 and 345 nm when  $\text{Al}^{3+}$  concentration get bigger in the solution. The UV-Vis spectrum of compound **2**, shows that while we increased the  $\text{Al}^{3+}$  concentration from 1.25 to 7.5  $\mu\text{M}$  the intensity of the band at 397 nm decreases, and after the addition of 10  $\mu\text{M}$  of  $\text{Al}^{3+}$ , this signal disappear and a new band at 370 nm appears, increasing its intensity as the concentration of the metal rises (**figure 12**). Absorption graphic of compound **3** (**figure 13**) displays that the band at 417nm decreases as the concentration of  $\text{Al}^{3+}$  increases and the spectrum of compound **4** (**figure 14**) shows the absorption band at 473 nm gradually decrease while the band at 310 nm is increasing as the concentration of  $\text{Al}^{3+}$  grow.

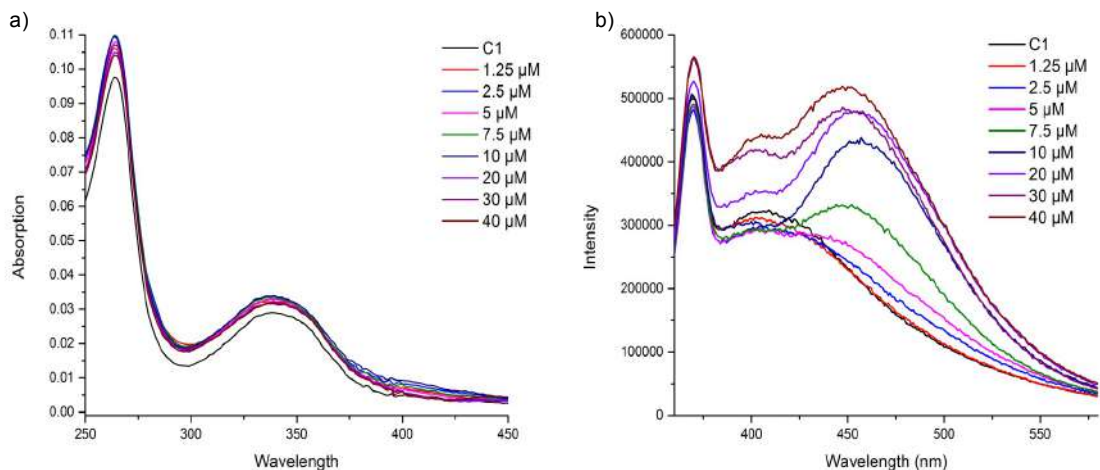


**Figure 11.** a) UV–Vis and b) fluorescence spectra (excited at 330 nm) of Compound 1 (10  $\mu\text{M}$ ) in presence of different concentrations of  $\text{Al}^{3+}$  (0–40  $\mu\text{M}$ ).

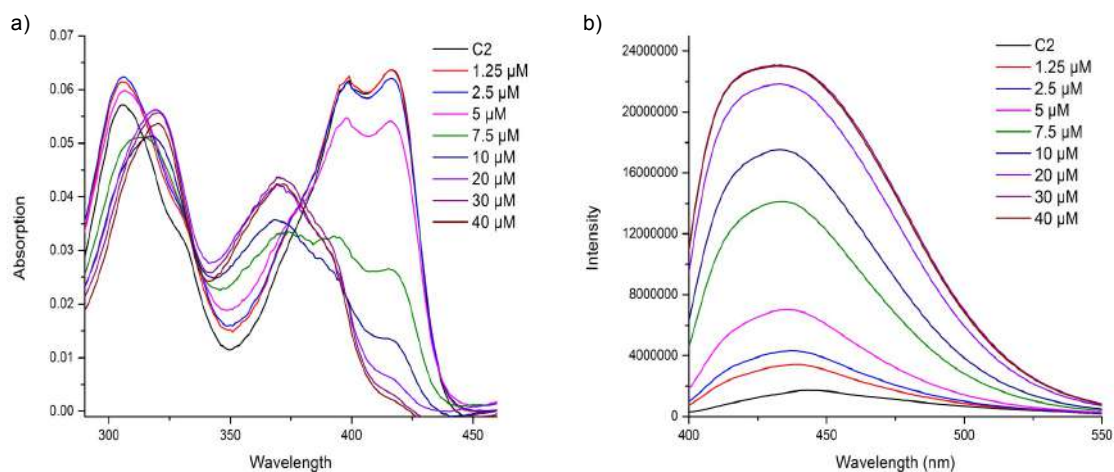


**Figure 12.** a) UV–Vis and b) fluorescence spectra (excited at 390 nm) of Compound 2 (10  $\mu\text{M}$ ) in presence of different concentrations of  $\text{Al}^{3+}$  (0–40  $\mu\text{M}$ ).

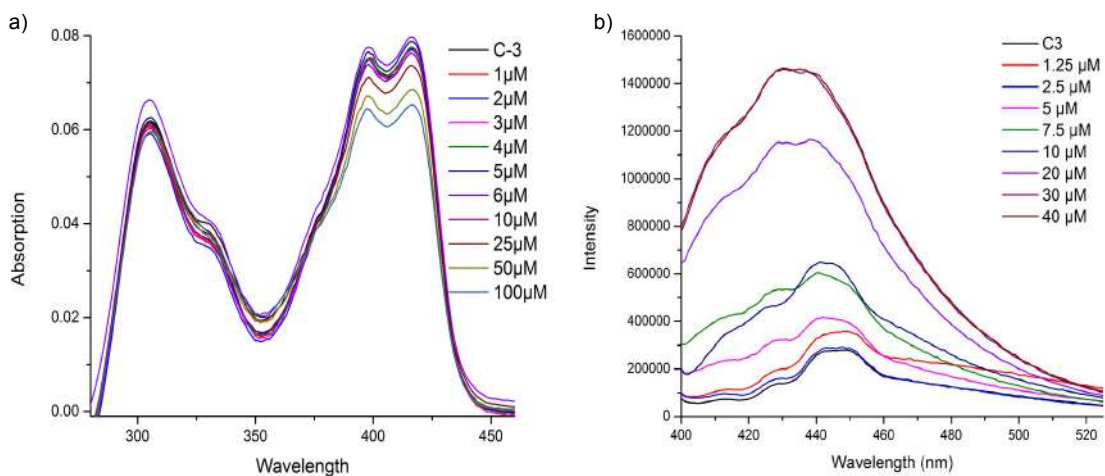




**Figure 13.** a) UV–Vis and b) fluorescence spectra (excited at 390 nm) of Compound **3** (10  $\mu\text{M}$ ) in presence of different concentrations of  $\text{Al}^{3+}$  (0–40  $\mu\text{M}$ ).

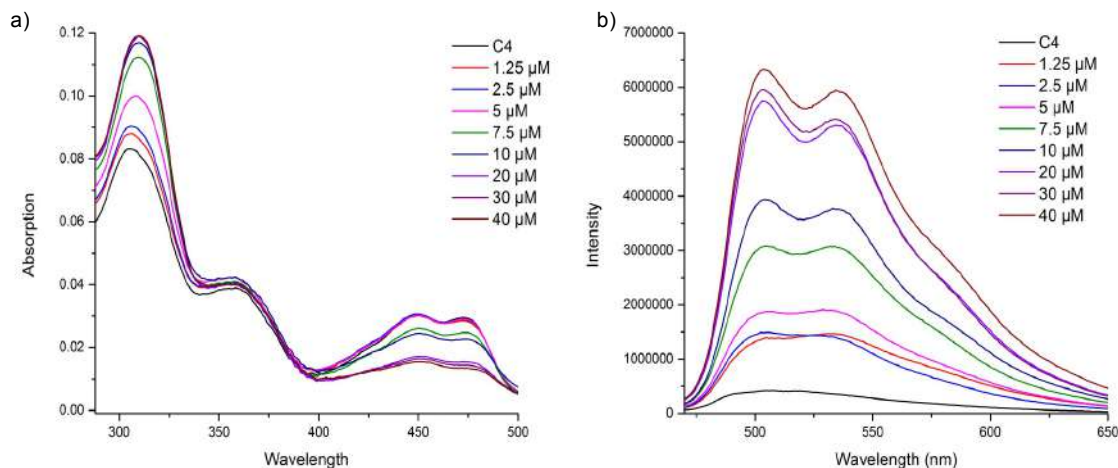


**Figure 14.** a) UV–Vis and b) fluorescence spectra (excited at 440 nm) of Compound **4** (10  $\mu\text{M}$ ) in presence of different concentrations of  $\text{Al}^{3+}$  (0–40  $\mu\text{M}$ ).

### 6.3.6 Detection limit

The detection limit (LOD) of each compound was calculated (**table 5**) according to the equation  $\text{DL} = 3\sigma/K$ , where  $\sigma$  is the standard deviation of the blank solution (measured 12 times) and  $K$  is the slope of the calibration curve from the fluorescence titration experiments (**figure 15**).

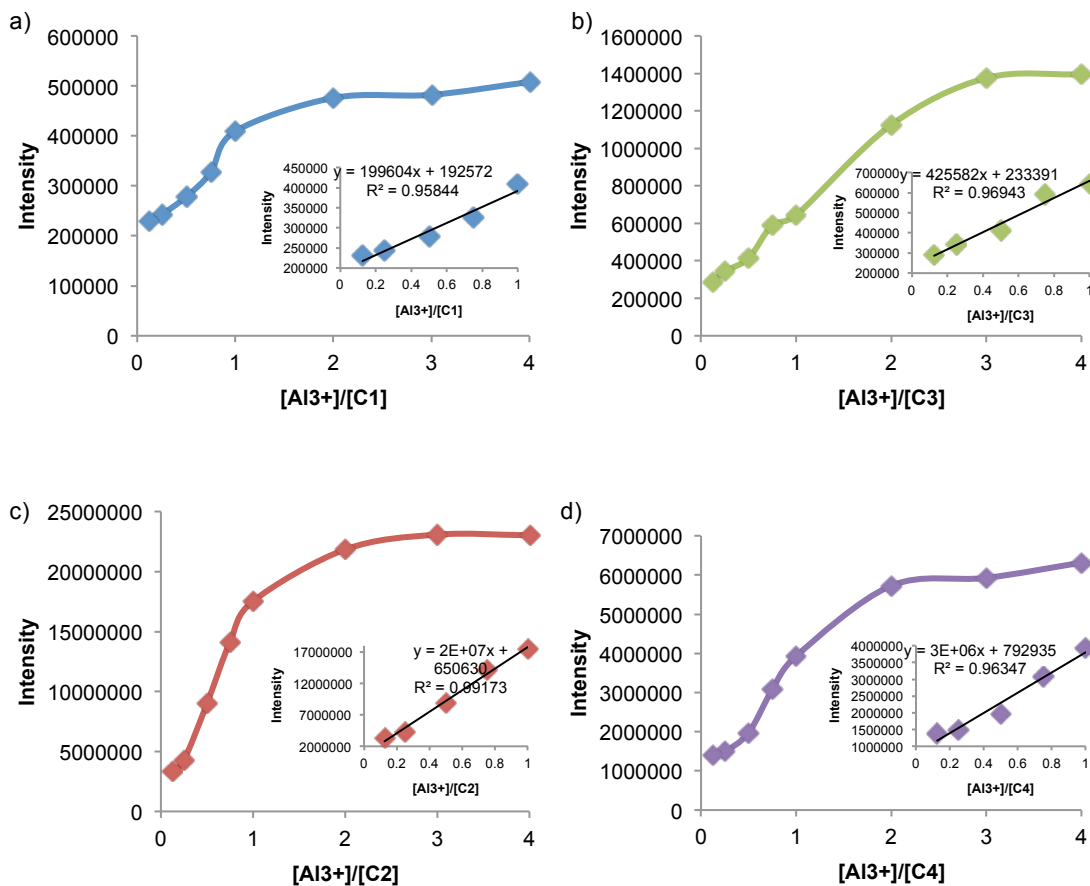


**Figure 15.** Changes of emission intensity of compounds **1-4** at a) 465 nm (Compound **1**); b) 433 nm (Compound **2**); c) 433 nm (Compound **3**) and c) 505 nm (Compound **4**).

All compounds exhibit a good detection limit from 0.09 to 1.02, which is below the WHO acceptable limit (0.05 mg/L or 1.85  $\mu\text{M}$  of  $\text{Al}^{3+}$ ) in drinking water. Compounds **2**, **3** and **4** displays a LOD lower than previous molecules derived from Schiff bases reported (**figure 16**).<sup>xliii, xliiv</sup>

**TABLE 5**  
LOD data of compounds **1-4**

Compound	LOD ( $\mu\text{M}$ )
<b>1</b>	1.022
<b>2</b>	0.103
<b>3</b>	0.317
<b>4</b>	0.091

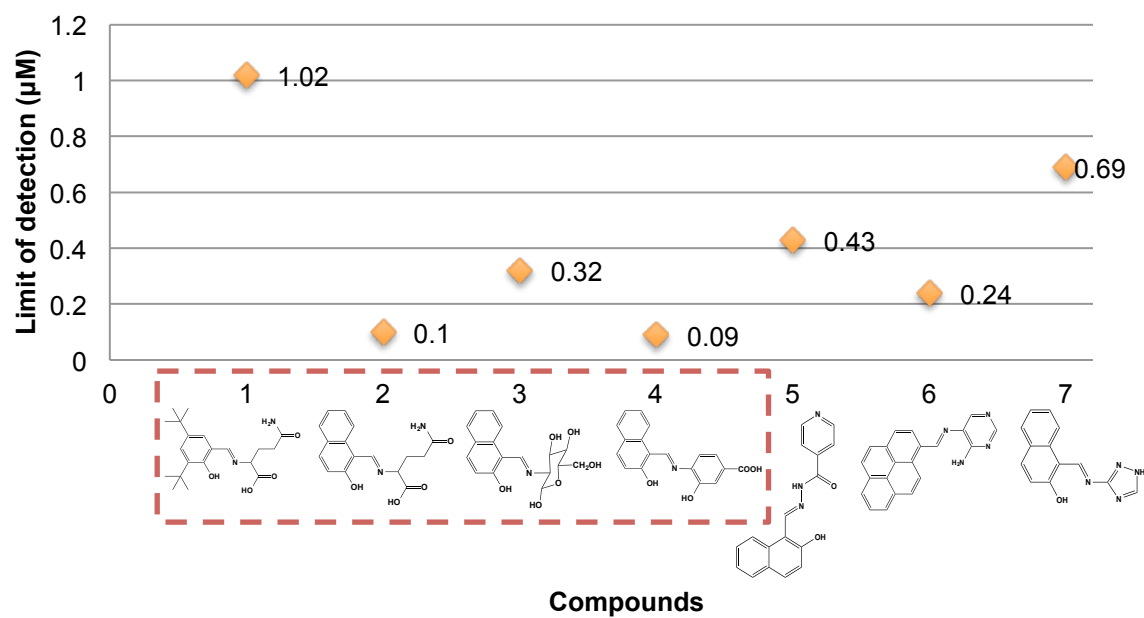


**Figure 16.** Comparison of the limits of detection between compounds **1-4** and molecules previously reported ( $5^{\text{xliii}}$ ,  $6^{\text{ix}}$  and  $7^{\text{xliv}}$ ).

### 6.3.7 Binding stoichiometry

The binding stoichiometry of compounds **1-4** to  $\text{Al}^{3+}$  was determined by the Job's method on the basis of fluorescence emission spectrum by keeping the sum of the concentration of the  $\text{Al}^{3+}$  and the complexes constant and varying the molar fraction of each compound from 0.1 to 0.9. It could be seen from **figure 17** that the fluorescence intensity at 465 nm (Compound **1**), 433 nm (Compound **2**), 433 nm (Compound **3**) and 505 nm (Compound **4**) exhibited a maximum when the molar fraction of each compound was 0.5 demonstrating a possible 1:1 binding stoichiometry between the compounds and  $\text{Al}^{3+}$ .

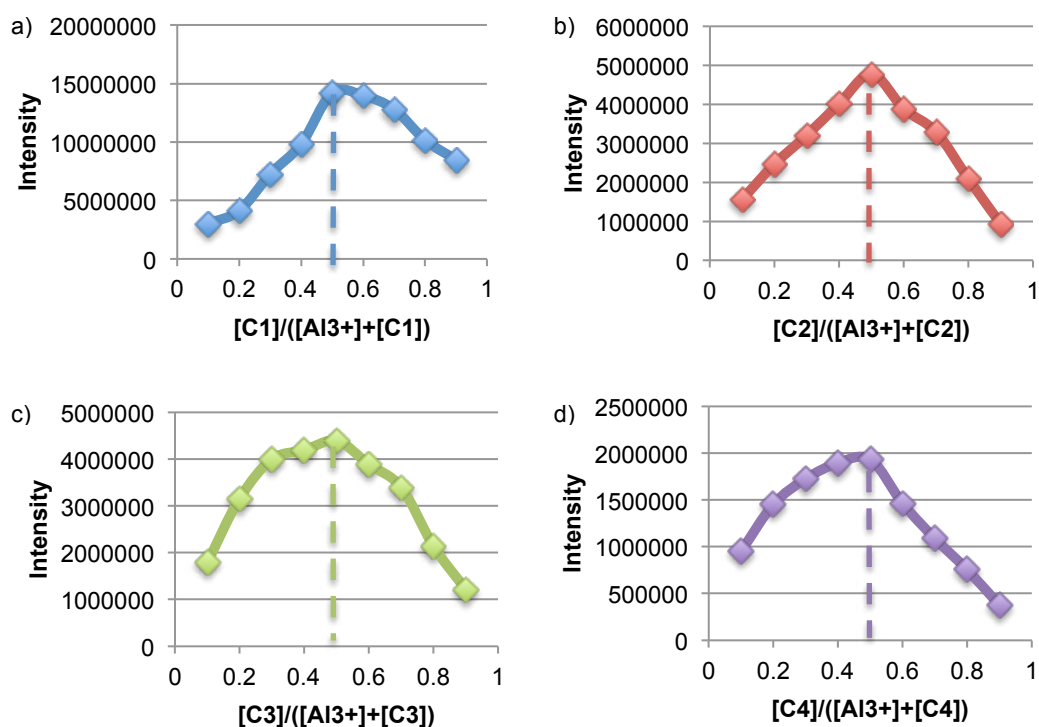


**Figure 17.** Job's plot for the complexation of a) compound **1**; b) compound **2**; c) compound **3**; d) compound **4**, with  $\text{Al}^{3+}$  in a mixture acetonitrile : water (1:1).

#### 6.4 Fluorescence Imaging of $\text{Al}^{3+}$ in Living Cells

To evaluate the capacity of the compounds to penetrate the cell membrane and produce a fluorescent signal when  $\text{Al}^{3+}$  is present in cell culture, confocal fluorescence microscopy measurement was carried out. Briefly, human epithelial cells Hs27 (ATCC-CRL-1634) were seeded in 6-well plates in Dulbecco's Modified Eagle Media, 24 hours later the medium was renewed and cells were loaded with  $\text{Al}^{3+}$  at concentrations of 100 and 50  $\mu\text{M}$  (37 °C for 60 min). After removal of free  $\text{Al}^{3+}$  by washing with media, cells were exposed to the compounds (20  $\mu\text{M}$ ) and incubated for 30 minutes. After washing with PBS, cells were analyzed using a confocal laser microscopy (Olympus BX61WI).

Compounds **3** and **4** (20  $\mu\text{M}$ ) did not produce any staining and when exposed to  $\text{Al}^{3+}$  (100  $\mu\text{M}$ ) this behavior remains. (**Figure 18**) This comportment can be attributed to the incapability of the molecules to penetrate the cell membrane and sense the  $\text{Al}^{3+}$  present in the cells, compound **4** have a carboxylic group that, depending on the pH of its environment and on the acid pKa, can loss a proton and produce a negative charge, this charge makes difficult the diffuse of the molecule across the lipid membrane, and similar with compound **3** that have five  $-\text{OH}$  groups that can be deprotonated making hard the membrane penetration.

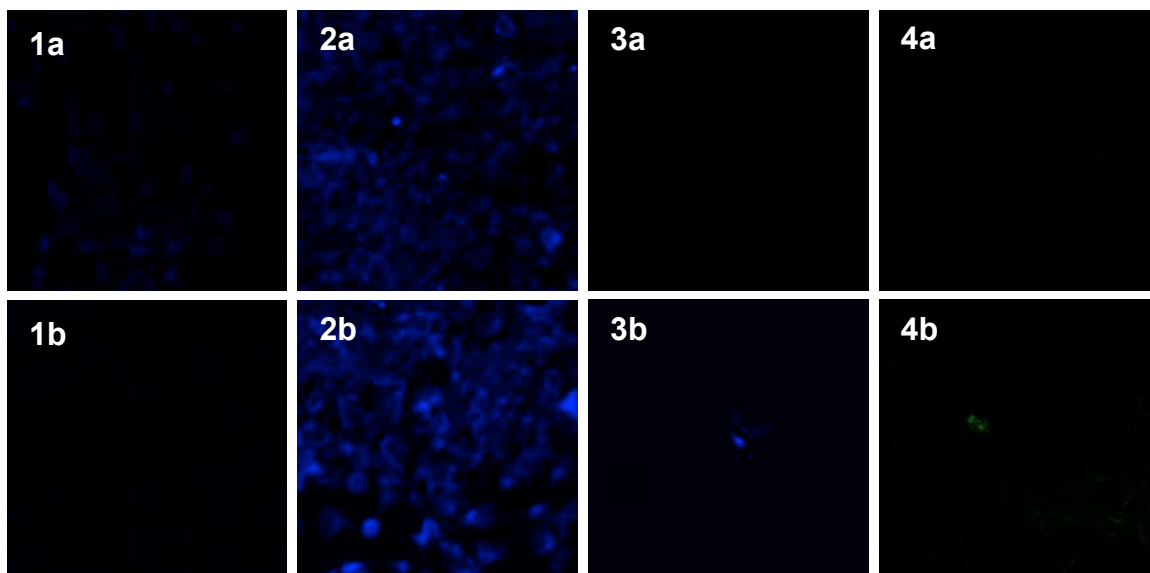


**Figure 18.** Confocal microscopic images of human epithelial cells Hs27 treated with (1) compound **1**, (2) compound **2**, (3) compound **3** and (4) compound **4** (20  $\mu\text{M}$ ); images in the absence (a) and presence (b) of  $\text{Al}^{3+}$  (100  $\mu\text{M}$ ). Incubation temperature is 37  $^{\circ}\text{C}$ .

Cells exposed to compound **1** (20  $\mu\text{M}$ ) present a weak blue staining that disappears when  $\text{Al}^{3+}$  (100  $\mu\text{M}$ ) is present in the cells. (**Figure 18**) Treatment of cells with 20  $\mu\text{M}$  of compound **2** showed a blue staining pattern that arises when  $\text{Al}^{3+}$  is present in the cell culture, producing a stronger stain in the nucleus and cytoplasm, demonstrating the membrane penetrability of compound **2** and the complexation with  $\text{Al}^{3+}$  inside the cells (**Figure 19**).

Access of compound **1** and **2** in to the cells may be ascribed to the presence of glutamine fragment in the molecules, this amino acid can easily penetrate the cell membrane thanks to transport systems. As we can see in the fluorescence spectra of each compound, both molecules present low

fluorescence by itself, which arises when  $\text{Al}^{3+}$  is present, this compartment is the same in cell culture for compound **2**, where we can appreciate the enhancement of fluorescent in presence of the metal, not the same for compound **1**, where the fluorescence is quenched.

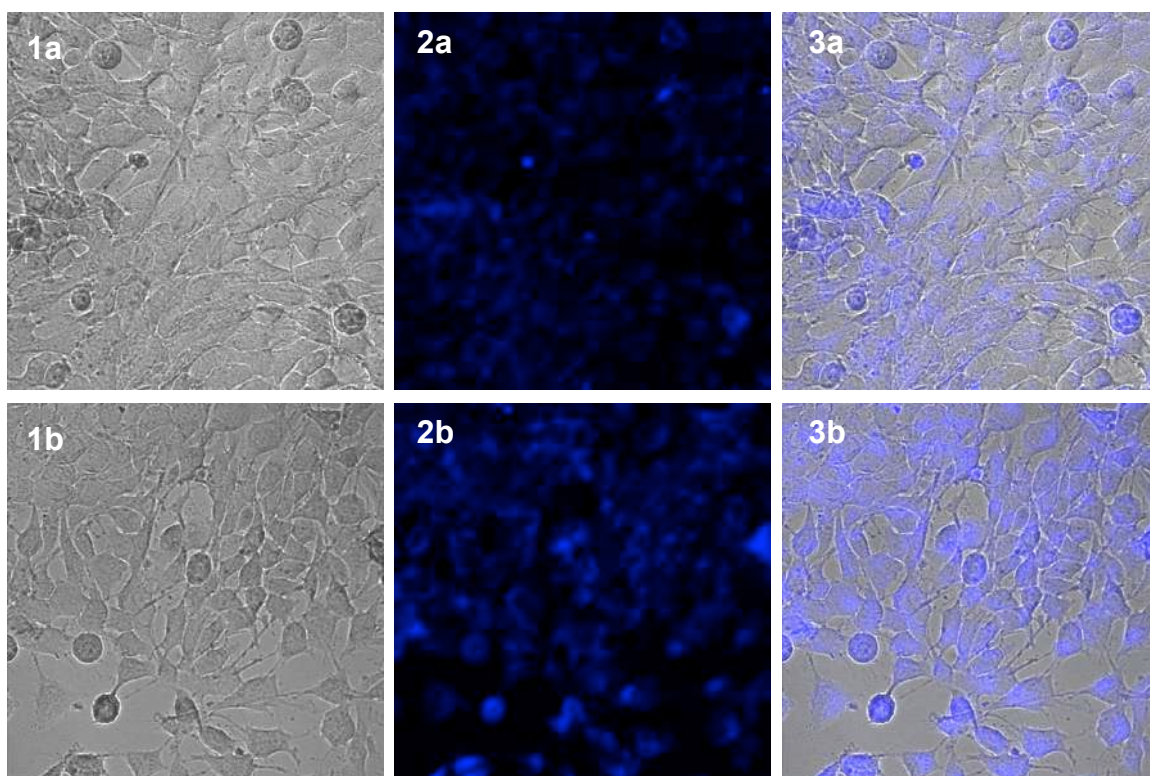


**Figure 19.** Confocal microscopic images of human epithelial cells Hs27 treated with compound **2** ( $20\ \mu\text{M}$ ) in the absence (a) and presence (b) of  $\text{Al}^{3+}$  ( $100\ \mu\text{M}$ ); bright-field (1), fluorescent (2) and the overlay image (3). Incubation temperature is  $37\ ^\circ\text{C}$ .

## 7. CONCLUSIONS

In summary, we have synthesized and characterized four new compounds derivative from Schiff bases. We proved that the four compounds could trap the aluminum and produce an increase in the emission intensity compared with the ligand without the metal and this complex present good quantum yields in solution. Only compounds **3** and **4** showed their selectivity toward aluminum ions. Compound **2** exhibited the higher emission intensity with aluminum, but the emission peak with zinc still high, while compound **1** exhibit better response in presence of Zinc. As we notice in the fluorescent competitive experiments, the existence of iron, cupper and mercury ions, decreases the fluorescence intensity, and this may act as interference when sensing aluminum. Fluorescence bio images only work for compound **2** thanks to the presence of the amino acid in the molecule that favors the membrane penetration. The high quantum yields and the low detection limits of the four compounds make molecules **2**, **3** and **4** auspicious for aluminum detection, and molecules **1** and **2**, for zinc detection in liquid samples.



## **7.1 Perspectives**

As part of the knowledge generated in this research work was demonstrated that this Schiff base compounds can sense aluminum ions and produce a fluorescent response in solution with low detection limit and high quantum yields. New molecules with tertbutyl fragment must be synthesized and probed with different metals, to corroborate that this fragments favors the union with zinc over aluminum.

## 8. REFERENCES

---

<sup>i</sup>(a) R. Yokel. Toxicity of aluminum exposure to the neonatal and immature rabbit. *Fundam. Appl. Toxicol.*, **1987**, 9, 795; (b) G. Muller, V. Bernuzzi, D. Desor, M. Hutin, P. Lehr. Developmental alterations in offspring of female rats orally intoxicated by aluminum lactate at different gestation periods. *Teratology*, **1990**, 42, 253; (c) J. Donald, M. Golub, M. Gershwin, C. Keen. Neurobehavioral effects in offspring of mice given excess aluminum in diet during gestation and lactation. *Neurotoxicol. Teratol.*, **1989**, 11, 341.

<sup>ii</sup> WHO. Aluminum in drinking-water. [[http://www.who.int/water\\_sanitation\\_health/water-quality/guidelines/chemicals/aluminium.pdf?ua=1](http://www.who.int/water_sanitation_health/water-quality/guidelines/chemicals/aluminium.pdf?ua=1)]

<sup>iii</sup> (a) J. Barcelo and C. Poschenrieder. Fast root growth responses, root exudates, and internal detoxification as clues to the mechanisms of aluminium toxicity and resistance: a review. *Environ. Exp. Bot.*, **2002**, 48, 75; (b) B. Valeur and I. Leray. Design principles of fluorescent molecular sensors for cation recognition. *Coord. Chem. Rev.*, **2000**, 205, 3; (c) Z. Krejpcio and R. Wojciak. The Influence of Al<sup>3+</sup> Ions on Pepsin and Trypsin Activity in Vitro. *Environ. Stud.*, **2002**, 11, 251.

<sup>iv</sup> L. Tomljenovic. Aluminum and Alzheimer's Disease: After a Century of Controversy, Is there a Plausible Link?. *J. of Alzheimer's Disease*, **2011**, 23, 567-598.

<sup>v</sup> (a) D. Perl. Relationship of aluminum to Alzheimer's disease. *Environ Health Perspect.* **1985**, 63, 149-53.; (b) T. Flaten. Aluminium as a risk factor in Alzheimer's disease, with emphasis on drinking water. *Brain Res Bull*, **2001**, 55 (2), 187-196.; (c) J. Savorya, O. Ghribia, M. Forbesa, M. Hermanc. Aluminium and neuronal cell injury: inter-relationships between neurofilamentous arrays and apoptosis. *J. of Inorg. Biochem.*, **2001**, 87, 15-19. ; (d) C. Martyn, C. Osmond, J. Edwardson, D. Barker, E. Harris, R. Lacey. Geographical relation between Alzheimer's disease and aluminium in drinking water. *Lancet*, **1989**, 333 (8629), 61-62.

---

<sup>vi</sup> D. Perl, D. Gajdusek, R. Garruto, R. Yanagihara, C. Gibbs. Intraneuronal aluminum accumulation in amyotrophic lateral sclerosis and Parkinsonism-dementia of Guam. *Science*, **1982**, 217, 1053.

<sup>vii</sup> T. Han, X. Feng, B. Tong, J. Shi, L. Chen, J. Zhic and Y. Dong. A novel "turn-on" fluorescent chemosensor for the selective detection of Al<sup>3+</sup> based on aggregation-induced emission, *Chem. Commun.*, **2012**, 48, 416–418.

<sup>viii</sup> M. Vendrell, D. Zhai, J. Cheng Er, and Y. Chang. Combinatorial Strategies in Fluorescent Probe Development, *Chem. Rev.*, **2012**, 112 (8), 4391–4420.

<sup>ix</sup> S. Das, A. Sahana, A. Banerjee, S. Lohar, D. Safin, M. Babashkina, M. Bolte, Y. Garcia, I. Hauli, S. Mukhopadhyay and D. Das. Ratiometric fluorescence sensing and intracellular imaging of Al<sup>3+</sup> ions driven by an intramolecular excimer formation of a pyrimidine–pyrenescaffold. *Dalton Trans.*, **2013**, 42, 4757.

<sup>x</sup>(a) D. Wana, Y. Lib, P. Zhu, A series of emission "turn-on" probes derived from rhodamine for Hg(II) recognition and sensing: Synthesis, characterization and performance. *Sensor. Actuat. B: Chem*, **2015**, 221, 1271-1278; (b) C. Zhao, Y. Chena, H. Zhanga, B. Zhoua, X. Lva, W. Fu, A BODIPY-based fluorescent chemosensor for Cu<sup>2+</sup> and biological thiols, and application as Cu<sup>2+</sup> probe in live cell imaging. *J. Photochem. Photobiol. A: Chem.*, **2014**, 282, 41-46; (c) V. Gupta, N. Mergu, A. Singh, Fluorescent chemosensors for Zn<sup>2+</sup> ions based on flavonol derivatives, *Sensor. Actuat. B: Chem*, **2014**, 202, 674-682; (d) H. Li, S. Gao, Z. Xi, A colorimetric and "turn-on" fluorescent chemosensor for Zn(II) based on coumarin Schiff-base derivative. *Inorg. Chem. Commun.*, **2009**, 12 (4), 300-303.

<sup>xi</sup> C. Chang, L. De, W. Chin and W. An. A turn-on and reversible Schiff base fluorescence sensor for Al<sup>3+</sup> ion. *Analyst*, **2013**, 138, 2527.

<sup>xii</sup> Y. Jang, U. Nama, H. Kwon, I. Hwang, C. Kim. A selective colorimetric and fluorescent chemosensor based-on naphthol for detection of Al<sup>3+</sup> and Cu<sup>2+</sup>. *Dyes and Pigm*, **2013**, 99, 6-13.

<sup>xiii</sup> S. Choudhary, J. Morrow. Dynamic Acylhydrazone Metal Ion Complex Libraries: A Mixed-Ligand Approach to Increased Selectivity in Extraction. *Angew. Chem.*, **2002**, 114, 4270.

---

<sup>xiv</sup>V. Silveira, J. Luz, C. Oliveira, I. Graziani, M. Ciriolo, A. Ferreira. Double-strand DNA cleavage induced by oxindole-Schiff base copper(II) complexes with potential antitumor activity. *J. Inorg. Biochem.* **2008**, 102, 1090.

<sup>xv</sup>Y. Li, Z. Yang. DNA binding affinity and antioxidative activity of copper(II) and zinc(II) complexes with a novel hesperetin Schiff base ligand, *Inorg. Chim. Acta*, **2009**, 362, 4823.

<sup>xvi</sup>a) S. Kasselouri, A. Garoufis, A. Katehanakis, G. Kalkanis, S. Perlepes, N. Hadjiliadis, 1:1 Metal complexes of 2-(2'-pyridyl)quinoxaline, a ligand unexpectedly formed by the reaction between 2-acetylpyridine and 1,2-phenylenediamine. *Inorg. Chim. Acta*, **1993**, 207, 255; b) A. Caballero, A. Espinosa, A. Tárraga, P. Molina, Ferrocene-Based Small Molecules for Dual-Channel Sensing of Heavy- and Transition-Metal Cations. *J. Org. Chem.* **2008**, 73, 5489-5497.

<sup>xvii</sup>D. Maity and T. Govindaraju, Naphthaldehyde–Urea/Thiourea Conjugates as Turn-On Fluorescent Probes for Al<sup>3+</sup> Based on Restricted C=N Isomerization. *Eur. J. Inorg. Chem.* **2011**, 5479–5485.

<sup>xviii</sup>K. Soroka, R. Vithanage, D. Phillips, B. Walker and P. Dasgupta, Fluorescence Properties of Metal Complexes of 8-Hydroxyquinoline-5-sulfonic Acid and Chromatographic Applications, *Anal. Chem.*, **1987**, 59, 629.

<sup>xix</sup>S. Al-Kindy, F. Suliman and A. Pillay, Fluorimetric determination of aluminium using sequential injection analysis (SIA): state of our art and future developments. *Instrum. Sci. Technol.*, **2006**, 34, 619-633.

<sup>xx</sup>N. Chattopadhyay, A. Mallick and S. Sengupta, Photophysical studies of 7-hydroxy-4-methyl-8-(4'-methylpiperazin-1'-yl) methylcoumarin: A new fluorescent chemosensor for zinc and nickel ions in water. *J. Photochem. Photobiol., A*, **2006**, 177, 55.

<sup>xxi</sup>V. Jiménez, M. García, B. Muñoz, R. Chan, J. Berrones, R. Dias, I. Moggio, E. Arias, J. Serrano, A. Chavez. New application of fluorescent organotin compounds derived from Schiff bases: synthesis, X-ray structures, photophysical properties, cytotoxicity and fluorescent bioimaging. *J. Mater. Chem. B*, **2015**, 3, 5731.

<sup>xxii</sup>J. Lehn. *Supramolecular Chemistry: Concepts and Perspectives*. Federal Republic of Germany, **1995**, 262.

- 
- <sup>xxiii</sup> B. Valeur. *Molecular fluorescence: principles and applications*. Wiley-VCH: Weinheim, **2002**.
- <sup>xxiv</sup> a) L. Prodi, F. Bolletta, M. Montalti, N. Zaccheroni. Luminescent chemosensors for transition metal ions. *Coord. Chem. Rev.* **2000**, 205 (1), 59-83; b) W. Czarnik. Fluorescent chemosensors of ion and molecule recognition. In *Interfacial Design and Chemical Sensing*, *J. Am. Chem. Soc.*, **1994**, 561, 314-323; c) M. Keefe, K. Benkstein, J. Hupp. Luminescent sensor molecules based on coordinated metals: a review of recent developments. *Coord. Chem. Rev.*, **2000**, 205 (1), 201-228.
- <sup>xxv</sup> C. Bargossi, M. Fiorini, M. Montalti, L. Prodi, N. Zaccheroni. Recent developments in transition metal ion detection by luminescent chemosensors. *Coord. Chem. Rev.*, **2000**, 208 (1), 17-32.
- <sup>xxvi</sup> J. Anastassopoulou, T. Theophanides (1995) *The Role of Metal Ions in Biological Systems and Medicine*. In: Kessissoglou D.P. (eds) *Bioinorganic Chemistry*. NATO ASI Series (Series C: Mathematical and Physical Sciences), vol 459. Springer, Dordrecht.
- <sup>xxvii</sup> K. S. Egorova and V. P. Ananikov, Toxicity of metal compounds: knowledge and myths. *Organometallics* **2017**, 36 (21), 4071 - 4090.
- <sup>xxviii</sup> L. Fabbrizzi, M. Licchelli, P. Pallavicini, A. Perotti, D. Sacchi, An Anthracene-Based Fluorescent Sensor for Transition Metal Ions. *Angew. Chem. Int. Ed. in English* **1994**, 33 (19), 1975-1977.
- <sup>xxix</sup> L. Ma, H. Li, Y. Wu, A pyrene-containing fluorescent sensor with high selectivity for lead(II) ion in water with dual illustration of ground-state dimer. *Sensors Actuat. B: Chem.* **2009**, 143 (1), 25-29.
- <sup>xxx</sup> M. Dong, Y. Wang, Y. Peng, Highly Selective Ratiometric Fluorescent Sensing for Hg<sup>2+</sup> and Au<sup>3+</sup>, Respectively, in Aqueous Media. *Org. Lett.*, **2010**, 12 (22), 5310-5313.
- <sup>xxxi</sup> a) E. Altschuler, Aluminum-containing antacids as a cause of idiopathic Parkinson's disease. *Med. Hypotheses*, **1999**, 53, 22-23; b) B. Wang, W. Xing, Y. Zhao, X. Deng, Effects of chronic aluminum exposure on memory through multiple signal transduction pathways. *Environ. Toxicol. Pharmacol.* **2010**, 29,

---

308–313; c) J.R. Walton, Aluminum in hippocampal neurons from humans with Alzheimer's disease, *Neuro. Toxicol.*, **2006**, 27, 385–394.

<sup>xxxii</sup> D. Krewski, R. Yokel, E. Nieboer, D. Borchelt, J. Cohen, J. Harry, S. Kacew, J. Lindsay, A. Mahfouz, and V. Rondeau. Human health risk assessment for aluminium, aluminium oxide, and aluminium hydroxide. *J Toxicol Environ Health B Crit Rev*, **2007**, 10, 1–269.

<sup>xxxiii</sup> a) K. Soroka, R. Vithanage, D. Phillips, B. Walker, P. Dasgupta, Fluorescence properties of metal complexes of 8-hydroxyquinoline-5-sulfonic acid and chromatographic applications, *Anal. Chem.*, **1987**, 59, 629–636; b) S. Kim, H. Choi, J. Kim, S. Lee, D. Quang, J. Kim, Reaction-Based Fluorescent Sensing of Au(I)/Au(III) Species: Mechanistic Implications on Vinylgold Intermediates, *Org. Lett.*, **2010**, 12, 560–563.

<sup>xxxiv</sup> L. Wong and C. Wong. A New Method for Heavy Metals and Aluminium Detection Using Biopolymer-Based Optical Biosensor *IEEE Sens. J.*, **2015**, 15(1), 471–475.

<sup>xxxv</sup> V. Suryawanshi, A. Gore, P. Dongare, P. Anbhul, S. Patil, G. Kolekar. A novel pyrimidine derivative as a fluorescent chemosensor for highly selective detection of Aluminum (III) in aqueous media. *Spectrochim. Acta A: Mol. Biomol. Spectrosc.*, **2013**, 114, 681–686.

<sup>xxxvi</sup> W- Lin, L. Yuan, and J. Feng, A Dual-Channel Fluorescence-Enhanced Sensor for Aluminum Ions Based on Photoinduced Electron Transfer and Excimer Formation, *Eur. J. Org. Chem.* **2008**, 3821–3825.

<sup>xxxvii</sup> J. Qin, T. Li, B. Wang, Z. Yang, L. Fan. A sensor for selective detection of Al<sup>3+</sup> based on quinoline Schiff-base in aqueous media. *Synthetic Met.*, **2014**, 195, 141–146.

<sup>xxxviii</sup> S. Rollas, G. Küçükgül. Biological Activities of Hydrazone Derivatives. *Molecules* **2007**, 12, 1910–1939.

<sup>xxxix</sup> (a) S. Adewuyi, D. Ondigo, R. Zügler, Z. Tshentu, T. Nvokong, N. Torto, A highly selective and sensitive pyridylazo-2-naphthol-poly(acrylic acid) functionalized electrospun nanofiber fluorescence turn-off chemosensory system for Ni<sup>2+</sup>. *Anal. Method.*, **2012**, 6, 1729–1735; (b) A. Kumar, V. Kumar, K.K. Upadhyay, An Al<sup>3+</sup> and H<sub>2</sub>PO<sub>4</sub><sup>(-)</sup>/HSO<sub>4</sub><sup>(-)</sup> selective conformational arrest and bail to a pyrimidine-naphthalene anchored molecular switch. *Analyst*, **2013**, 6, 1891–1897; (c) R. Azadbakht, J. Khanabadi, A highly sensitive and selective off-on

---

fluorescent chemosensor for Al<sup>3+</sup> based on naphthalene derivative, *Inorg. Chem. Commun.*, **2013**, 30, 21-25; (d) Y.W. Liu, C.H. Chen, A.T. Wu, A turn-on and reversible fluorescence sensor for Al<sup>3+</sup> ion. *Analyst.*, **2012**, 22, 5201-5203.

<sup>xi</sup> (a) A. Sahana, A. Banerjee, S. Das, S. Lohar, D. Karak, B. Sarkar, S.K. Mukhopadhyay, A.K. Mukherjee, D. Das, A naphthalene-based Al<sup>3+</sup>-selective fluorescent sensor for living cell imaging. *Org. Biomol. Chem.*, **2011**, 9, 5523-5529; (b) S. Sen, T. Mukherjee, A. Basu, Chattopadhyay, A. Moirangthem, J. Basu, P. Marek, Chattopadhyay, A water soluble Al<sup>3+</sup> selective colorimetric and fluorescent turn-on chemosensor and its application in living cell imaging. *Analyst.*, **2012**, 137, 3781-3795; (c) R. Azadbakht, J. Khanabadi, A novel aluminum-sensitive fluorescent nano-chemosensor based on naphthalene macrocyclic derivative. *Tetrahedron*, **2013**, 69, 3206-3211.

<sup>xii</sup> Q. Wei, J. Dong, P. Zhao, M. Li, F. Cheng, J. Kong, L. Li. DNA binding, BSA interaction and SOD activity of two new nickel(II) complexes with glutamine Schiff base ligands. *J. Photochem. Photobiol. B: Biology*, **2016**, 161, 355–367.

<sup>xiii</sup> B. Muñoz, R. Santillan, M. Rodriguez, J. Méndez, M. Romero, N- Farfán, P. Lacroix, K. Nakatani, G. Ramos, J. Maldonado et. al. Synthesis, crystal structure and non-linear optical properties of boronates derivatives of salicylidenediminophenols. *J. Organomet. Chem.* **2008**, 690, 2351- 2357.

<sup>xiii</sup> X. Yue, Z. Wang, C. Li and Z. Yang. Naphthalene-derived Al<sup>3+</sup>-selective fluorescent chemosensor based on PET and ESIPT in aqueous solution. *Tetrahedron Let.*, **2017**, 58, 4532.

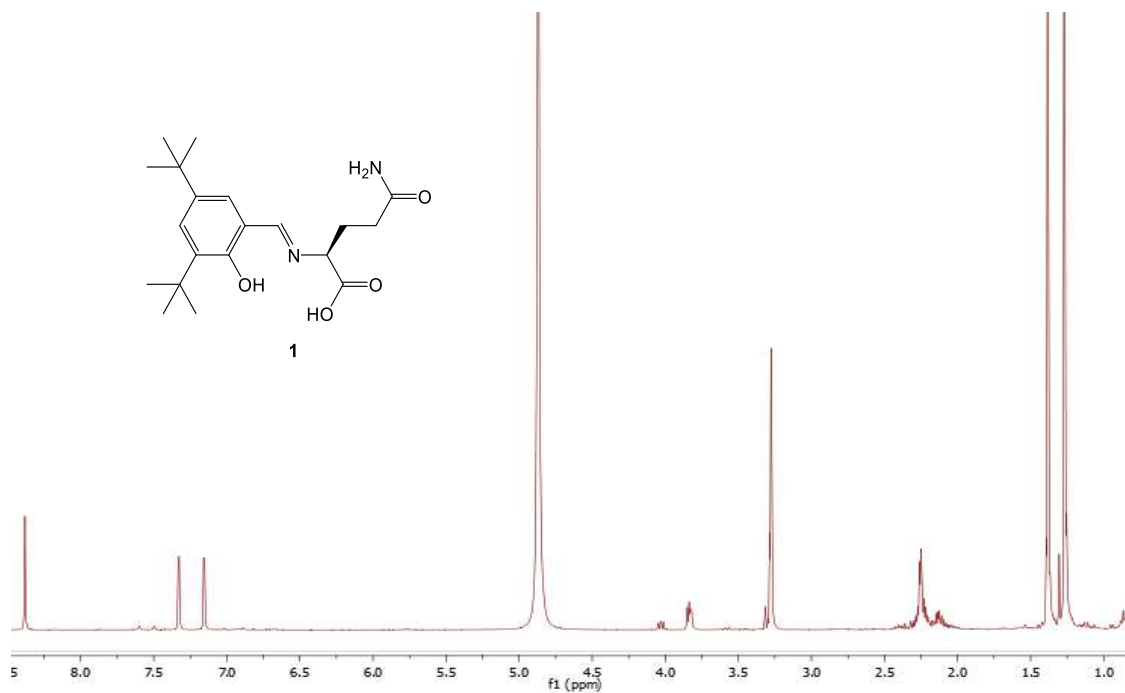
<sup>xiv</sup> T. Jia, W. Cao, X. Zheng and L. Jin. A turn-on chemosensor based on naphthol–triazole for Al(III) and its application in bioimaging. *Tetrahedron Let.*, **2013**, 54, 3471-3474.

## **9.APPENDIX**

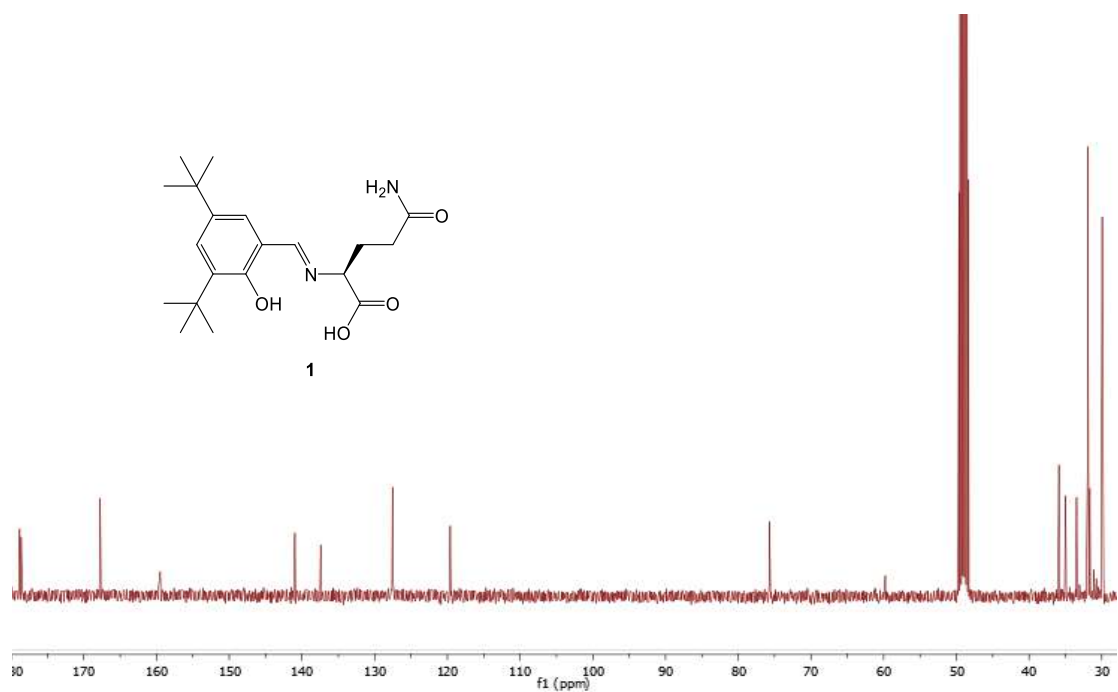
### APPENDIX A

### CHARACTERIZATION

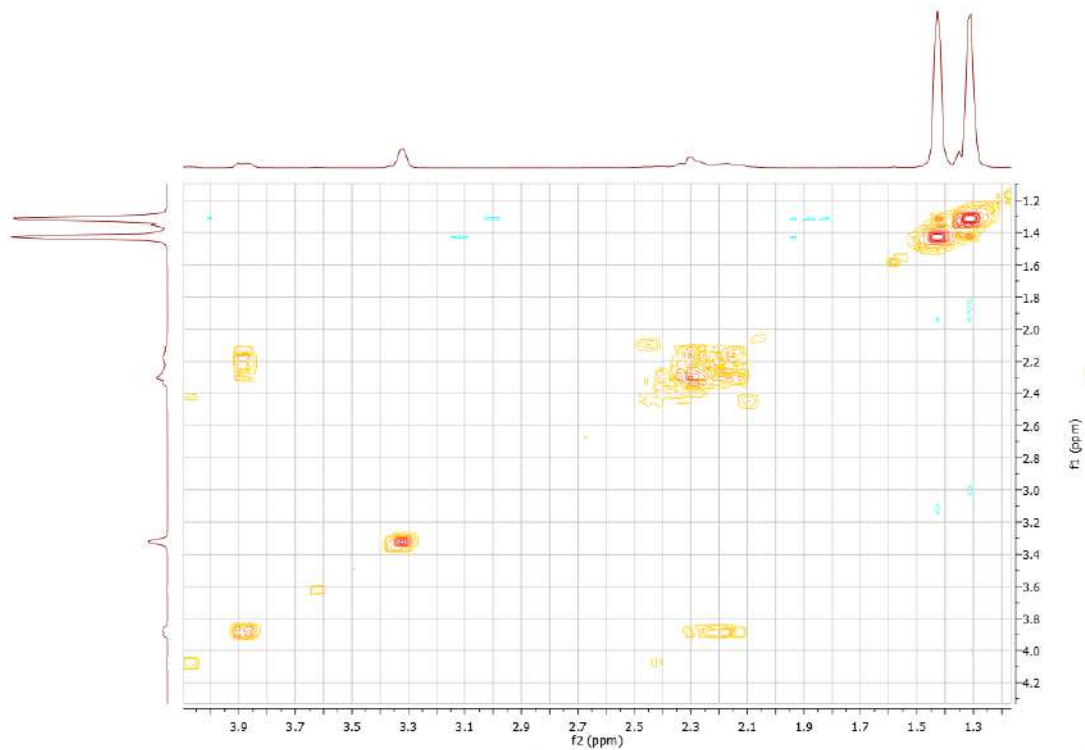




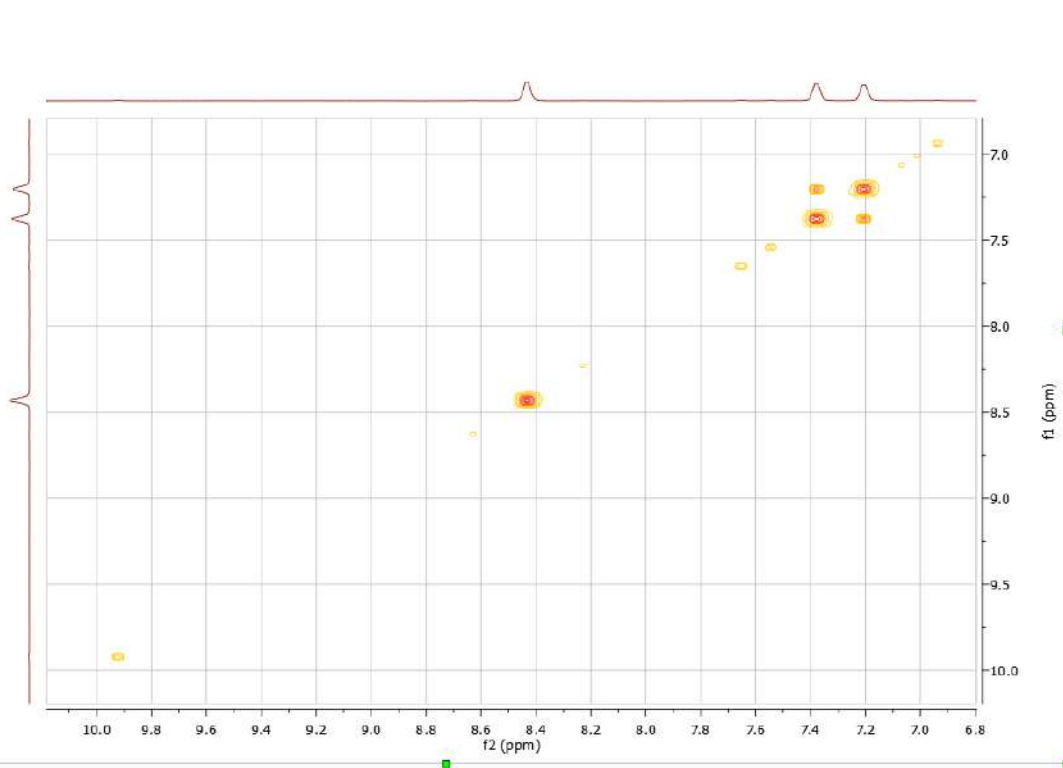
<sup>1</sup>H-NMR (400 MHz, CD<sub>3</sub>OD, 298 K) spectrum of compound 1.



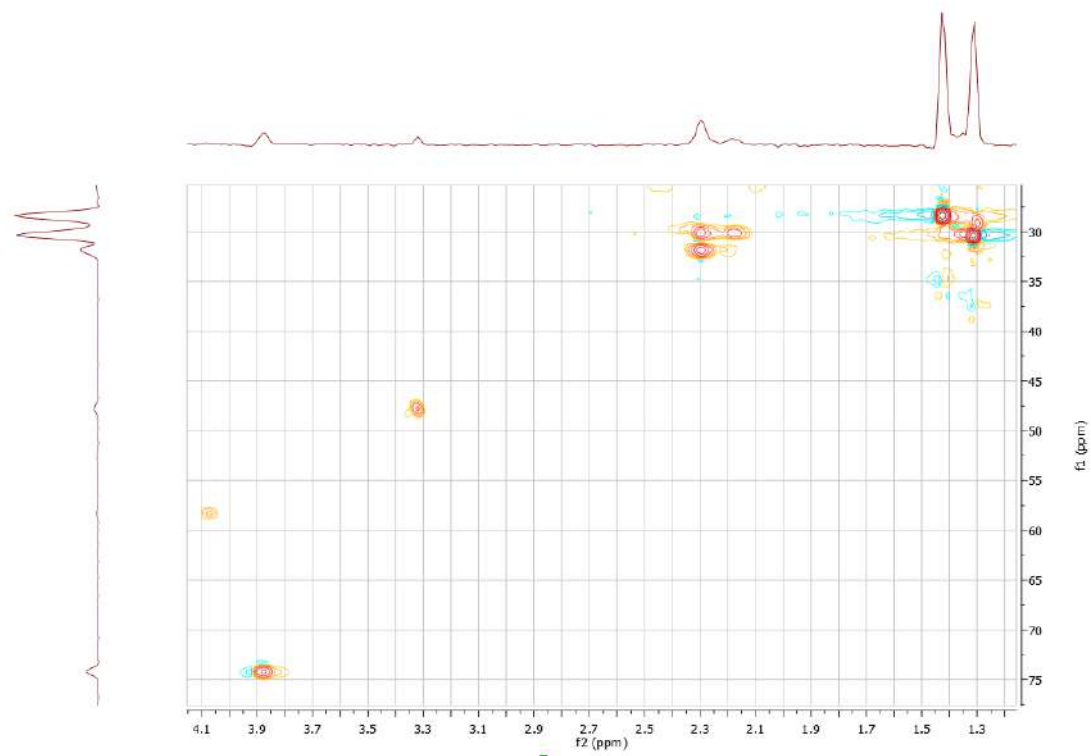
<sup>13</sup>C-NMR (400 MHz, CD<sub>3</sub>OD, 298 K) spectrum of compound 1.



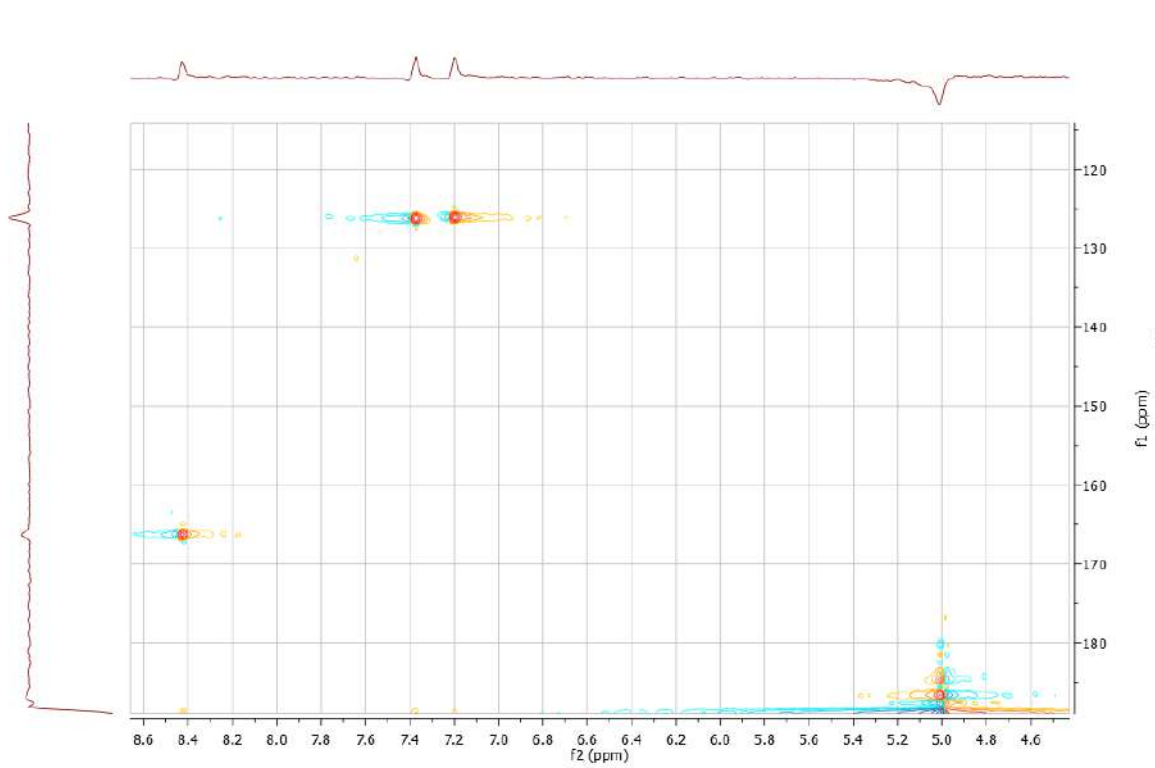
<sup>1</sup>H/<sup>1</sup>H COSY spectrum of compound **1** (aliphatic region).



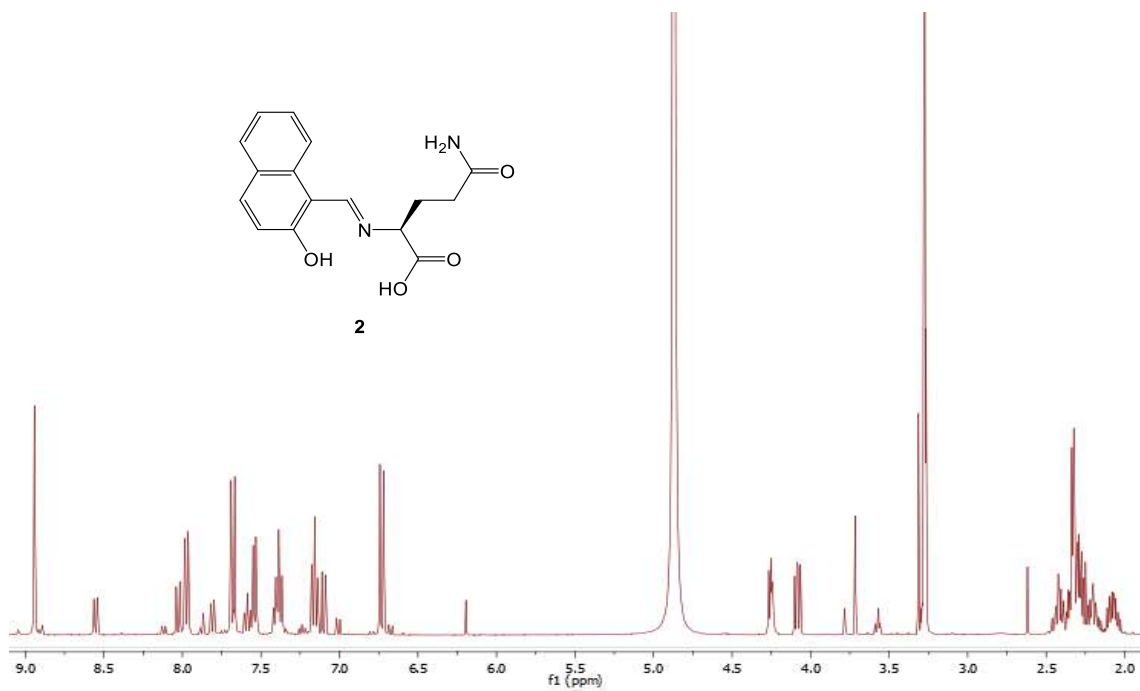
<sup>1</sup>H/<sup>1</sup>H COSY spectrum of compound **1** (aromatic region).



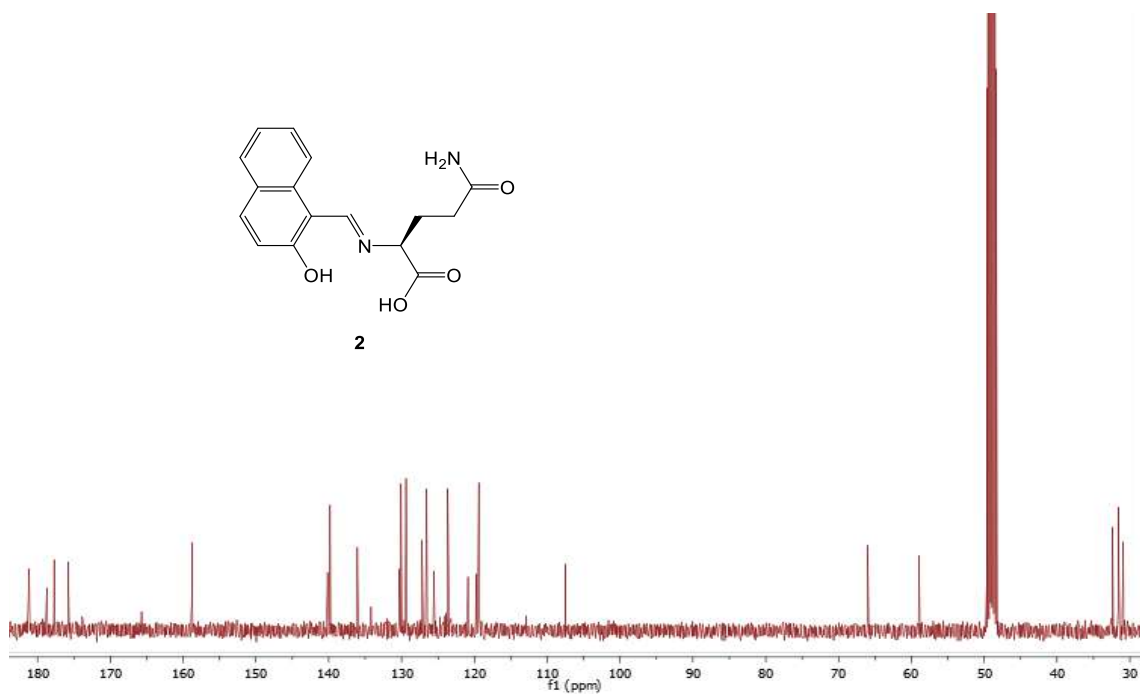
$^1\text{H}/^{13}\text{C}$  HETCOR spectrum of compound **1** (aliphatic region).



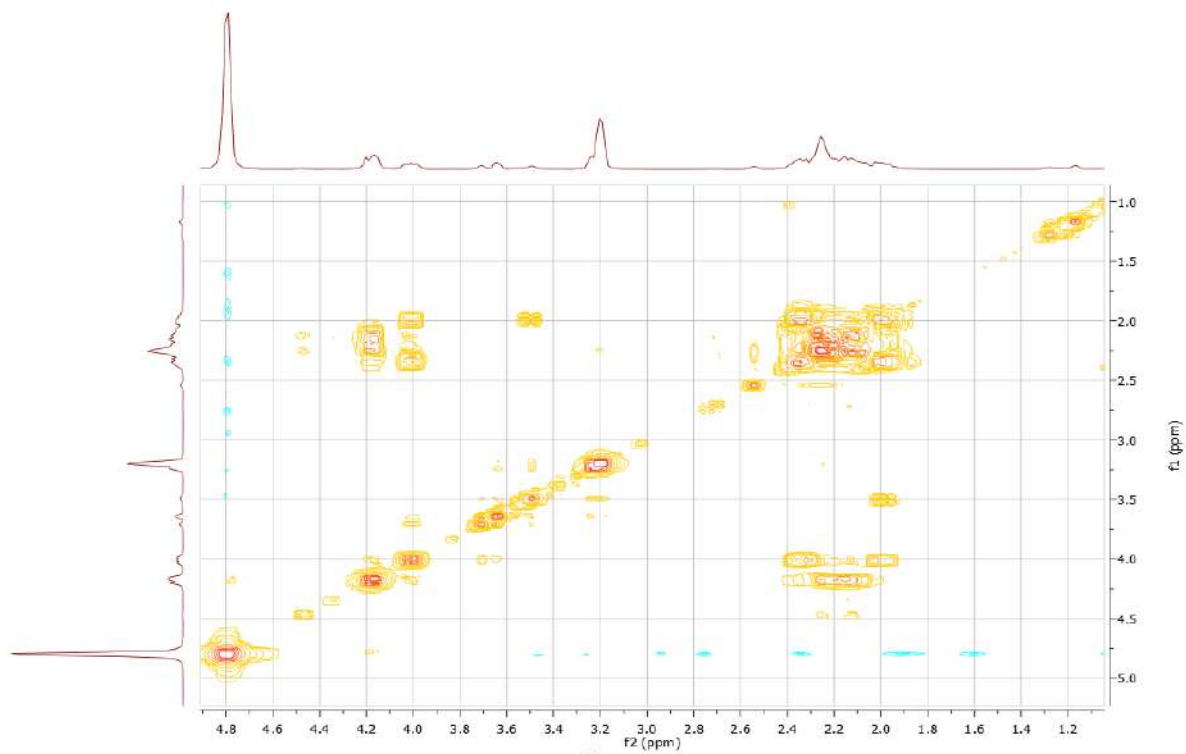
$^1\text{H}/^{13}\text{C}$  HETCOR spectrum of compound **1** (aromatic region).



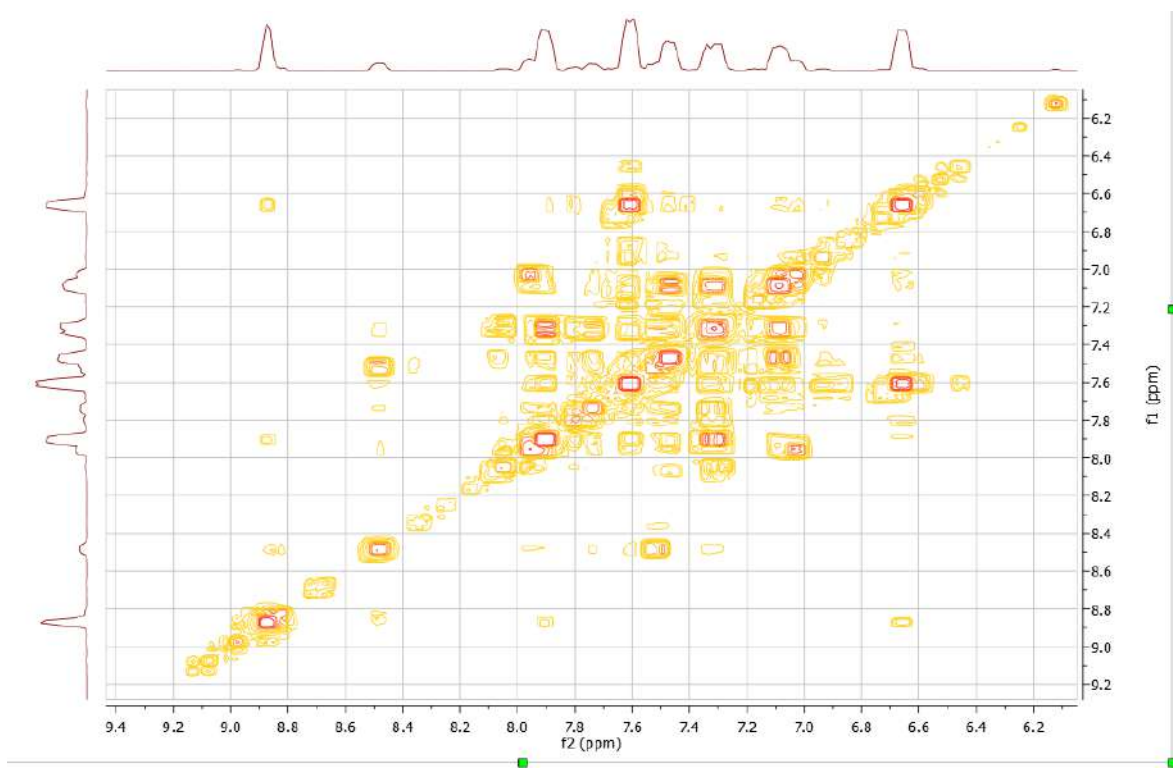
<sup>1</sup>H-NMR (400 MHz, CD<sub>3</sub>OD, 298 K) spectrum of compound 2.



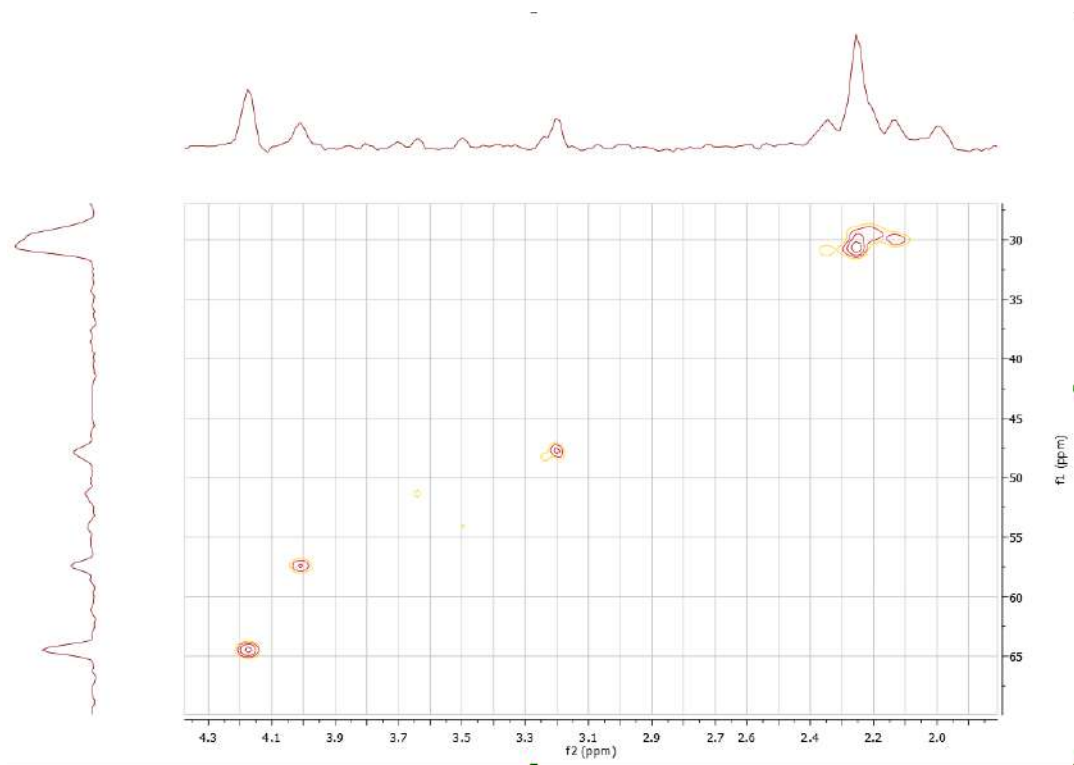
<sup>13</sup>C-NMR (400 MHz, CD<sub>3</sub>OD, 298 K) spectrum of compound 2.



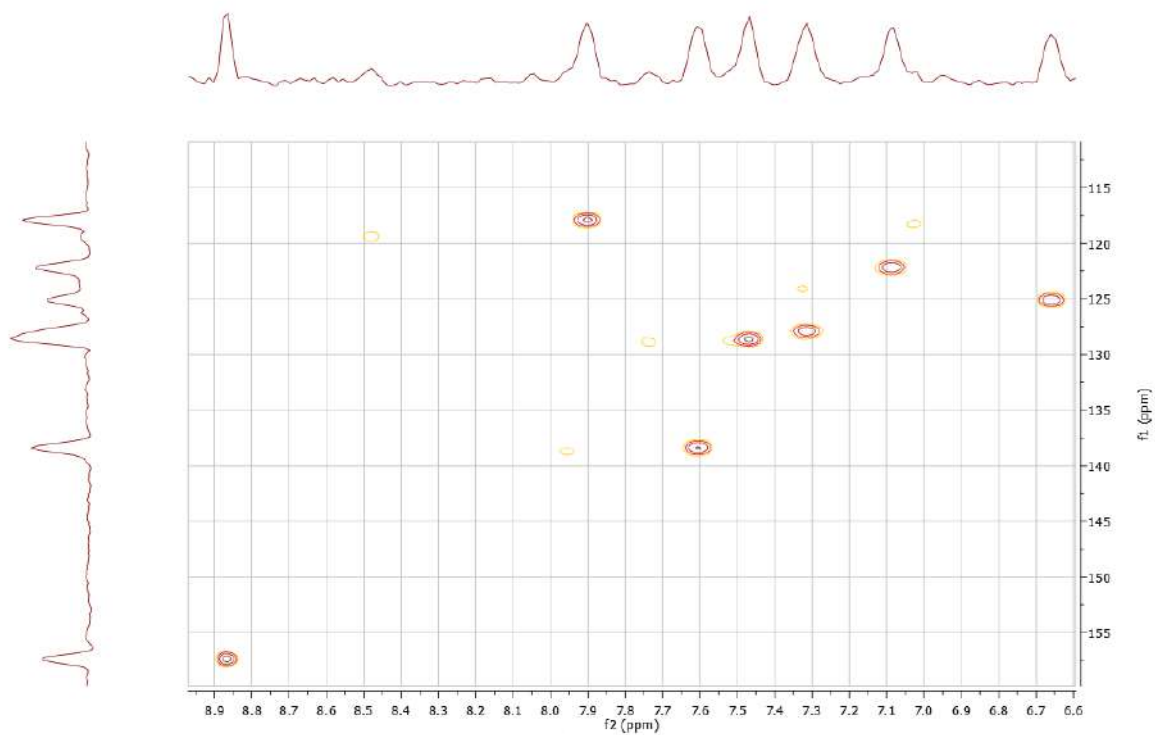
$^1\text{H}/^1\text{H}$  COSY spectrum of compound **2** (aliphatic region).



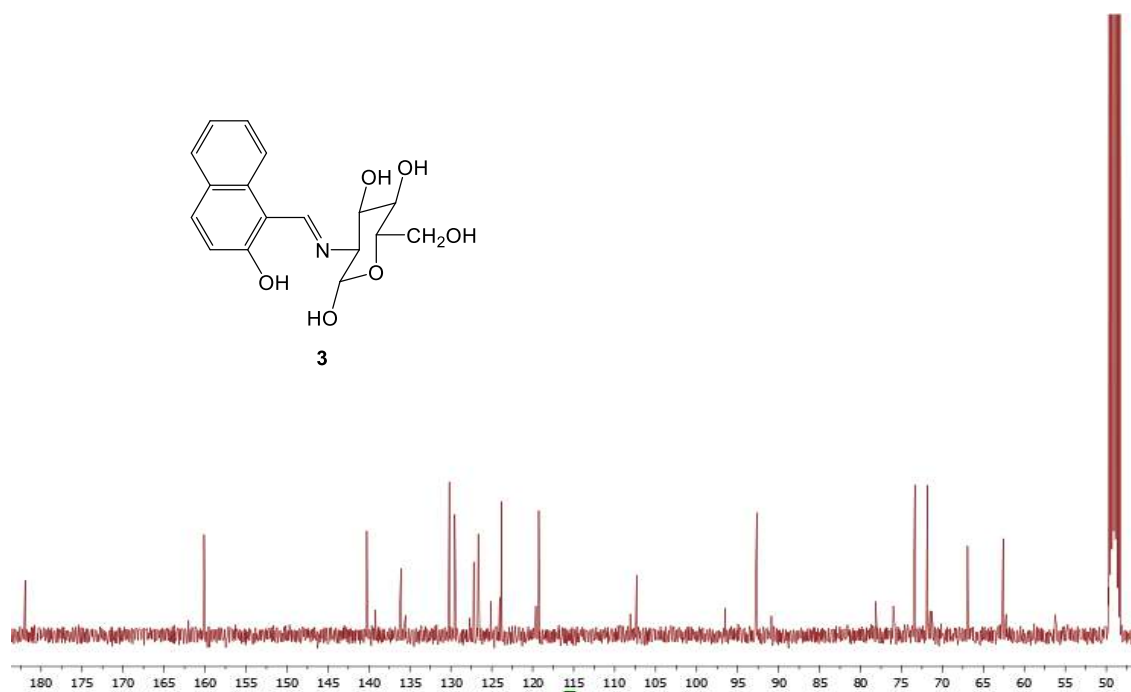
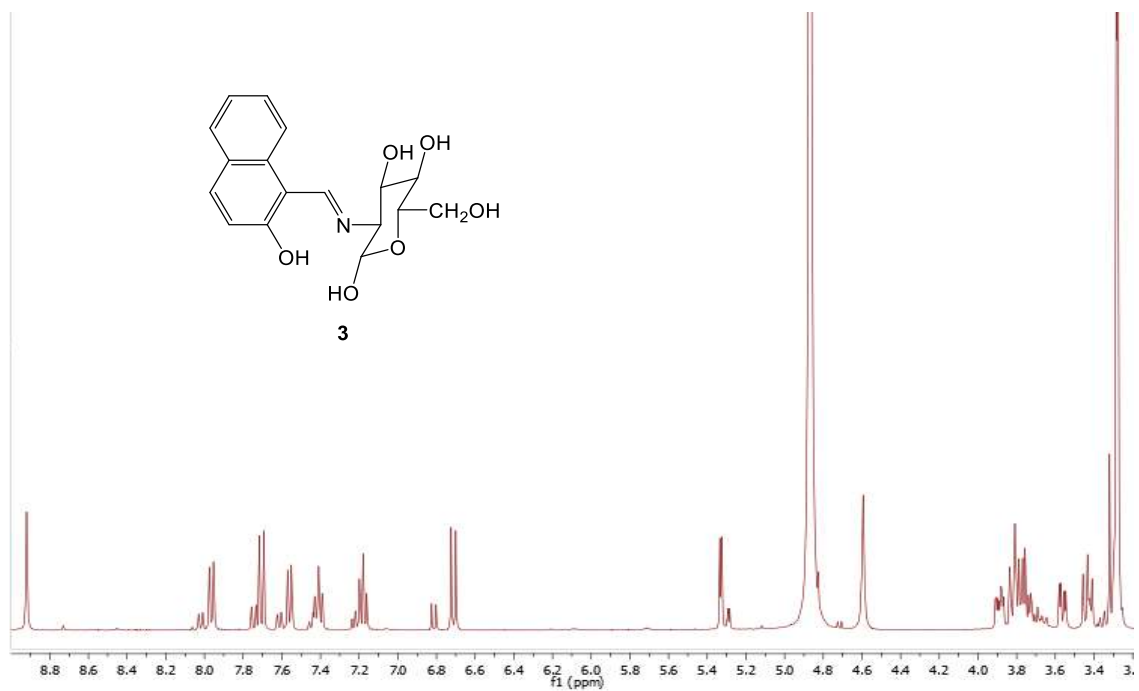
$^1\text{H}/^1\text{H}$  COSY spectrum of compound **2** (aromatic region).

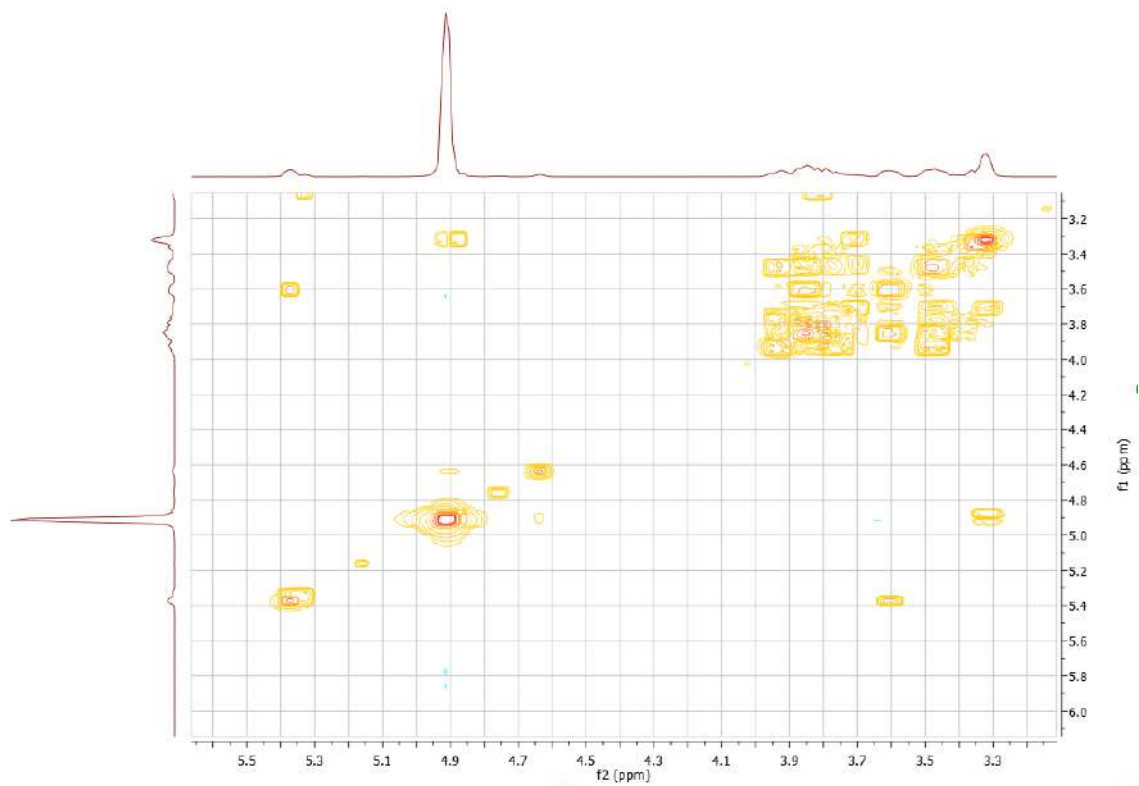


$^1\text{H}/^{13}\text{C}$  HETCOR spectrum of compound **2** (aliphatic region).

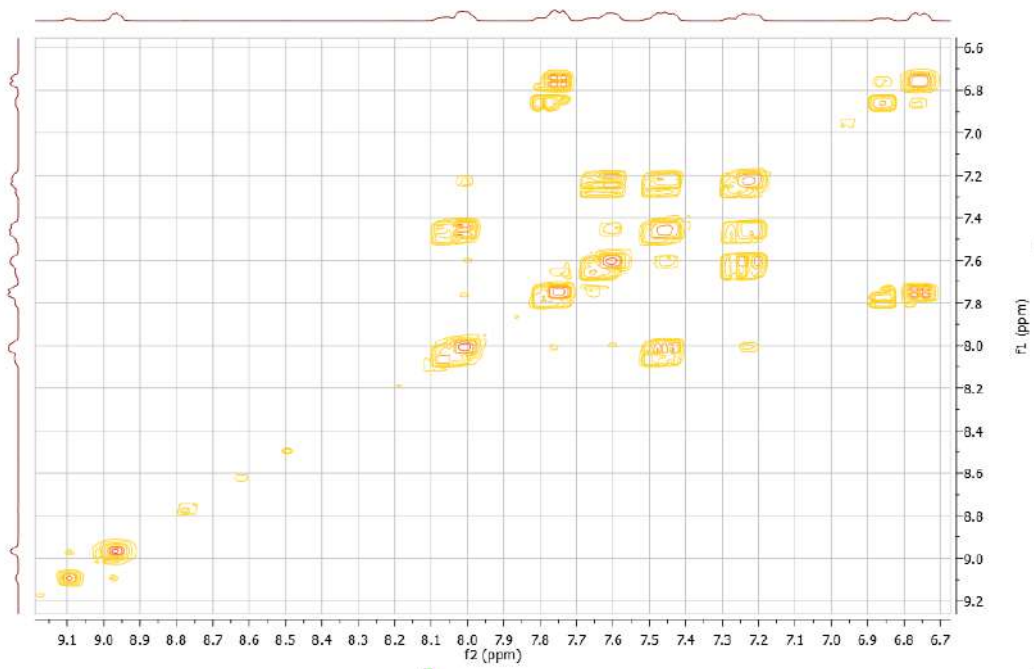


$^1\text{H}/^{13}\text{C}$  HETCOR spectrum of compound **2** (aromatic region).



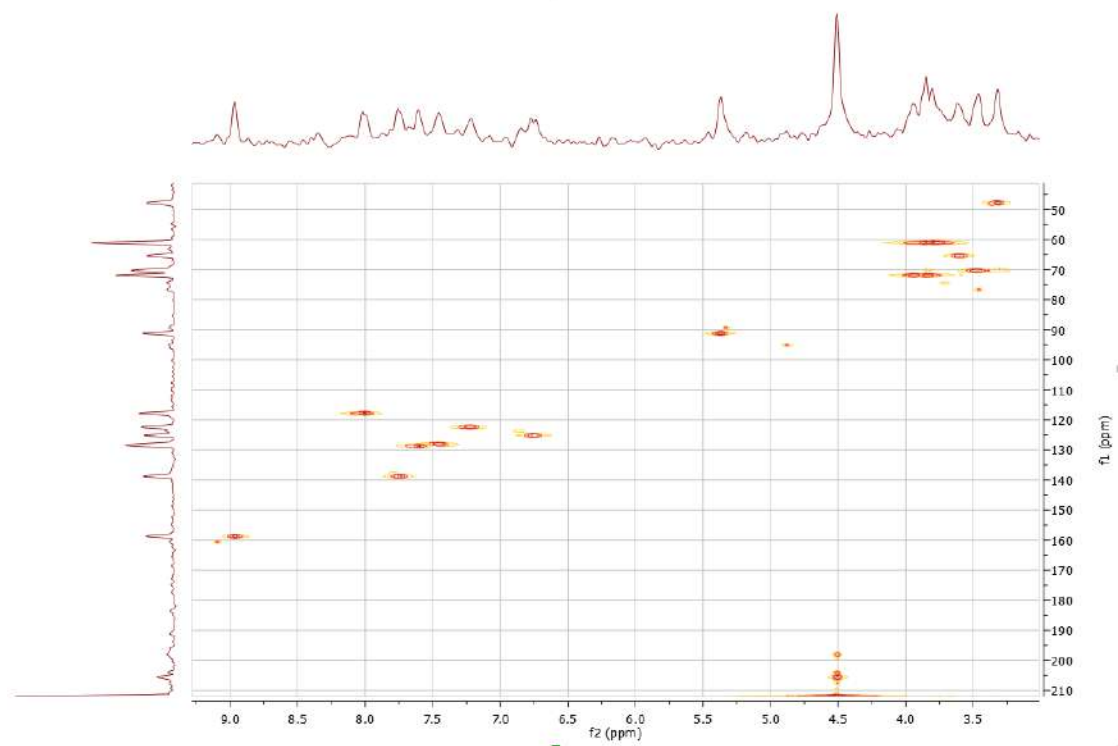


$^1\text{H}/^1\text{H}$  COSY spectrum of compound **3** (aliphatic region).

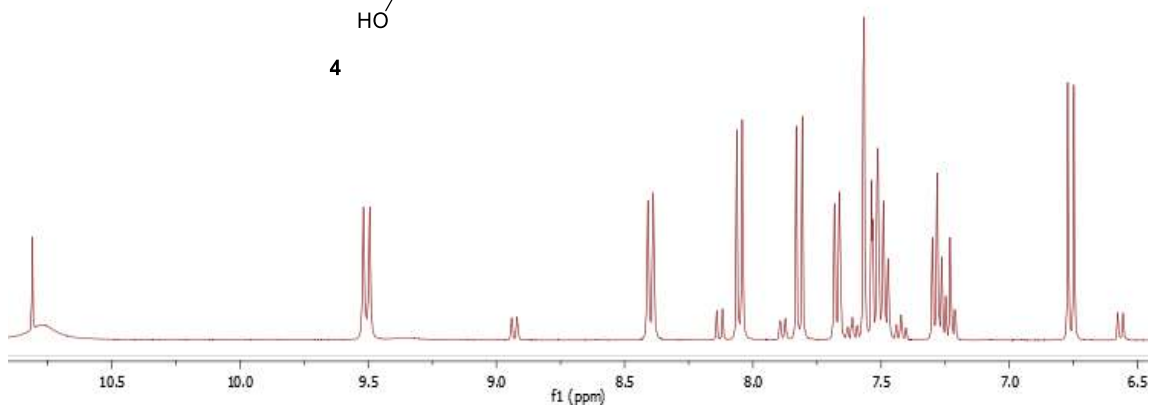
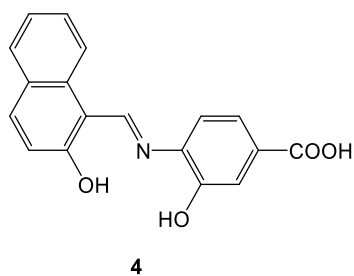


$^1\text{H}/^1\text{H}$  COSY spectrum of compound **3** (aromatic region).

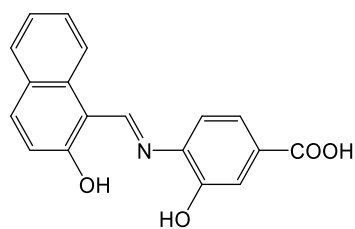




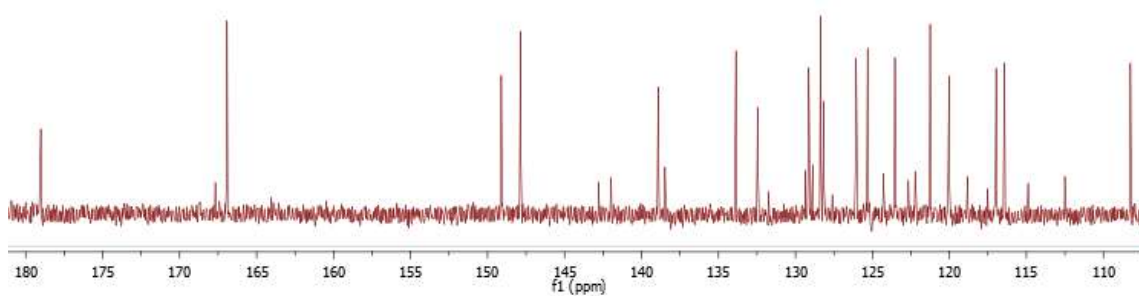
$^1\text{H}/^{13}\text{C}$  HETCOR spectrum of compound **3** (alifatic and aromatic region).



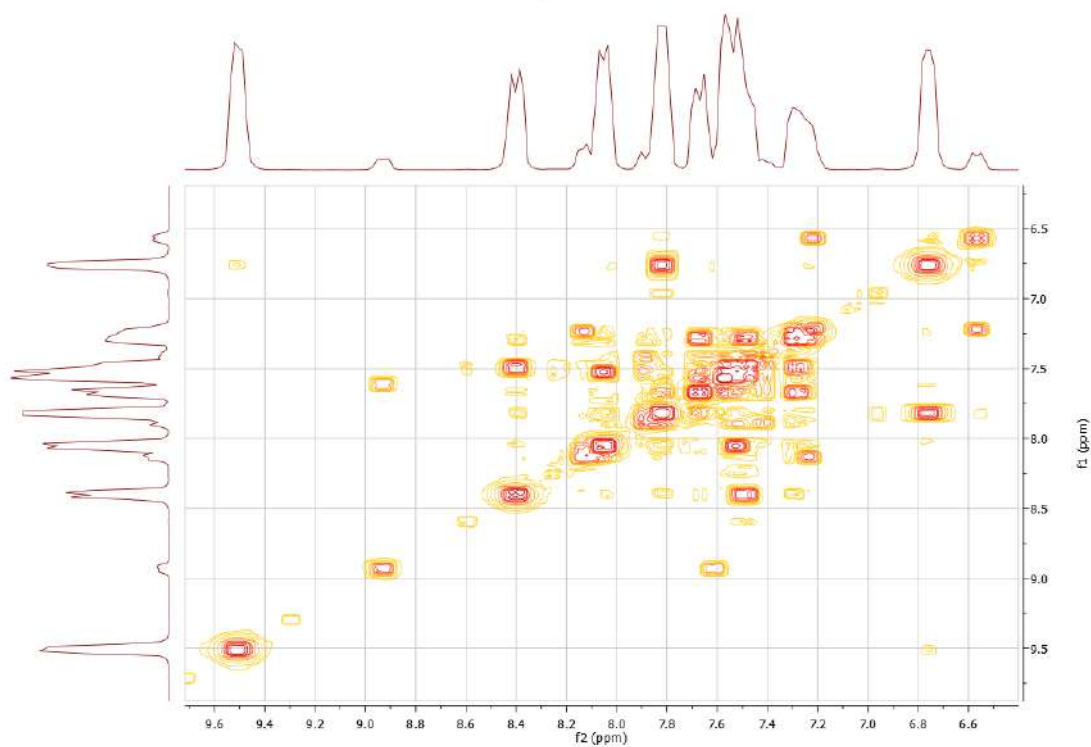
$^1\text{H}$ -NMR (400 MHz,  $\text{CD}_3\text{OD}$ , 298 K) spectrum of compound **4**.



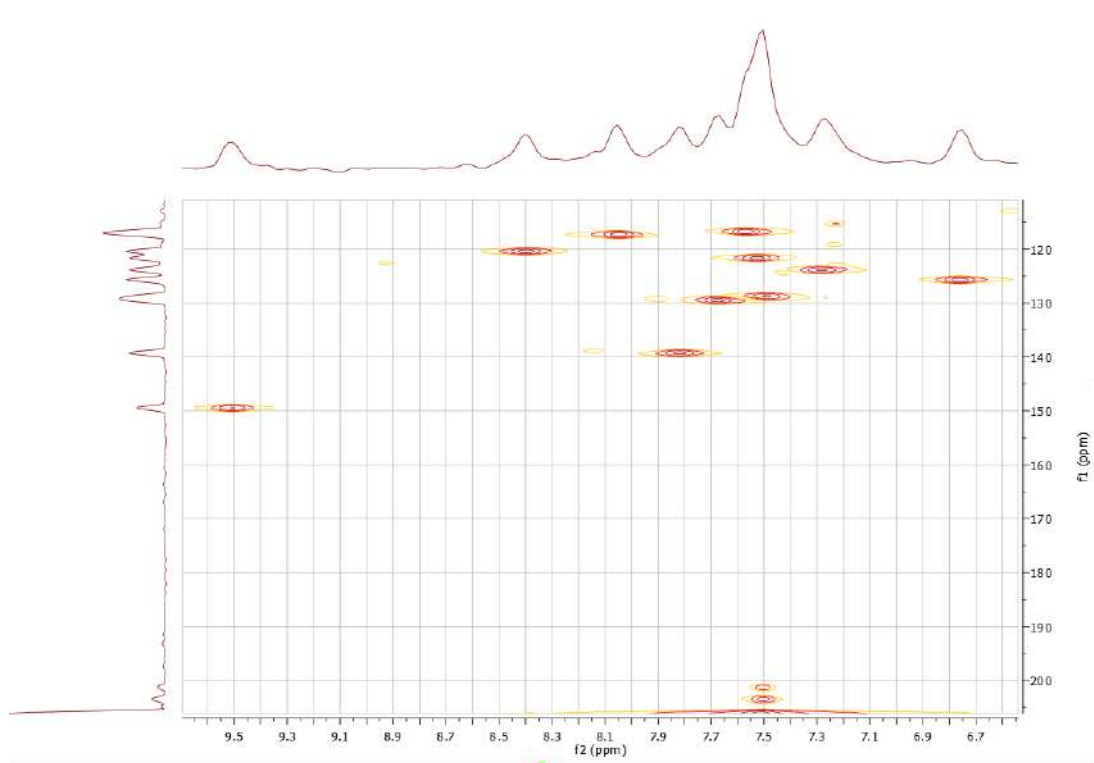
4



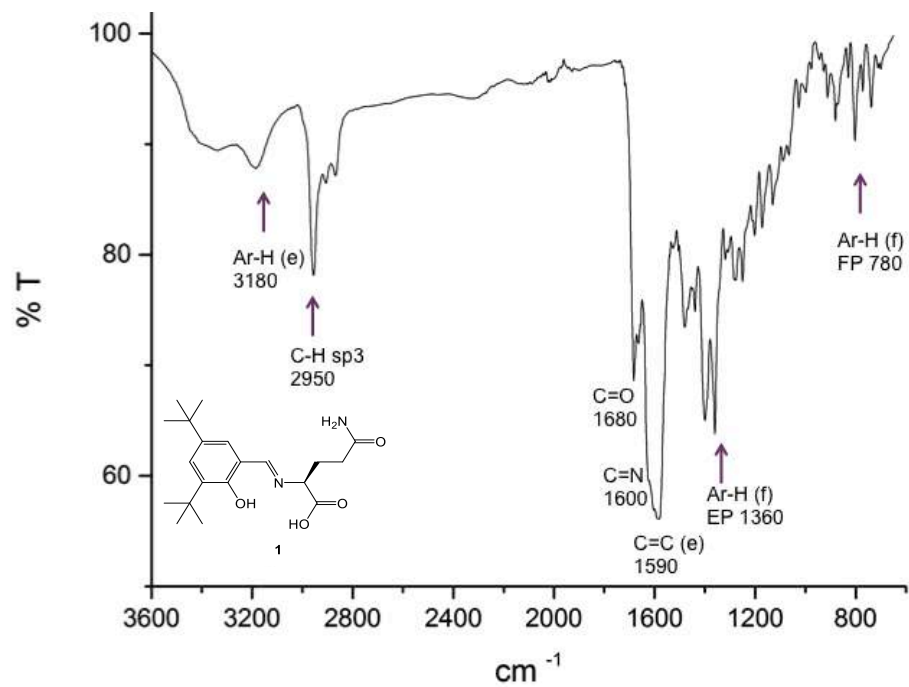
$^{13}\text{C}$ -NMR (400 MHz,  $\text{CD}_3\text{OD}$ , 298 K) spectrum of compound 4.



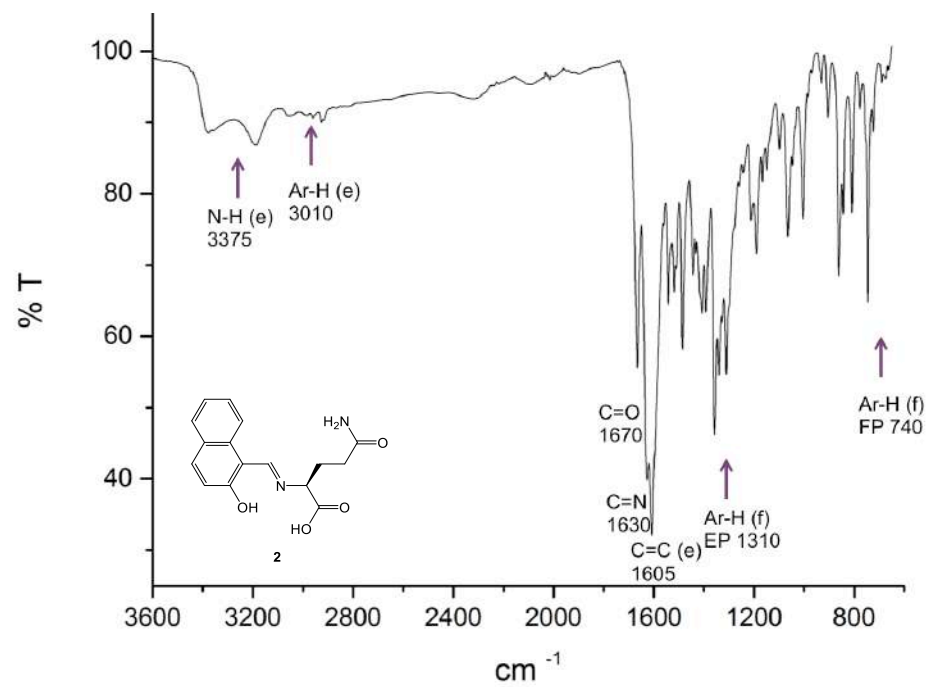
$^1\text{H}/^1\text{H}$  COSY spectrum of compound 4 (aromatic region).



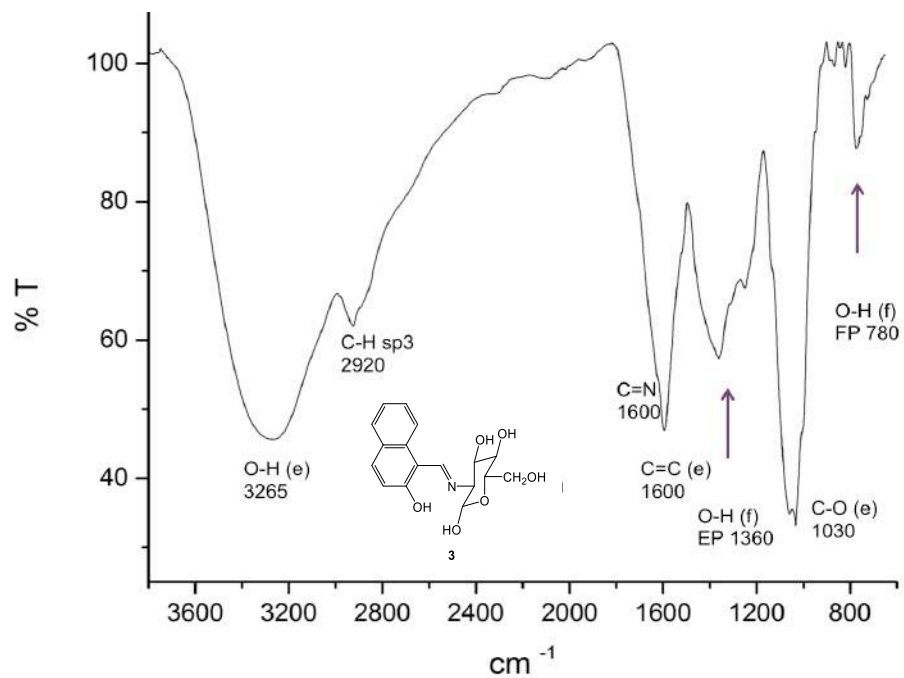
$^1\text{H}/^{13}\text{C}$  HETCOR spectrum of compound **4** (aromatic region).



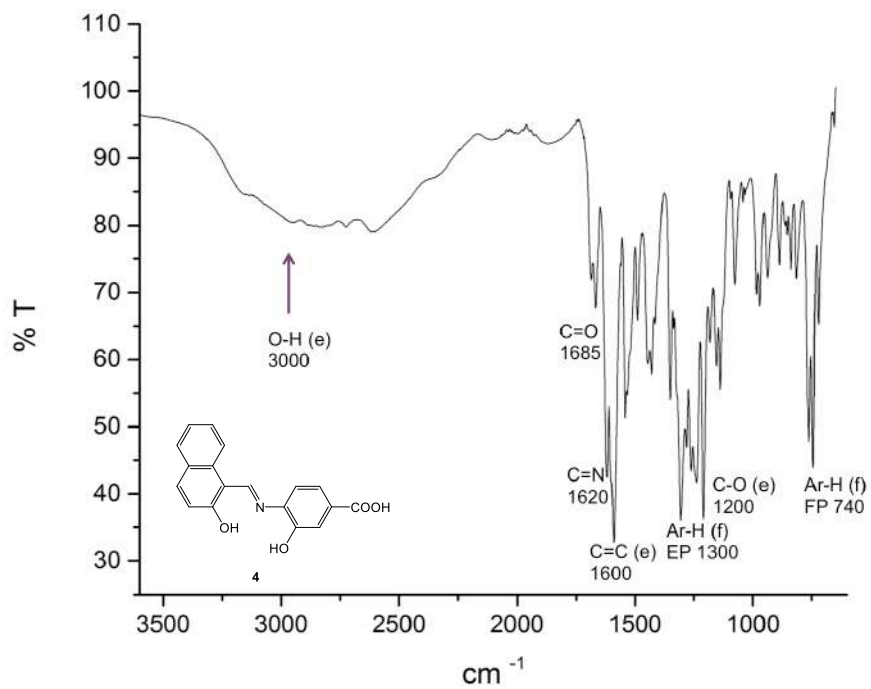
IR spectrum of compound 1.



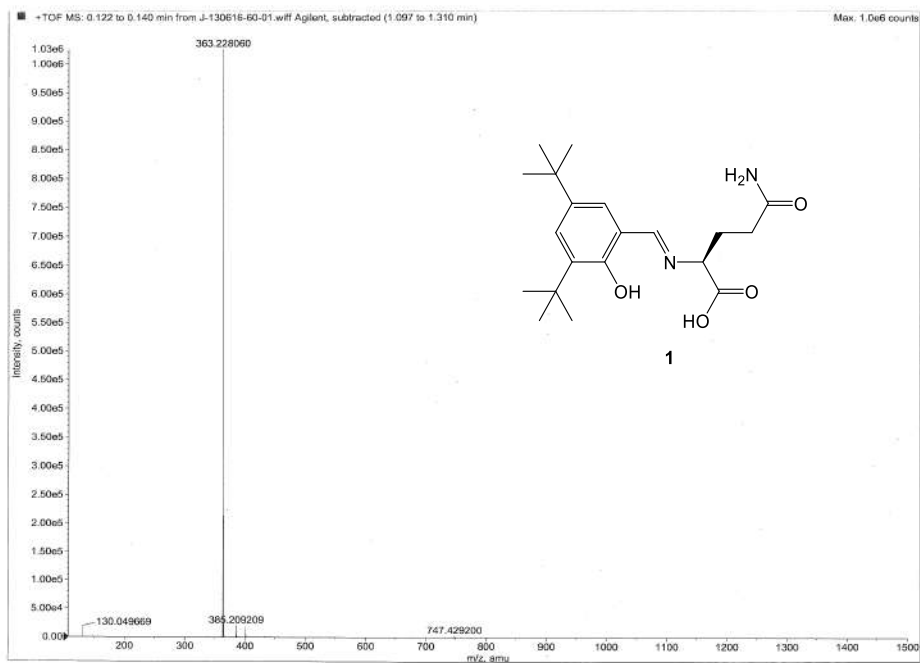
IR spectrum of compound 2.



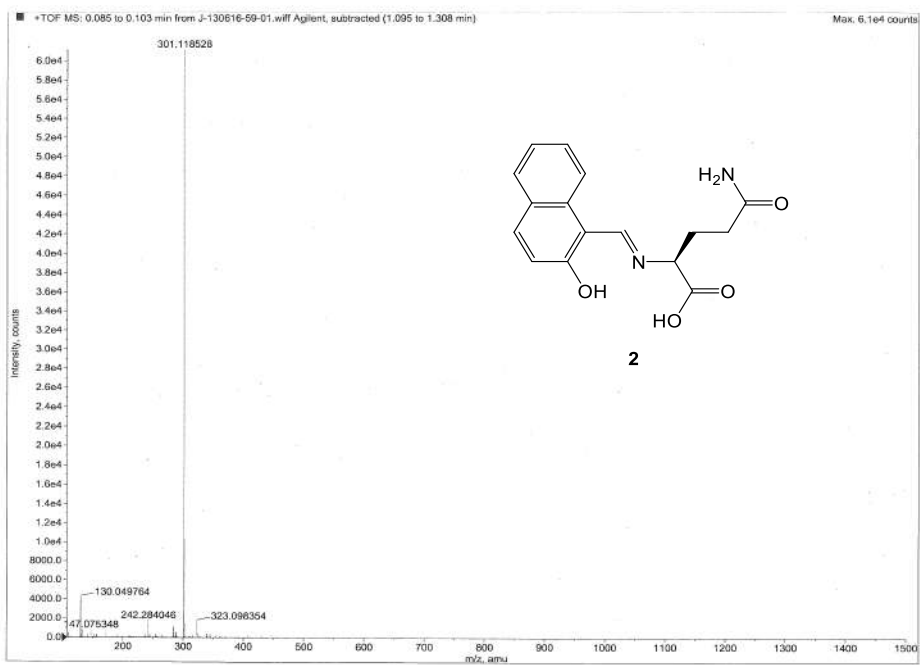
IR spectrum of compound **3**.



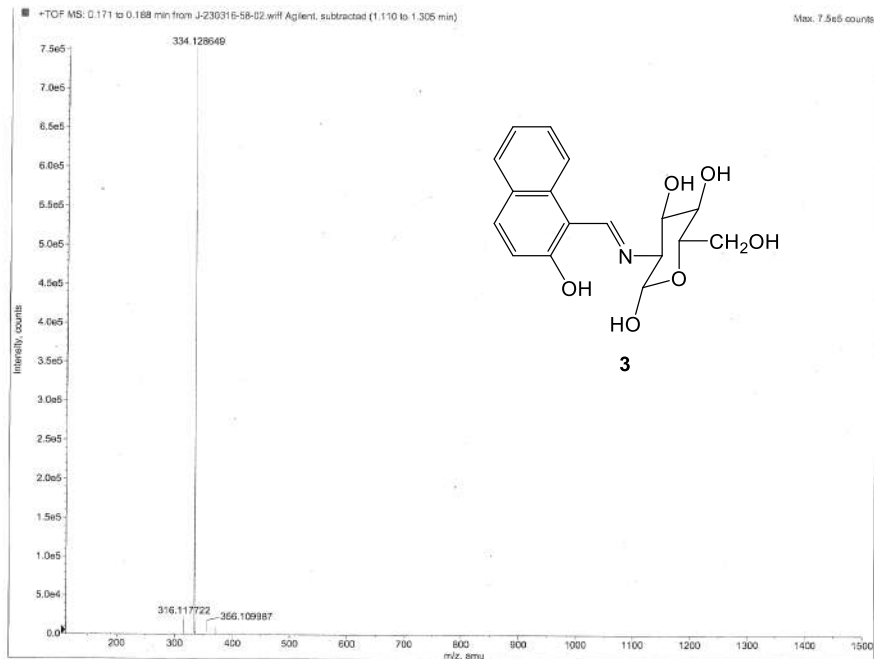
IR spectrum of compound **4**.



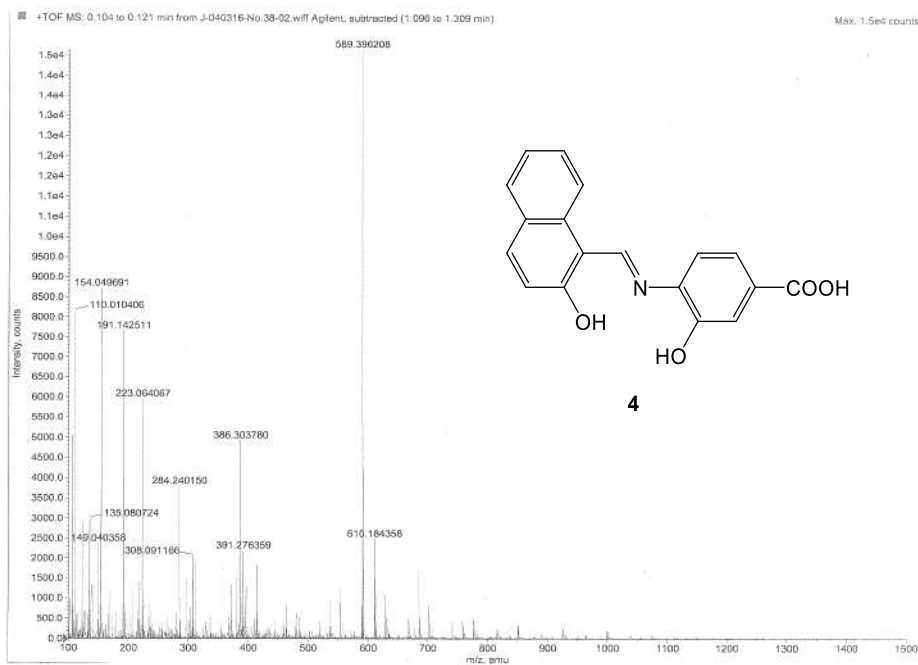
Mass spectrum of compound **1**.



Mass spectrum of compound **2**.



Mass spectrum of compound **3**.

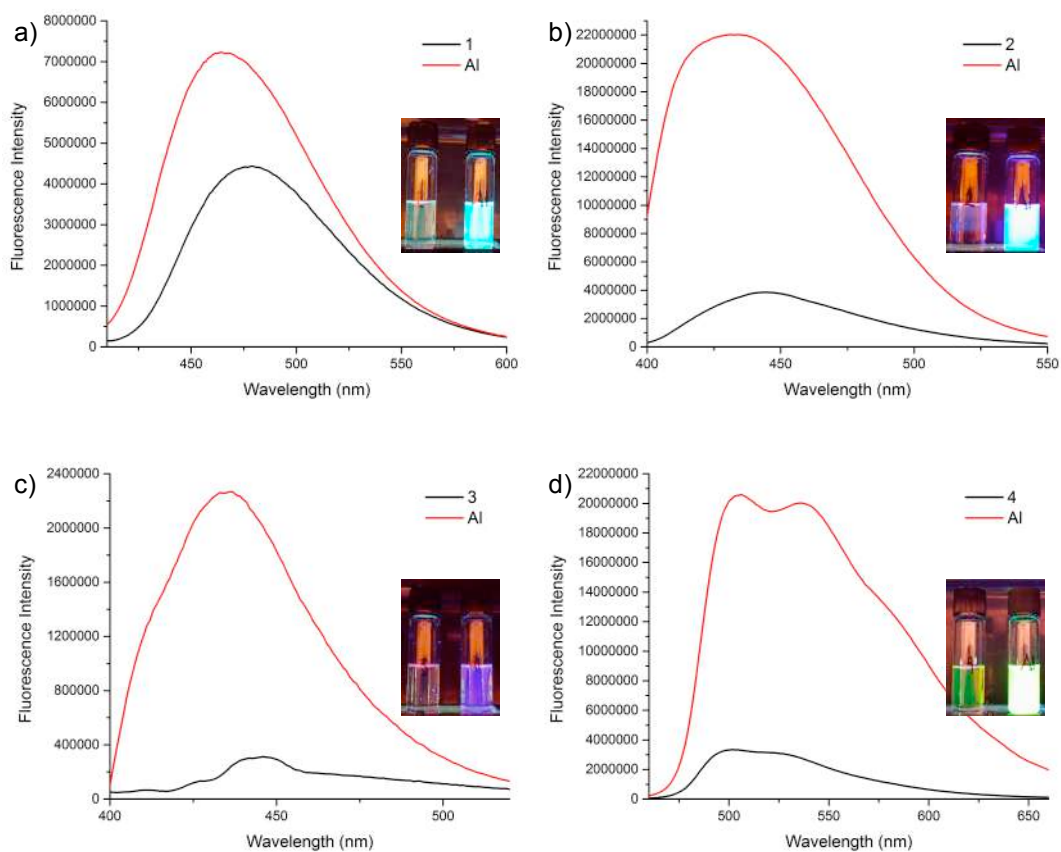


Mass spectrum of compound **4**.

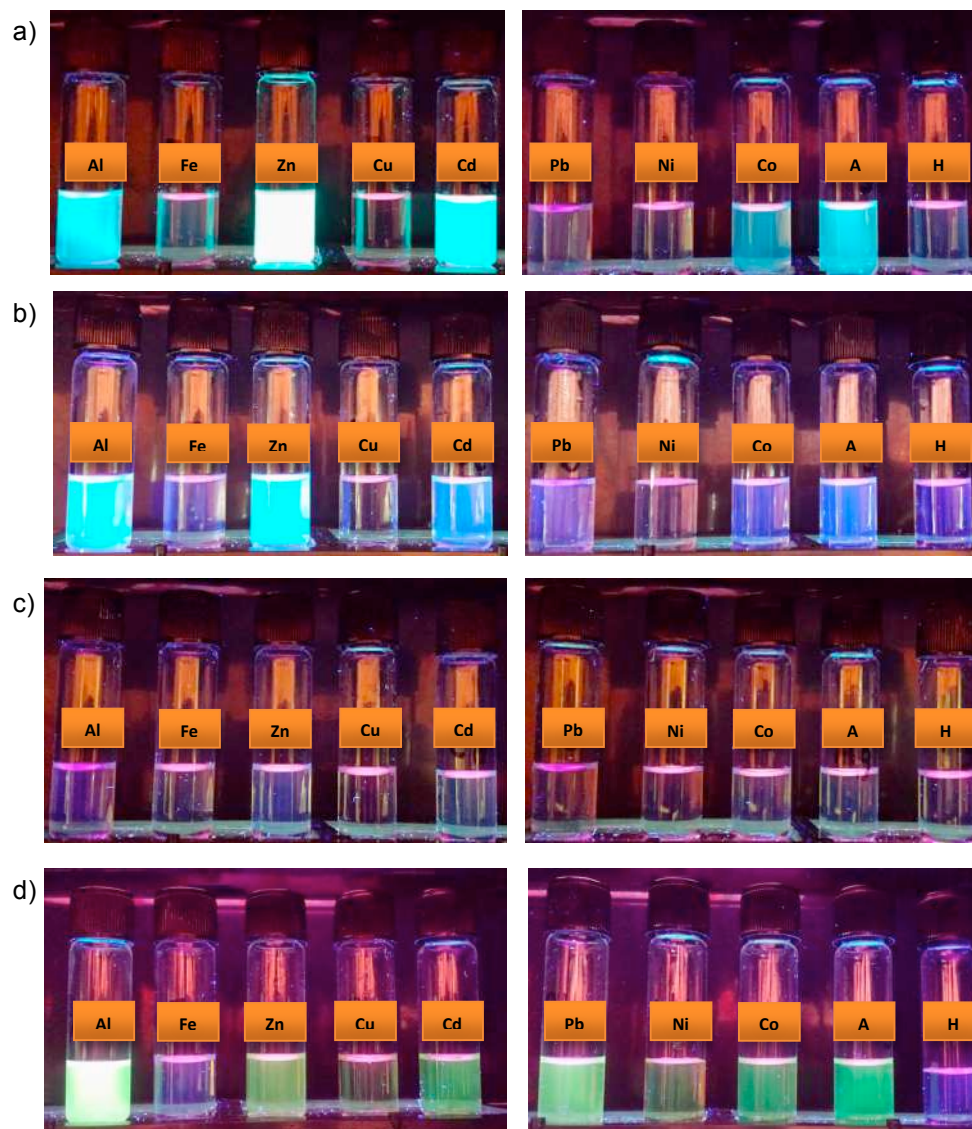
## APPENDIX B

### Fluorescence Measurement





Fluorescence spectra of a) compound **1**, b) compound **2**, c) compound **3** and d) compound **4**, ( $10\mu\text{M}$ , acetonitrile/ $\text{H}_2\text{O}$  = 1:1) in the absence and presence of  $\text{Al}^{3+}$  ( $50\mu\text{M}$ ), inserted: Photographs of the solutions under UV lamp (365 nm).



Photographs of a) compound **1**, b) compound **2**, c) compound **3** and d) compound **4**, (10  $\mu\text{M}$ ) with different metal ions (50  $\mu\text{M}$ ) under UV lamp (365 nm).

## 10. AUTOBIOGRAPHIC SUMMARY

**MC JESSICA CECILIA BERRONES REYES**

Candidate for the degree of  
Doctor of Science with Orientation in in Chemistry of Materials.

**Thesis:**

SYNTHESIS AND CHARACTERIZATION OF NEW LUMINESCENT  
BIOSENSORS OF Al (III), DERIVATIVES FROM SCHIFF BASE WITH  
POTENTIAL USE AS PREVENTIVE DIAGNOSIS METHOD IN  
NEURODEGENERATIVE DISEASES.

**Field of study:** Chemistry of Materials

**Biography:** Born in Cd. Victoria Tamaulipas, México, on September 28th of 1990.

**Education:** Graduated from the Universidad Autónoma de Nuevo León, degree obtained: Chemistry Pharmaceutical Biologist in 2013, second place of the generation. Master in Science with orientation in Pharmacy from the Universidad Autónoma de Nuevo León in 2015.

**Professional experience:** Professional practices in the department of controlled drugs Hospital Universitario Dr. José Eluterio González, UANL, 2012.